1 OF 3
AD-
A076255

1·0

2·8   2·5

3·15   2·2

3·5   2·0

1·1

1·8

1·25   1·4   1·6

NATIONAL BUREAU OF STANDARDS
MICROCOPY RESOLUTION TEST CHART

LEVEL

AD A076255

CRLS-229 Solar X-Ray
Spectrometer/Spectroheliograph Experiment

P. B. LANDECKER, W. T. CHATER, C. K. HOWEY, D. L. McKENZIE,
H. R. RUGGE, R. L. WILLIAMS, and R. M. YOUNG
Laboratory Operations
The Aerospace Corporation
El Segundo, Calif. 90245

DDC
RECEIVED
NOV 5 1979
E

5 October 1979

Interim Report
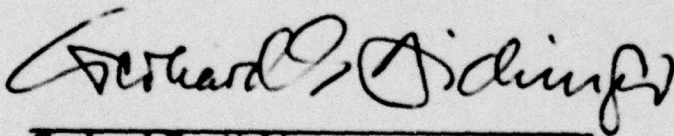
Prepared for

79 11 05 046

This interim report was submitted by The Aerospace Corporation, El Segundo, CA 90245, under Contract No. F04701-79-C-0080 with the Space and Missile Systems Organization, Contracts Management Office, P.O. Box 92960, Worldway Postal Center, Los Angeles, CA 90009. It was reviewed and approved for The Aerospace Corporation by G. A. Paulikas, Director, Space Sciences Laboratory. Gerhard E. Aichinger, was the project officer for Mission-Oriented Investigation and Experimentation (MOIE) Programs.

This report has been reviewed by the Information Office (OI) and is releasable to the National Technical Information Service (NTIS). At NTIS, it will be available to the general public, including foreign nations.

This technical report has been reviewed and is approved for publication. Publication of this report does not constitute Air Force approval of the report's findings or conclusions. It is published only for the exchange and stimulation of ideas.

Gerhard E. Aichinger
Project Officer

FOR THE COMMANDER

Frank J. Bane, Chief
Contracts Management Office

REPORT DOCUMENTATION PAGE		READ INSTRUCTIONS BEFORE COMPLETING FORM
1. REPORT NUMBER SAMSO-TR-79-76	2. GOVT ACCESSION NO.	3. RECIPIENT'S CATALOG NUMBER
4. TITLE (and Subtitle) CRLS-229 SOLAR X-RAY SPECTROMETER/ SPECTROHELIOGRAPH EXPERIMENT.		5. TYPE OF REPORT & PERIOD COVERED Interim rept's
		6. PERFORMING ORG. REPORT NUMBER TR-0080(5960-01)-1
7. AUTHOR(s) P. B. Landecker, W. T. Chater, C. K. Howey, D. L. McKenzie, H. R. Rugge, R. L. Williams, R. M. Young		8. CONTRACT OR GRANT NUMBER(s) F04701-79-C-0080
9. PERFORMING ORGANIZATION NAME AND ADDRESS The Aerospace Corporation El Segundo, Calif. 90245		10. PROGRAM ELEMENT, PROJECT, TASK AREA & WORK UNIT NUMBERS
11. CONTROLLING OFFICE NAME AND ADDRESS Space and Missile Systems Organization Air Force Systems Command Los Angeles, Calif. 90009		12. REPORT DATE 5 October 1979
		13. NUMBER OF PAGES 210
14. MONITORING AGENCY NAME & ADDRESS(if different from Controlling Office)		15. SECURITY CLASS. (of this report) Unclassified
		15a. DECLASSIFICATION/DOWNGRADING SCHEDULE

16. DISTRIBUTION STATEMENT (of this Report)

Approved for public release; distribution unlimited

17. DISTRIBUTION STATEMENT (of the abstract entered in Block 20, if different from Report)

18. SUPPLEMENTARY NOTES

19. KEY WORDS (Continue on reverse side if necessary and identify by block number)

X-Ray Spectrometers
Solar X-Rays
Soft X-Rays

20. ABSTRACT (Continue on reverse side if necessary and identify by block number)

The CRLS-229 Solar X-ray Spectrometer/Spectroheliograph was launched in the solar pointed section of the United States Air Force Space Test Program P78-1 satellite on 24 February 1979. The SOLEX collimated Bragg crystal spectrometer experiment and the MONEX solar X-ray monitor experiment were built by The Aerospace Corporation, and the Naval Research Laboratory supplied the SOLFLEX uncollimated solar flare crystal spectrometer and the MAGMAP magnesium mapping experiment. The SOLEX A spectrometer has a

DD FORM 1473
(FACSIMILE)

009 575

micrometer   angstroms

20 arc sec multigrid collimator, an ADP or RAP crystal, and a proportional counter detector with a 25 µm thick beryllium window. The SOLEX B spectrometer has a 60 arc sec collimator, an ADP or RAP crystal, and a channel electron multiplier array detector. The SOLEX crystals and detectors can be driven so that either spectrometer exposes RAP to the collimated solar X-rays while the other exposes ADP. The spacecraft pointing system can raster the SOLEX collimator over the whole sun or a 5×5 arc minute region to build up a monochromatic image, or it can point the instrument anywhere on the sun so that spectra in the 3-25 Å range are obtained. The MONEX experiment is currently recording broadband observations of both hard and soft X-ray emission from solar flares and active regions in the energy range 1-140 keV with time resolution of 32 msec. The hardware consists of proportional counter detectors which view the entire sun. Twelve channels of pulse height analysis are employed. This report provides a detailed description of the design, function and overall operation of the SOLEX and MONEX experiments. It is intended for use during post-launch data processing and for potential guest investigators who may wish to devise an observing program using this payload.

SUMMARY

The CRLS-229 Solar X-ray Spectrometer/Spectroheliograph payload was launched in the solar pointed section of the U. S. Air Force Space Test Program P78-1 satellite on 24 February 1979. Aerospace built the SOLEX collimated X-ray spectrometer and the MONEX X-ray monitor experiments, whereas the Naval Research Laboratory built the SOLFLEX uncollimated solar flare X-ray spectrometer and the MAGMAP magnesium line mapping experiments. The SOLEX experiment is currently obtaining solar raster maps in individual X-ray spectral lines and recording spectra in the 3-25 Å wavelength interval. The basic CRLS-229 SOLEX hardware consists of a 20 arc sec and a 1 arc min multigrid collimator for spatial resolution, RAP and ADP scanning high-resolution Bragg crystals, and detectors consisting of an array of channel electron multipliers and a proportional counter. The MONEX experiment is currently recording broadband observations of both hard and soft X-ray emission from flares and active regions in the energy range 1-140 keV with time resolution of 32 msec. The hardware consists of proportional counter detectors which view the entire sun. A total of 12 channels of pulse height analysis are employed. The detailed design of both the SOLEX and MONEX experiments is given in this report.

<u>Preface</u>

This report provides a general description of the design, function and overall operation of the Aerospace parts of the CRLS-229 Solar X-Ray Spectrometer/ Spectroheliograph Experiment. It is intended for use during post-launch data processing and for potential guest investigators who may wish to devise an observing program using this payload. As a consequence, it covers the most important aspects of the experiment in considerable detail, all of which may not be of interest to the casual reader of this report.

iii

Figure 1. The People Associated with the Design, Fabrication, and Testing of the CRLS-229 Payload. The flight instrument is bagged and ready for shipment to Ball Brothers Research Corporation, the spacecraft contractor. The protective coating will be removed in Boulder, Colo., and the highly reflecting thermal coating then will be exposed.

CONTENTS

CONTENTS (Continued)

FIGURES

FIGURES (Continued)

FIGURES (Continued)

TABLES

1. INTRODUCTION

1.1 Payload Summary

CRLS-229, a joint payload of the Space Sciences Laboratory of The Aerospace Corporation and the Naval Research Laboratory, was launched in the pointed section of the United States Air Force Space Test Program P78-1 satellite on 24 February 1979. The satellite, built by the Ball Corporation, provides an accurate solar pointing platform for this payload which consists of four experiments. A photograph of CRLS-229 installed in the P78-1 satellite is given in Figure 1.1. Aerospace has responsibility for the chassis and the SOLEX and MONEX experiments. R. Kreplin of NRL[*] has responsibility for the MAGMAP and SOLFLEX experiments. The entire CRLS-229 payload weighs 127 lbs and is 52 in long.

The four experiments contained in the CRLS-229 payload are described below.

(i) The SOLEX experiment makes solar maps in individual X-ray spectral lines and records spectra of individual active regions and the quiet Sun in the 3-25Å wavelength interval. The maps are generated in a 5 arc min x 5 arc min or 45 arc min x 45 arc min raster pattern, whereas the spectra are, in general, recorded in the spacecraft offset point mode. The basic hardware consists of a 20 arc sec and a 1 arc min multigrid collimator, RAP (Rubidium Acid Phthalate) and ADP (Ammonium Dihydrogen Phosphate) scanning high-resolution Bragg crystals, and detectors consisting of a proportional counter, and a channel electron multiplier array associated with the 20 arc sec and 1 arc min collimators, respectively.

(ii) The MONEX experiment obtains broadband observations of both hard and soft X-ray emission from the sun in the energy range 1-140 keV with time resolution

[*]This and other abbreviations are listed in the glossary in Section 10.

CRLS-229
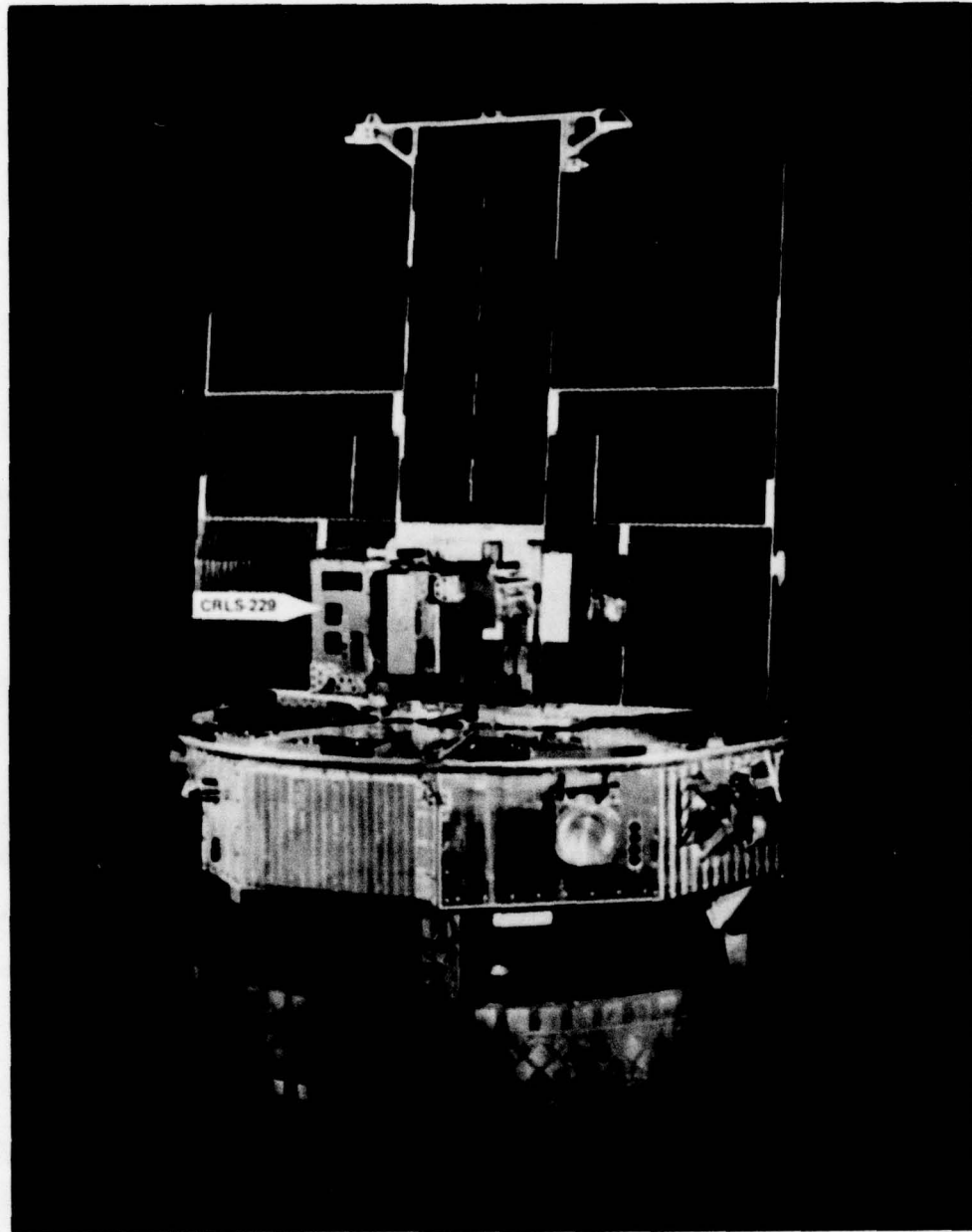
Figure 1.1. P78-1 Spacecraft. The P78-1 (a backup OSO, acquired by the Space Test Program from NASA) carries a complement of experiments designed to study solar and terrestrial radiations. The Aerospace experiment, indicated by the arrow, is mounted in the portion of the spacecraft that points at the sun.

of 32 msec. The hardware consists of uncollimated proportional counter detectors. A total of 12 channels of pulse height analysis are employed.

(iii) The SOLFLEX experiment studies selected wavelength regions of flare spectra with high spectral resolution in four wavelength bands: $1.823\text{Å}-1.966\text{Å}$ (iron lines), $2.982\text{Å}-3.088\text{Å}$ (Lyα Ca XX), $3.141\text{Å}-3.239\text{Å}$ (Ca XIX), and $8.249\text{Å}-8.514\text{Å}$ (iron lines). The hardware consists of uncollimated, scanning Bragg crystal spectrometers and stationary proportional counter detectors.

(iv) The MAGMAP experiment is designed to make 45 arc min x 45 arc min maps of solar Mg XI and XII emission in the $8-12\text{Å}$ spectral region. The instrument consists of two proportional counter detectors that view the Sun through the SOLEX 1 arc min collimator.

The four experiments cover the wavelength range $\simeq 0.1\text{Å}-25\text{Å}$. Since they will, in general, simultaneously observe the same phenomena, they can be used in combination during the data reduction phase of the CRLS-229 project. This payload represents one of the most sophisticated satellite experiments ever to make solar X-ray spectroscopic measurements.

A modular approach was used in the design of the various subsystems as is illustrated in Figure 1.2. This approach made it possible to build, test and calibrate each module separately as well as easily separate the Aerospace and NRL experiments.

This calibrated payload was delivered to the spacecraft contractor and all spacecraft/payload integrated system tests performed were successfully completed. The satellite was launched at 0820 UT on 24 February 1979 from Vandenberg Air Force Base. Quick-look data which is being processed at the Air Force Satellite Control Facility and production data processed at the Air Force Space and Missile Test Center will be analyzed at Aerospace and NRL.

SPACECRAFT INTERFACE

MONEX HEM

MONEX LEM

SOLFLEX

COMMAND AND TELEMETRY

FORWARD SECTION

SOLEX DETECTOR

SOLEX MOTOR CONTROL

MAGMAP

AFT SECTION
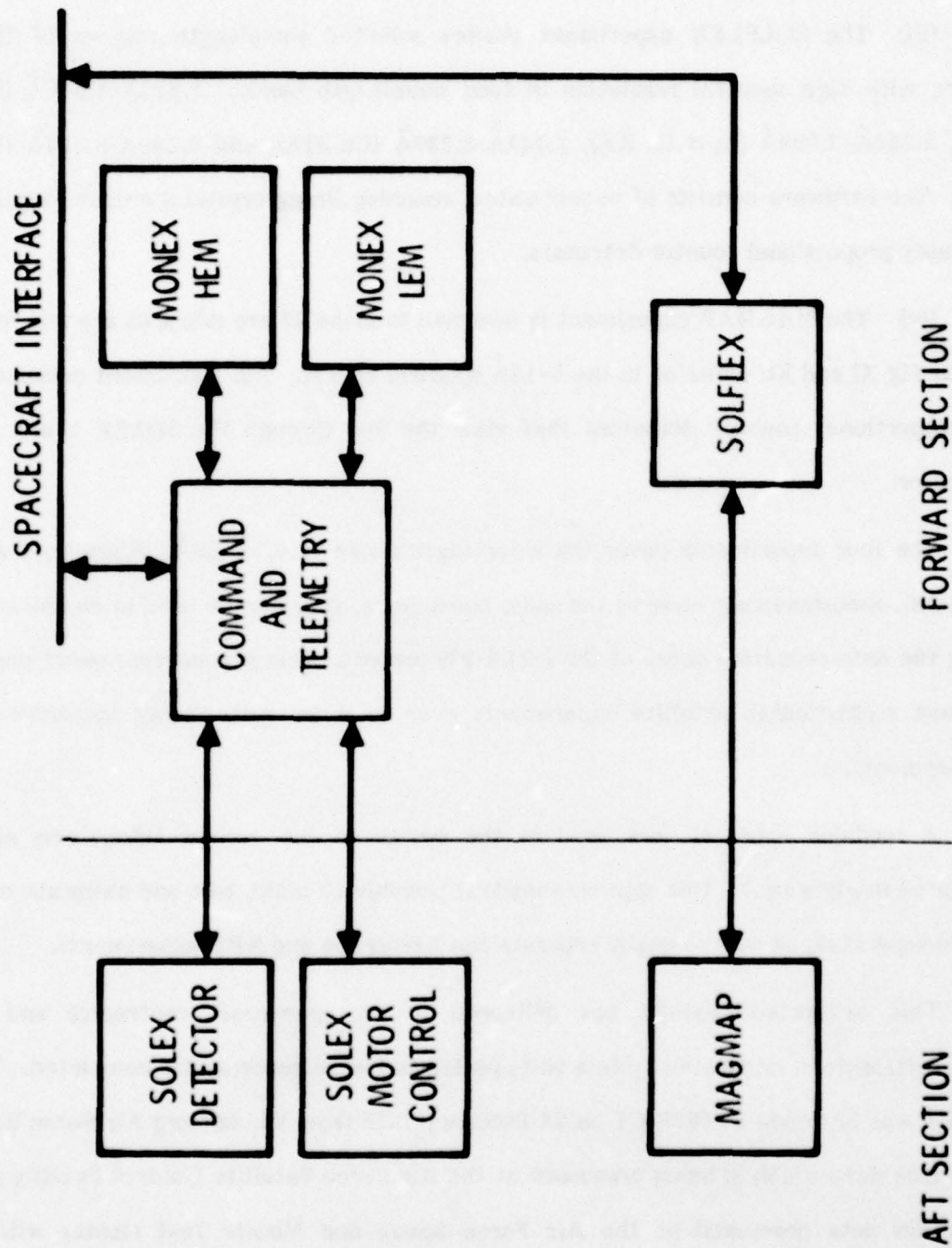
Figure 1.2. CRLS-229 Electrical Block Diagram. The forward section of CRLS-229 corresponds to the front (sun-facing) end of the payload.

1-4

2. CRLS-229 MECHANICAL CONFIGURATION

2.1 General Information

Much of the mechanical description of this instrument will be made with reference to applicable mechanical drawings. The drawing number will be in the format L - XXXX. Access to all drawings relevant to this progam can be obtained by examination of Aerospace Drawings L-6163 through L-6174. These are "Bill-of-Material" tabulations which are essentially an index to the drawing files. All drawings are on file in the Space Sciences Laboratory of The Aerospace Corporation.

The external appearance of CRLS-229 is illustrated by L-5202-H and shown in Figures 2.1-2.4. This payload, is approximately 52 in long, 14 in high and 7 in wide (132x36x18 cm). The primary shape of this package is a long rectangular section. The most prominent asymmetry consists of two large bulges at the aft (anti-solar) end; these are the Command and Data Processor (C and DP) units for the sail section of the P78-1 spacecraft. This payload conforms to the Mechanical Interface Control Drawing or MICD (Ball Drawing No. 49327).

The weight of the package is 126.59 lb (57.42 kg); this figure includes approximately 20 lb (9 kg) of spacecraft hardware. The center-of-gravity (CG) is constrained to lie on the axis of rotation (elevation axis of the PIA); it is not constrained in the spacecraft "Y-axis" direction (see Figure 2.1).

The instrument is mounted at three attachment points close to the axis of rotation (see Figure 2.4). Two top and two bottom attachment screws are also used, but they are not intended to be used as primary support points. The location of the payload in the spacecraft is determined by a spherical plug which has been lapped to a
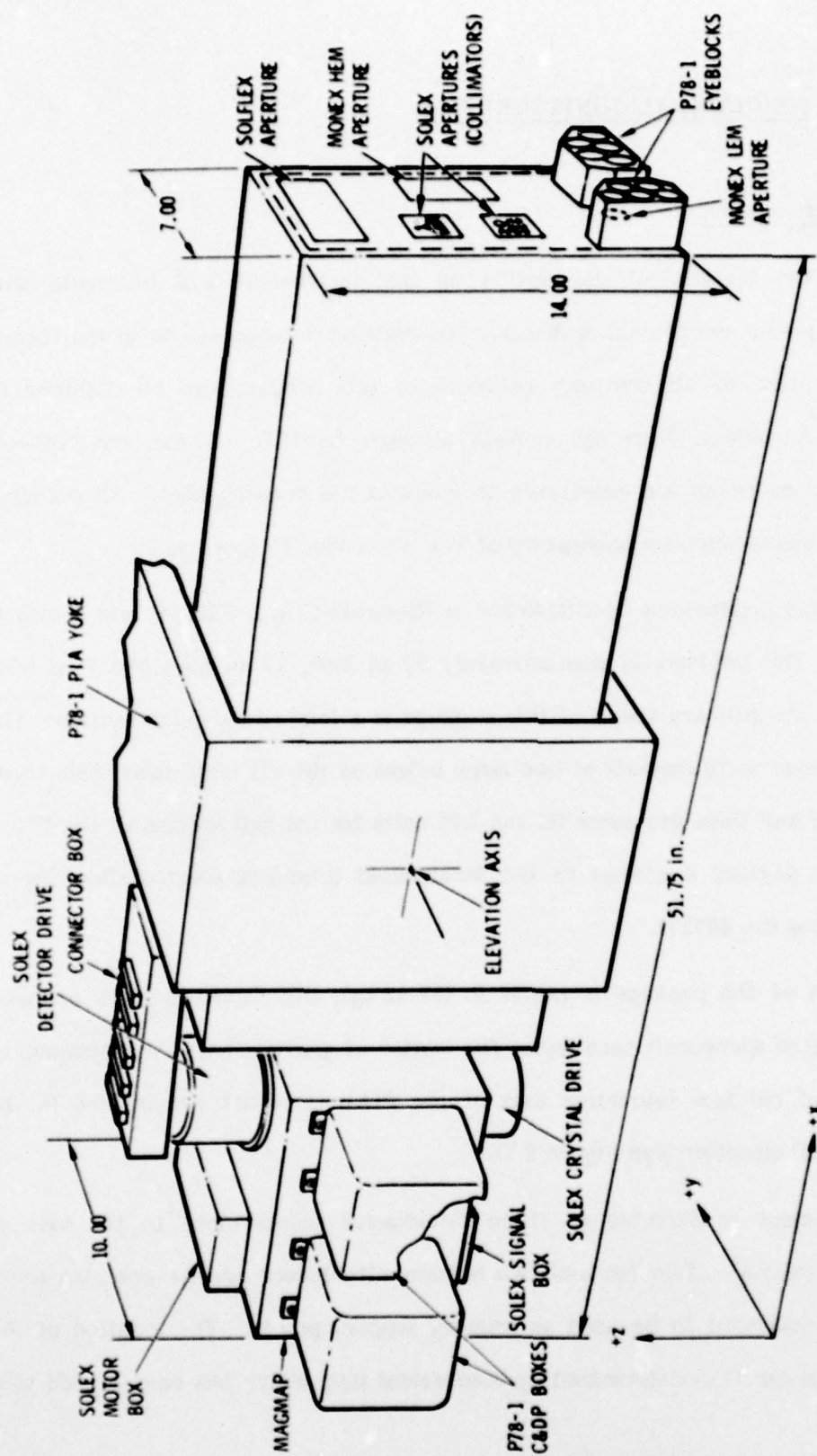
Figure 2.1. CRLS-229 Experiment Layout.

SOLFLEX APERTURE

MOMEX HEM APERTURE

SOLEX APERTURES (COLLIMATORS)

P78-1 EYEBLOCKS

MOMEX LEM APERTURE

7.00

14.00

P78-1 PIA YOKE

SOLEX DETECTOR DRIVE

CONNECTOR BOX

ELEVATION AXIS

51.75 in.

SOLEX CRYSTAL DRIVE

SOLEX MOTOR BOX

MAGMAP

SOLEX SIGNAL BOX

P78-1 C&DP BOXES

10.00

+x

+y

+z

Figure 2.2. CRLS-229 Outline and Mounting Drawing. Part 1 of 3.
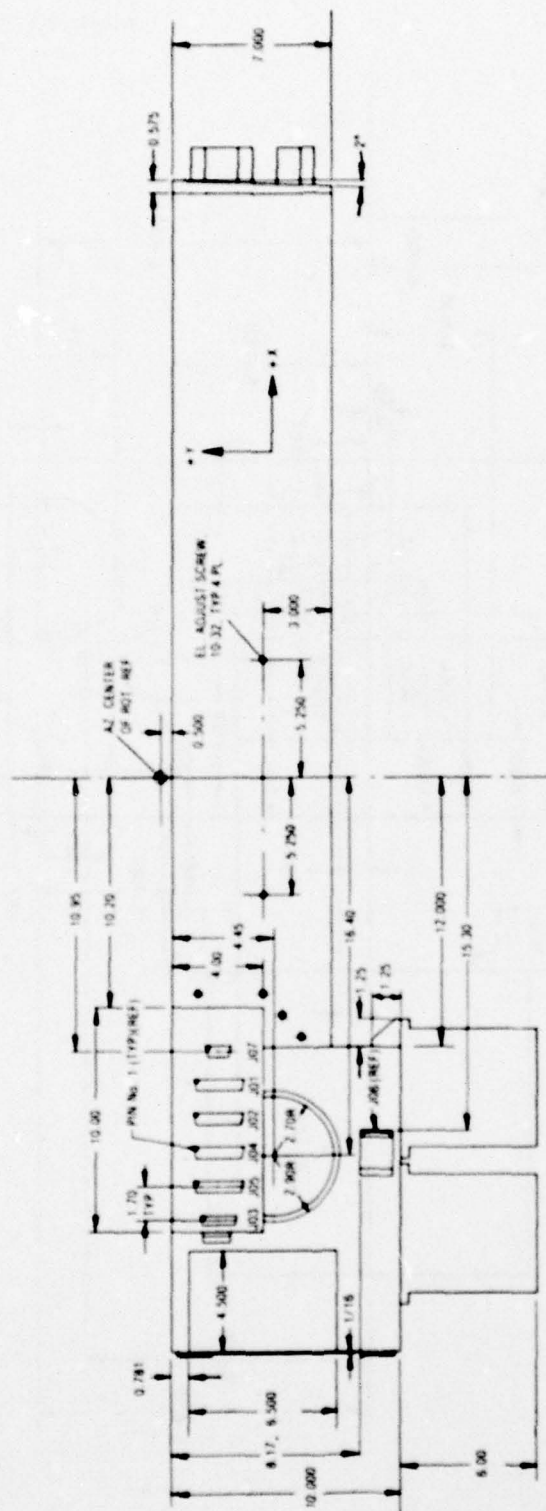
Figure 2.3.   CRLS-229 Outline and Mounting Drawing. Part 2 of 3.
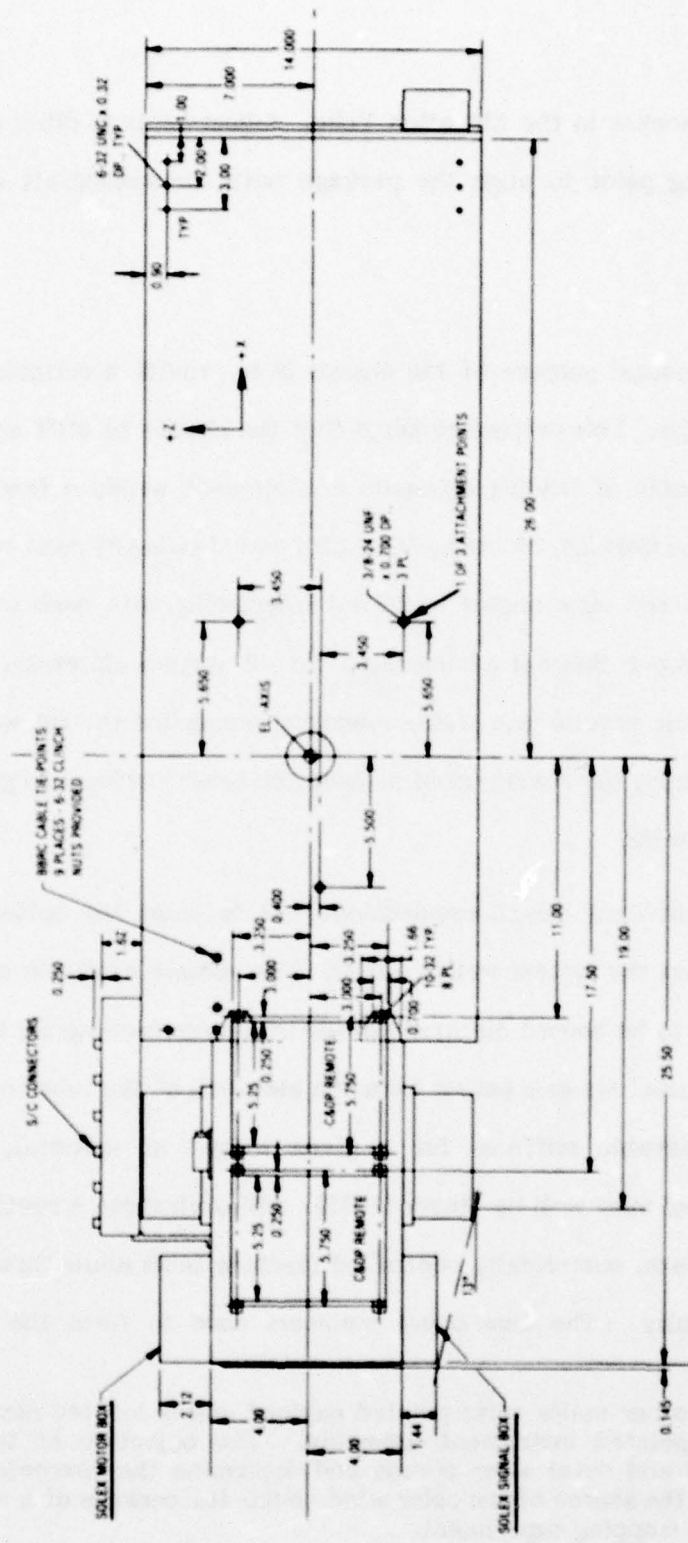
Figure 2.4. CRLS-229 Outline and Mounting Drawing, Part 3 of 3.

mating spherical socket in the Elevation Yoke. Adjustments in pitch and yaw are made about this locating point to align the package with the spacecraft and NRL-401* as required.

2.2   Chassis

The fundamental purpose of the chassis is to provide a suitable environment for the payload modules. This purpose requires that the chassis be stiff enough to act as an optical bench capable of holding elements in alignment within a few arc seconds. All instrument modules (SOLEX, MONEX, SOLFLEX and MAGMAP) must be located so as to achieve their required view angles while not interfering with each other. The chassis must provide a proper thermal environment for all system elements. In addition, the chassis must provide precise and stable mounting points for the spacecraft readout and control eyes. Finally, the chassis must provide the basic stiffness to get the instrument resonance above 50 Hz.

The most difficult design requirement was to meet the optical bench stiffness while staying within the system weight limits. The volume available and the number of internal elements to be housed dictated the use of a large rectangular tube for the major portion of the chassis. Iso-grid panels form the elements of the tube since they will have the greatest achievable stiffness for a given weight of material. This structural approach is covered very well by Meyer (1973). Although these structures would appear difficult to fabricate, numerically controlled machine tools allow them to be fabricated with little difficulty. The five panel members used to form the chassis tube are

---

*NRL-401 is the other major solar pointed payload and is located next to CRLS-229 in the spacecraft's pointed instrument assembly. The objective of this payload is to monitor the inner and outer solar corona and determine the character of the outward flow of plasma at the source of the solar wind. NRL-401 consists of a white light corona-graph and an XUV mapping experiment.

2-6

described by Drawings L-5555, 6, 7 and 8; two pieces shown in Drawing L-5556 are required. Since an iso-grid is formed of many small triangular elements it was easy to provide mount points for all internal elements by leaving extra material around the nearest triangle vertex. The drawings show this approach clearly; elements are mounted on base, top and side panels. The triangular (waffle-like) patterns face inward in order that smooth surfaces face the exterior world. These structural details are shown in a photograph of the chassis given in Figure 2.5. The chassis tube ends consist of panels containing only the cutouts necessary for apertures; these ends are required if the torsional stiffness is to be high. Access to the internal cavity is gained by removal of the cover panel shown in Drawing L-5558.

2.2.1   Eyemounts

Part of the instrument function is to provide a stable and optically flat surface to accept the spacecraft control and readout eyes. Section 3.2.4.1 of General Interface Control Drawing or GICD (Ball Drawing No. 49329) specifies the mounting requirements. The requirements are met by Drawing L-5559 (control eye bracket) and L-5560 (readout eye bracket). These parts are attached to the baseplate and lower side plate, respectively. After being permanently mounted to the chassis, the bracket pads forming the eye block mounting planes are lapped so as to form two planes co-aligned within a few arc seconds; the pads of each plane are required to form a surface flat within a few light fringes. All environmental and alignment testing indicates the goals have been achieved.

2.2.2   Chassis Balance

The GICD specifies that the instrument center of gravity (CG) in the X-Z plane be within 0.100 inches of the center of rotation of the so called "elevation axis." In the
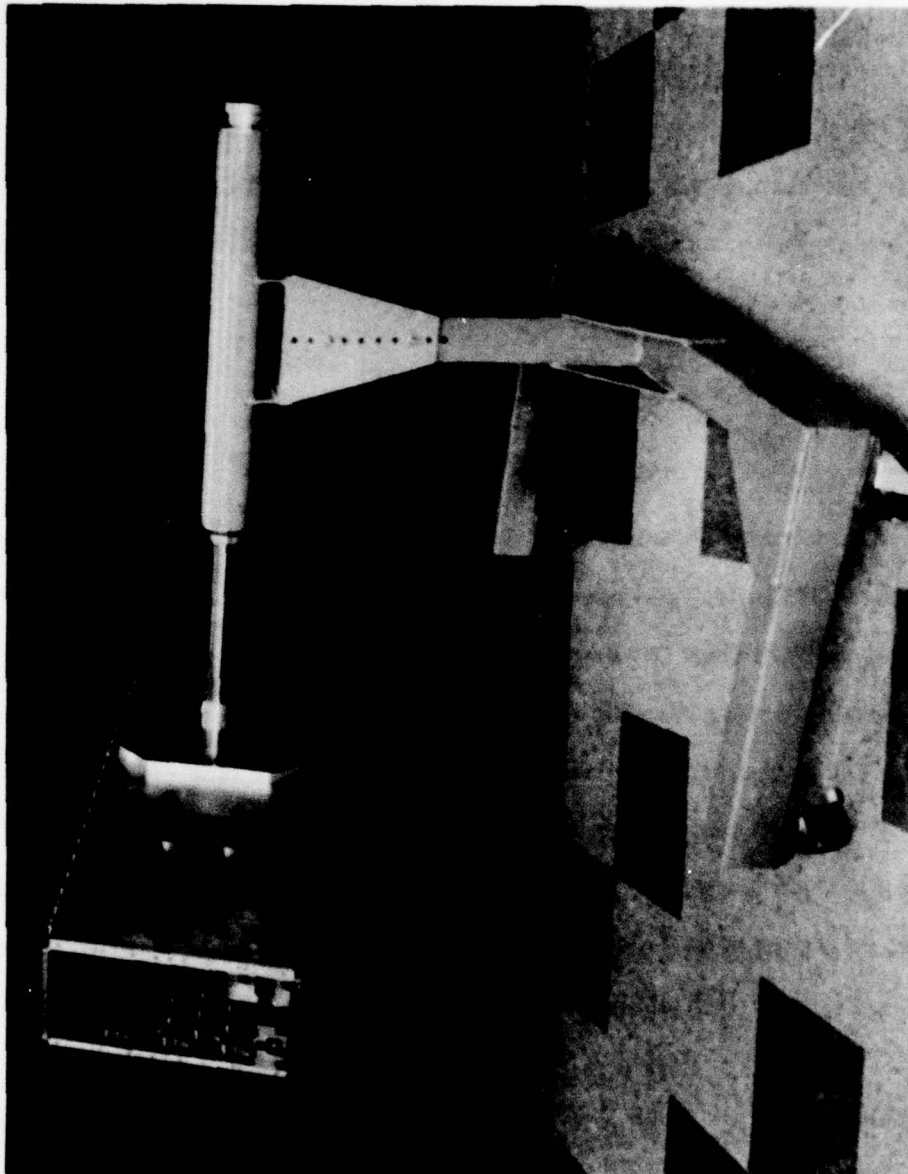
Figure 2.5. Chassis on which CRLS-229 Collimators, MONEX, SOLFLEX, and Data Processing Electronics Are Mounted. Weight relief of the panels was accomplished by computer-controlled milling machines. In this picture, the chassis is supported by a fixture used to balance the entire experiment.

initial attempt, the various internal modules were located to bring the CG near the geometric center of the package. Since there are limits and constraints on the movement of the internal modules, a final trim was to be achieved by optimally placing the center of rotation (C of R). Since the location of the C of R is machined into the structure long before the mass properties of the internal elements are known, estimates were made. The inaccuracy of the estimates resulted in a C of R location error of about an inch. Compensating for this required the addition of over 5 lb of ballast in the forward section of the chassis. Nearly 6 lb of additional forward ballast was required to make up for spacecraft generated unbalances (overweight C and DP units, wire harness, etc.). The balance weights are all brass plates bolted to the chassis panels by picking up the iso-grid triangle vertices.

2.2.3 Thermal Finish

The spacecraft contractor is required by the GICD to specify to the payload agency all exterior surface finishes to meet spacecraft thermal control requirements. Ball achieves thermal control using passive surface finishes rather than active elements. Only one small surface of CRLS-229 views the sun, and most of its surface area is exposed to cold space; the problem is in keeping the payload warm rather than cool. A very shiny surface meets this need. Rather than try to polish and maintain shiny metal outer surfaces, which would be difficult to protect through all the development phases, it was decided that a suitable thermal tape would be applied as one of the last assembly steps.

The tape used was Sheldahl Corporation thermal control tape G401-002. This is a 1.0 mil Kapton film having a 1000Å evaporated aluminum front surface. A good feature of this tape is that it has a "coverlay" protective film that can be left in place until the

2-9

final stages of preparing the spacecraft for thermal vacuum testing. This means that for the bulk of the program, extreme care about fingerprints and other contamination is not required as they will be removed when the "coverlay" is stripped off.

2.2.4 Thermistors

The three Aerospace furnished thermistors are located in CRLS-229 as follows.

Name	X (in)	Y (in)	Z (in)
T FRONT	+24	+0.8	-4
T MID	-9	+0.8	+5
T REAR	-24	+2	+3.5

The origin of the X and Z axes is at the PIA elevation axis; the Y axis origin is at the surface containing the spherical mount (see Figures 2.1-2.4).

Thermal calibration curves are given in Figure 7.5. Expected worst-case temperature extremes are $3^{o}C$ and $33^{o}C$. In fact, the temperatures measured in orbit during the first month of operation were $T_{FRONT} \simeq 26^{o}C$, $T_{MID} \simeq 21^{o}C$, $T_{REAR} \simeq 21^{o}C$, well within the design limits.

2.3 SOLEX

SOLEX is the most complicated experiment element in the CRLS-229 payload. In basic concept SOLEX is similar to other Bragg spectrometers designed, built and flown on both rockets and satellites by the Space Sciences Laboratory of The Aerospace Corporation; however, in detail it is an entirely new system.

2-10

Scientific considerations established that there would be two collimators arranged in an "over and under" configuration illuminating a crystal panel assembly carrying a set of four crystals. As shown in Figure 2.6, one detector, a channel electron multiplier array (CEMA), accepts radiation which has passed through the 60 arc sec collimator and been diffracted from either exposed surface of two back-to-back crystals (one at a time). The second detector, a proportional counter (PC), records photons which have passed through the 20 arc sec collimator and diffracted from a second pair of back-to-back crystals (again, one at a time).

One of two techniques can be used to maintain the required Bragg relationships. The first is to decouple the crystal drive and rotate the crystal panel 180 degrees to allow use of the companion crystal. The second technique is to move the detector assembly towards smaller and smaller Bragg angles until the angle goes negative and one is accepting reflections from the companion crystal. The first technique requires a complicated mechanical system with a substantial uncertainty in reliability and a certain loss in angular positional accuracy. Use of the second technique, in which the detector assembly sweeps out almost a full circle, creates substantial problems in mechanically coupling the crystal and detector assemblies together in order to develop the motion required to satisfy the Bragg condition. When the requirement that the detector assembly be parked out of the X-ray beam while the crystal assembly is at Bragg 0 degrees to allow the one minute collimator to illuminate the MAGMAP apertures (see Section 2.7) is considered, the idea of electronically (rather than mechanically) coupling the motions of the crystal and detector assemblies becomes very attractive. Once this gearing solution was chosen, the rest of the package design followed.
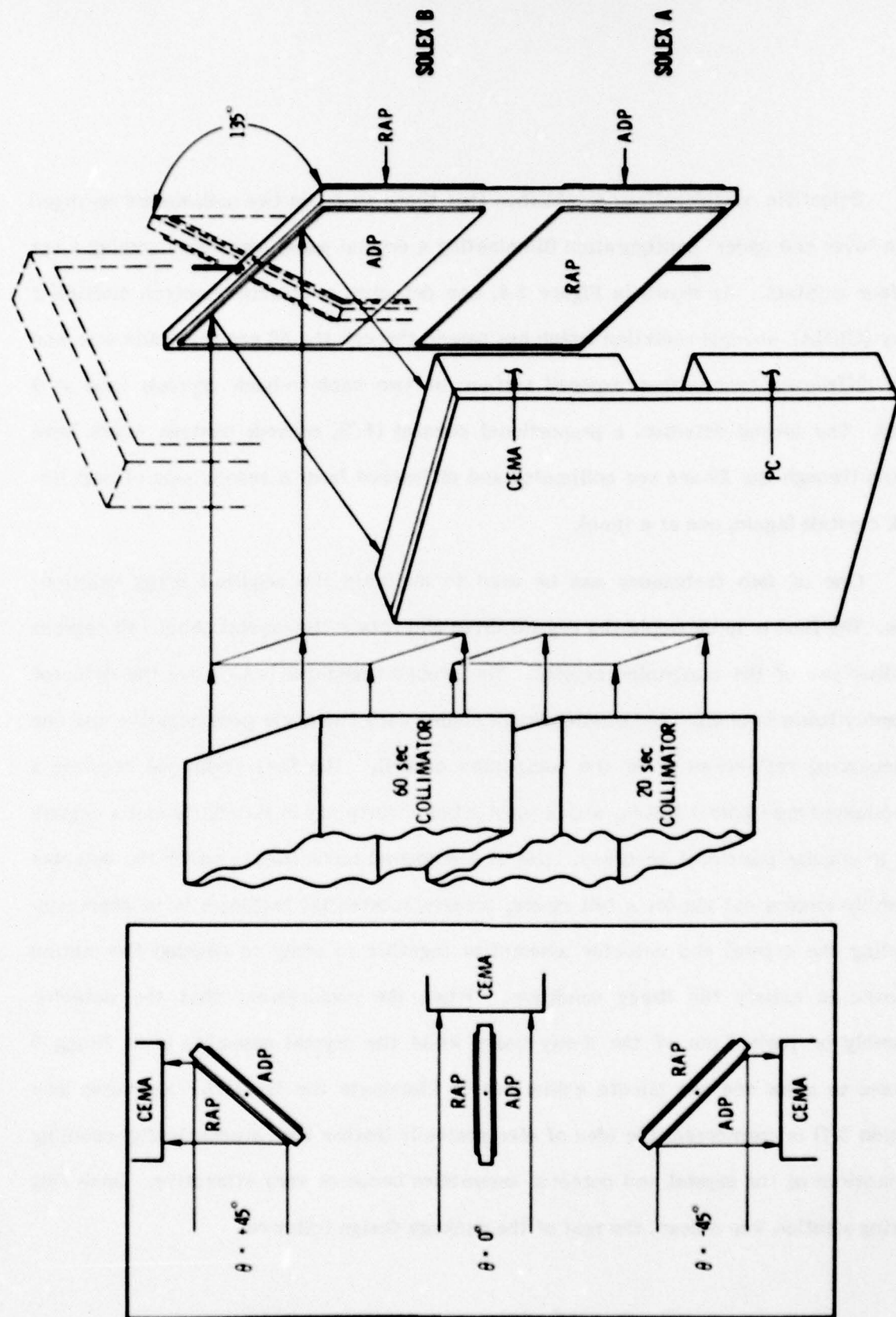
Figure 2.6. Layout of SOLEX Collimators, Crystals, and Detectors.

Some major constraints dictated much of the design. The first constraint is the limitation of a width of 7 inches in the forward section holding the collimators; this arises from the fixed width of the spacecraft elevation yoke through which the instrument must pass. Since the collimator optical centerline must intersect the rotation axis which passes through the center of the crystal panel, the collimators must be mounted as close as possible to the chassis baseplate.

Although the payload can bulge somewhat in the −Y direction at the aft end it cannot bulge in the +Y direction. Thus, the collimator optical center and the need for the detector sweep to be confined to the envelope of the chassis determines the maximum radius of the detector assembly. The thickness of the individual detector packages then determines the maximum length of the crystal panel. In this case, a 4 in long crystal panel will just clear the detector assembly. Crystal dimensions in the direction of the axis of rotation are also determined by the collimator aperture geometry. By placing the collimators as close together as possible, enough room in the ± Z directions was available to allow space for drive units within the permissible payload envelope.

The SOLEX design resulting from the various constraints is clearly illustrated by Drawing L-5814. The basic box structure containing the moving spectrometer elements is required to be very strong in order to carry the spacecraft Command and Data Processing (C and DP) units (each weighing about 8 lb). The C and DP packages are mounted in such a way that severe torsional moments are introduced during vibration. Iso-Grid panels were used in order to produce a strong, yet light assembly. This box carries on its exterior surfaces the crystal drive (motor, gears, etc.) unit, the detector drive unit, the motor drive electronics package, the detector electronics package, two C and DP units and the MAGMAP experiment. All of these elements are connector coupled

and could be removed for service. A photograph of the SOLEX Bragg crystal spectrometer compartment is shown in Figure 2.7. A photograph of this compartment attached to the chassis is given in Figure 2.8.

The entire SOLEX aft unit can be disconnected and removed from the rest of the CRLS-229 payload. The aft SOLEX weight is 21.3 lb. Since it is external to the rest of the payload, it had to include its own thermal finish; this was accomplished by use of the same tape as was used in the forward chassis section.

2.3.1 SOLEX Crystal Drive

The crystal drive requirement was to be able to position the crystal panel repeatably at any angle between Bragg -60 degrees and Bragg +75 degrees (a total angular travel of 135 degrees) with a high degree of precision. Since the crystal and detector drives were to be only electronically coupled, two stepper motors must be used. With adequate counting and driving electronics, open-loop control of the stepper motors may be reliably accomplished. Since the smallest motion possible from a stepper motor is one step (the motors we use have a 90 degree step), a large gear reduction is needed if the minimum crystal panel step is to be small. A large gear reduction is very helpful as a very small stepper motor will have more than adequate torque to drive the load. Also, since the inertia of the load is reduced by the square of the gear ratio when reflected through a gear train, the torque of the stepper motor is much enhanced. There are two factors limiting the maximum geartrain reduction: one is the time required to scan from point to point since the maximum step rate is limited, the second is the capacity of the control system to count and store step information. It was decided that the electronics would have a maximum of 2^{14} or 16,384 steps. If the crystal panel is to scan over 135 degrees, it follows that one step must be about 135/16,384 degrees or about 30 arc sec.
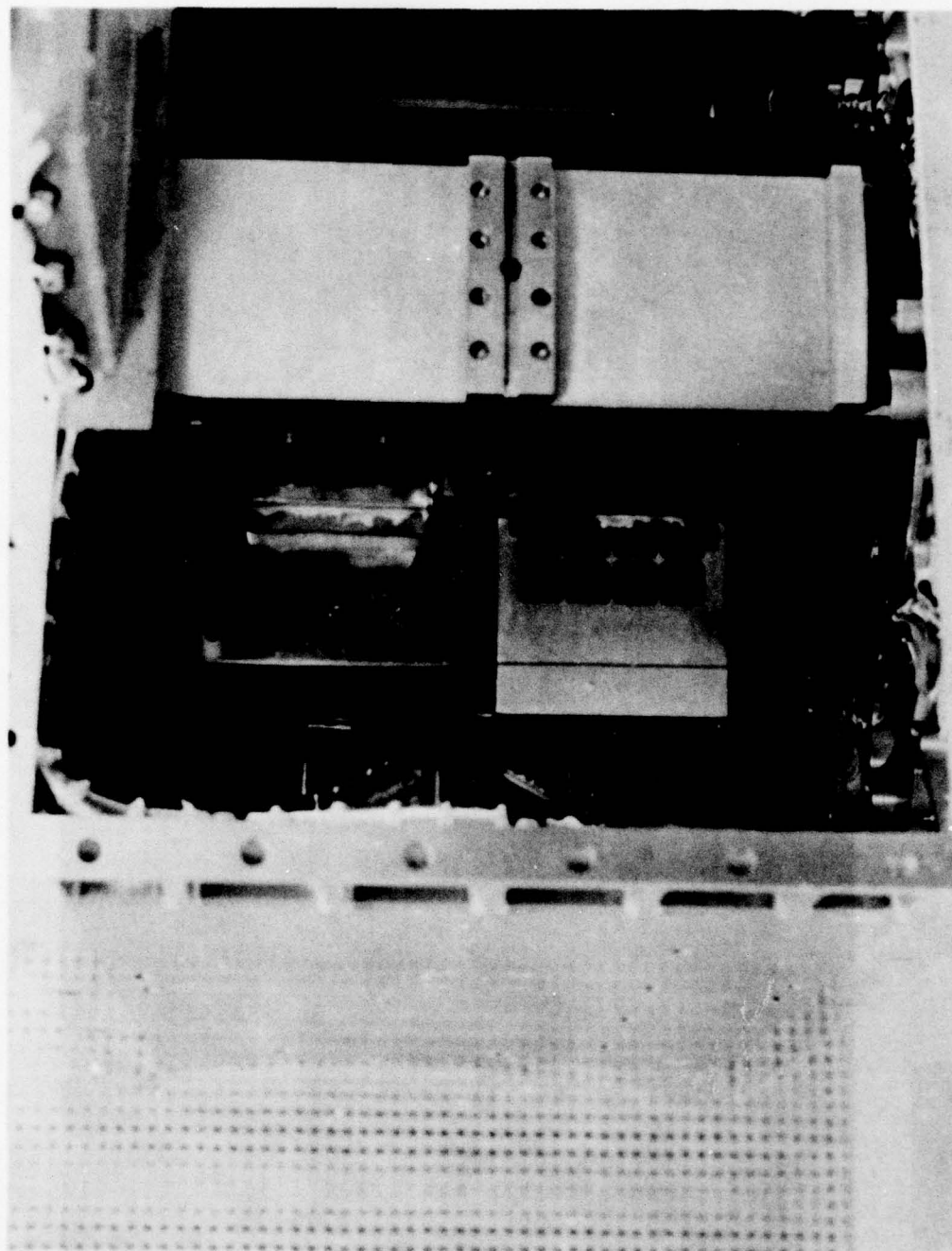
Figure 2.7. Detailed View of CRLS-229 X-Ray Bragg Crystal Spectrometer
Compartment. X-rays entering from the collimators on the
bottom are diffracted by ADP and RAP crystals and detected
by proportional counter and channel electron multiplier array
(CEMA) detectors. The crystals and detectors are scanned
separately to obtain high resolution solar X-ray spectra
between 0.5 and 4 keV (3-25 Å).

2-15
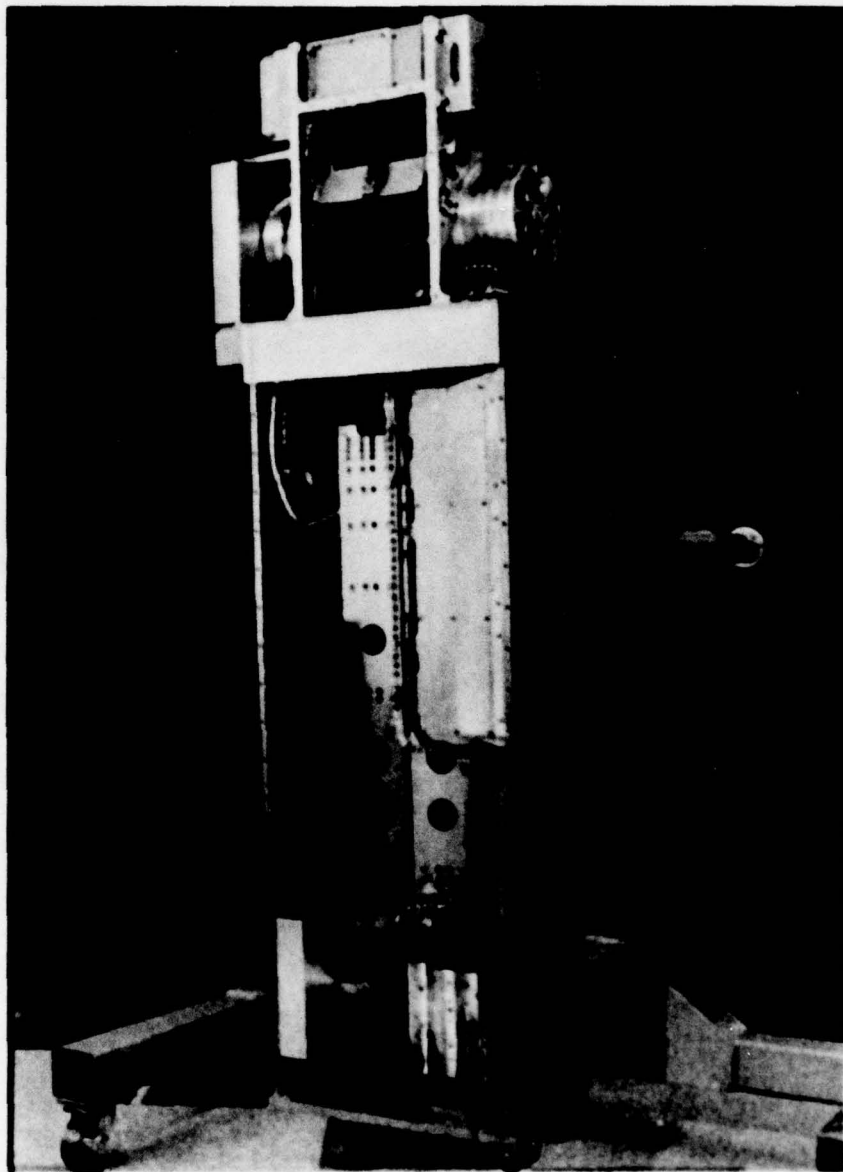
Figure 2.8. CRLS-229 Experiment (supported by balancing fixture) With
Several Covers Removed. Solar x-rays enter the experiment
from the bottom of the picture.

2-16

The crystal drive unit power flow starts with a size eight permanent magnet stepper motor driven at either 62.5 or 31.25 Hz. The motor drives an integral gearhead having a reduction ratio of 479 to one. The gearhead output drives through a ratio of 76:68 into a slipclutch adjusted to slip at 20 in-oz of torque. The function of the slipclutch is to protect the geartrain from any overloads accidentally introduced at the output end of the geartrain. Leaving the clutch assembly the drive passes through a mesh of ratio 21:105 followed by another mesh of 21:105 into the output shaft. The total reduction then is $(479/1) (68/76) (105/21)^2 = 10714.47:1$. If we divide one 90 degree step by this ratio we have 90/10714.47 = 0.008400 degree or 30.2 arc sec per step. A full scan of 135 degrees will take 4.29 minutes at a 62.5 Hz step rate.

Two other features were added to this assembly. The first was a precision potentiometer driven by the last gear in the train so that a convenient analog signal representing crystal panel position would be available. The output potentiometer is driven by the output shaft through a gear ratio of 105:76; therefore, it moves (135) (105/76) or 186 degrees in one 135 degree crystal panel scan. The second desirable feature was the incorporation of an anti-backlash element so that the crystal panel positioning would not be influenced by the direction of motion. Because the crystal panel motion is limited to 135 degrees a pre-loaded torsion spring on the output can remove geartrain backlash. In effect, the geartrain drives the output in one direction and acts as an escapement in the other. The drive elements are packaged in their own housing; the result is a modular element easily removed for service.

A substantial effort was made to measure the positioning performance of the drive unit. Analysis of the data allows one to make several statements.

1. The output angle measured from a zero point determined by a microswitch is 0.008393185 degrees per step (plus or minus two arc minutes in the 135 degree range).

2.   Using a calibration factor, the output can be positioned within plus or minus one arc minute.

3.   The reproduceability of motion is within 20 arc seconds except for one ten degree section where the uncertainty is up to 40 arc seconds.

2.3.2 SOLEX Detector Drive

The detector drive unit is identical to the crystal drive unit with two exceptions. The first difference stems from the fact that great precision on the motion of the detectors is not required; it is only required that the detector be positioned to accept the reflected radiation. For this reason no anti-backlash provision was built into the detector drive. The second difference arises from the need for the detector assembly to move at twice the crystal angular velocity to intercept the diffracted radiation. This detector motion was achieved by using a factor of two change in the last stages of the gear train.One 90 degree step at the input causes the detector assembly to move through twice the angle of the crystal panel motion. When properly synchronized, the Bragg condition is satisfied from one end of the spectrometer travel to the other.

2.3.2.1 Balance Weights

There is a requirement that SOLEX operation must not disturb the payload balance since any change in balance causes perturbations in the spacecraft solar pointing operation. Since the detector assembly is quite heavy (several pounds), its motion did disturb the system balance. The solution was to add balance weights to the SOLEX detector assembly so that it was balanced in all positions. A study of Drawings L-5809,

2-18

L-5811, and L-5814 will show that it was easy in concept, but very difficult in practice to find space for balance weights in locations where they would not interfere with the incoming beam. The addition of about 2 lb of brass weights did result in a balanced assembly. This local balance solution resulted in a total payload unbalance that could only be alleviated by the addition of ballast in the forward section.

2.3.2.2   Caging of SOLEX

One of the more vexing SOLEX design problems was the necessity to cage the system for resistance to vibration induced forces which would occur during launch. It could be established that since the crystal panel was of small mass and balanced it would survive vibration without undue strain. The detector assembly, on the other hand, was very heavy, and though balanced, was required by its function to be geometrically a very weak structural form.

The need for caging was met by designing a system using two semi-circular members to girdle the detector-balance weight assembly at the mid-point. In the caged position the ends of the semi-circles are drawn together as shown on Drawing L-5809. The girdle engages a circumferential slot in the balance weight and detector areas of the assembly. As a study of the drawing will show, the girdle members effectively restrain the detector assembly from movement in any direction. The ends of the girdle halves are held in the caged position by the forked end of the rod shown in Drawing L-5810. The rod is withdrawn on command by an Atlas Type IMT18CC pyrotechnic device. When the rod is withdrawn the springs visible in Drawing L-5809 open the girdle halves freeing the system for normal operations. The uncaging action is a one-shot event using the aforementioned pin-puller squib. Recaging requires the installation of a new squib.

2.3.3 SOLEX Crystal Panel

The crystal panel (Drawing L-5733) was designed as a one-piece stainless steel member which would allow mounting two pairs of 2 in x 4 in x 1/8 in crystals back-to-back. From geometrical considerations, the crystal panel should be as thin as possible. This crystal panel frame separates the back-to-back crystals by only 0.030 in. The crystals are held in place by bonding their rear surfaces to the panel and to the companion crystal. Care was required in the gluing process in order to avoid distorting the crystal surface. The crystals at final checkout were mounted in their frame with front surfaces flat within 1 to 2 arc minutes.

2.3.4 SOLEX Limits

With the crystal and detector assemblies coupled only electrically, synchronization of the system is required on occasion. This is accomplished in SOLEX by using 4 microswitches (one at each end of travel on both the crystal and detector assemblies). Synchronizing is easily accomplished by starting crystals and detectors towards one limit of travel and causing the control logic to hold one element at the limit until the second element also reaches that limit. A direction reversal at this time will start both elements moving together in a repeatable manner.

The switch activating arm for the crystal assembly is shown in Drawing L-5814, and for the detector assembly is illustrated in Drawing L-5811. The arms are pre-loaded spring beams. The pre-load ensures that the switch will be transferred with no arm deflection; this feature preserves the precision of the limit position (the switch opening and closure are very repeatable). The presence of the spring beam allows some

overtravel under an external force without destruction of the limit switch (switches of this type have an overtravel allowance of only 0.002 in). At the end of the moderate overtravel allowance both assemblies come up against firm mechanical limits. Once in orbital operation, the mechanical limits should never be reached.

2.3.5 Collimators

The most difficult mechanical development in the CRLS-229 payload was the design, fabrication, alignment and calibration of the 20 arc sec and 1 arc min collimators. Their design and construction is detailed by McKenzie, Howey and Young (1978). The functional design followed the procedure originated by McGrath (1968), but makes provision for grid nonuniformities and the inevitable small alignment errors or shifts. The mechanical design combines a firm and rigid mount with an intricate system of screws and levers that allow fine alignment adjustments to be made in a short period of time. When the alignment is complete the adjustment screws are bonded in place so that alignment is maintained over long periods of time and in severe environments. The assembly set-up is very similar to that described by Blake et al. (1976) and employs microscopes, a granite surface plate, and granite straight edges to align the grids visually.

The collimators were subjected to a comprehensive test program including visual inspection, performance tests using X-rays, checks with a ray-tracing computer program, and environmental tests to assure their proper performance in a space environment. Efficiency curves for each collimator determined using the computer program COLLIE are given in Figures 2.9-2.12. A summary of collimator properties is given in Table 2.1.
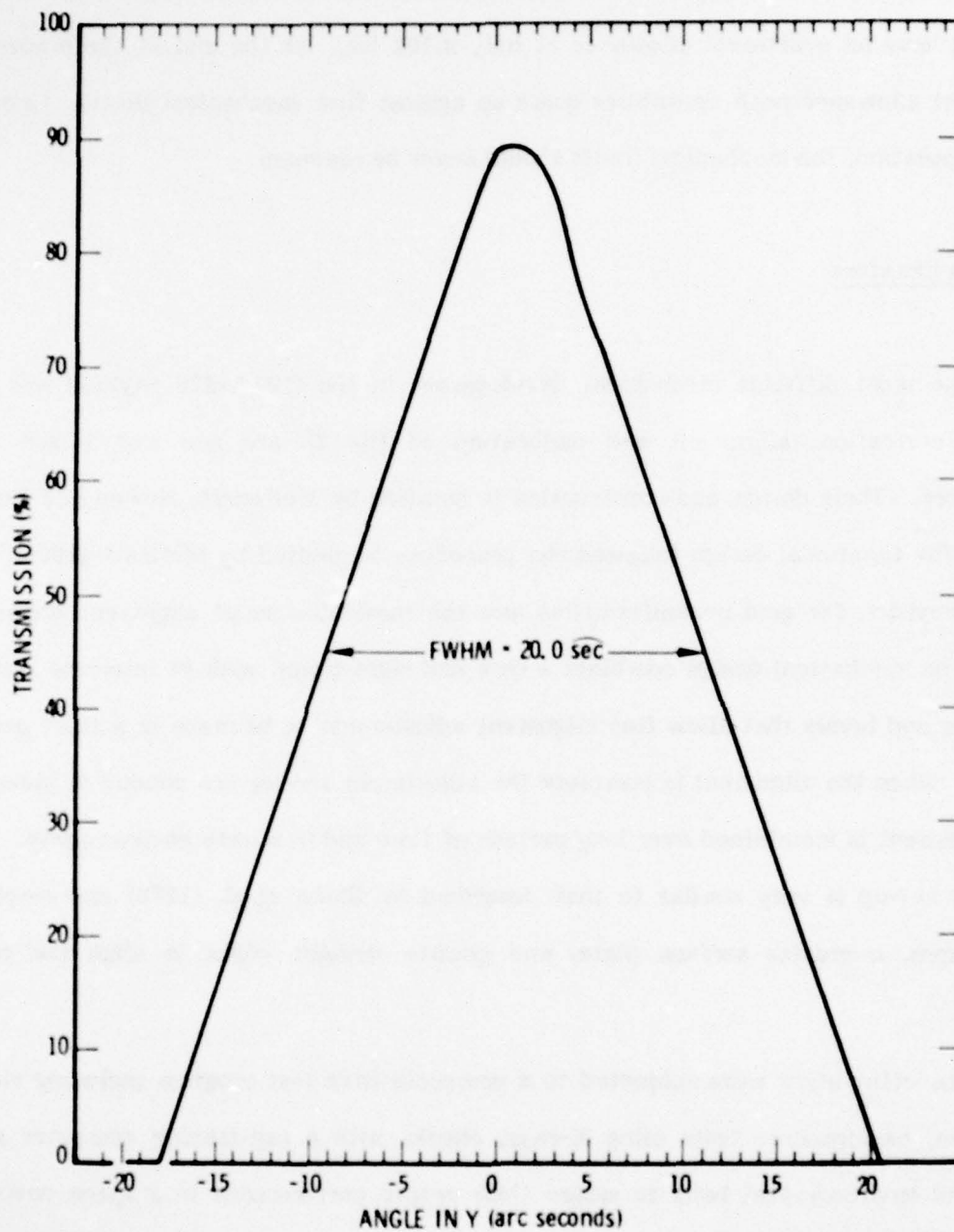
Figure 2.9.   CRLS-229 20 arc sec Collimator Efficiency
in the Vertical XY Plane.
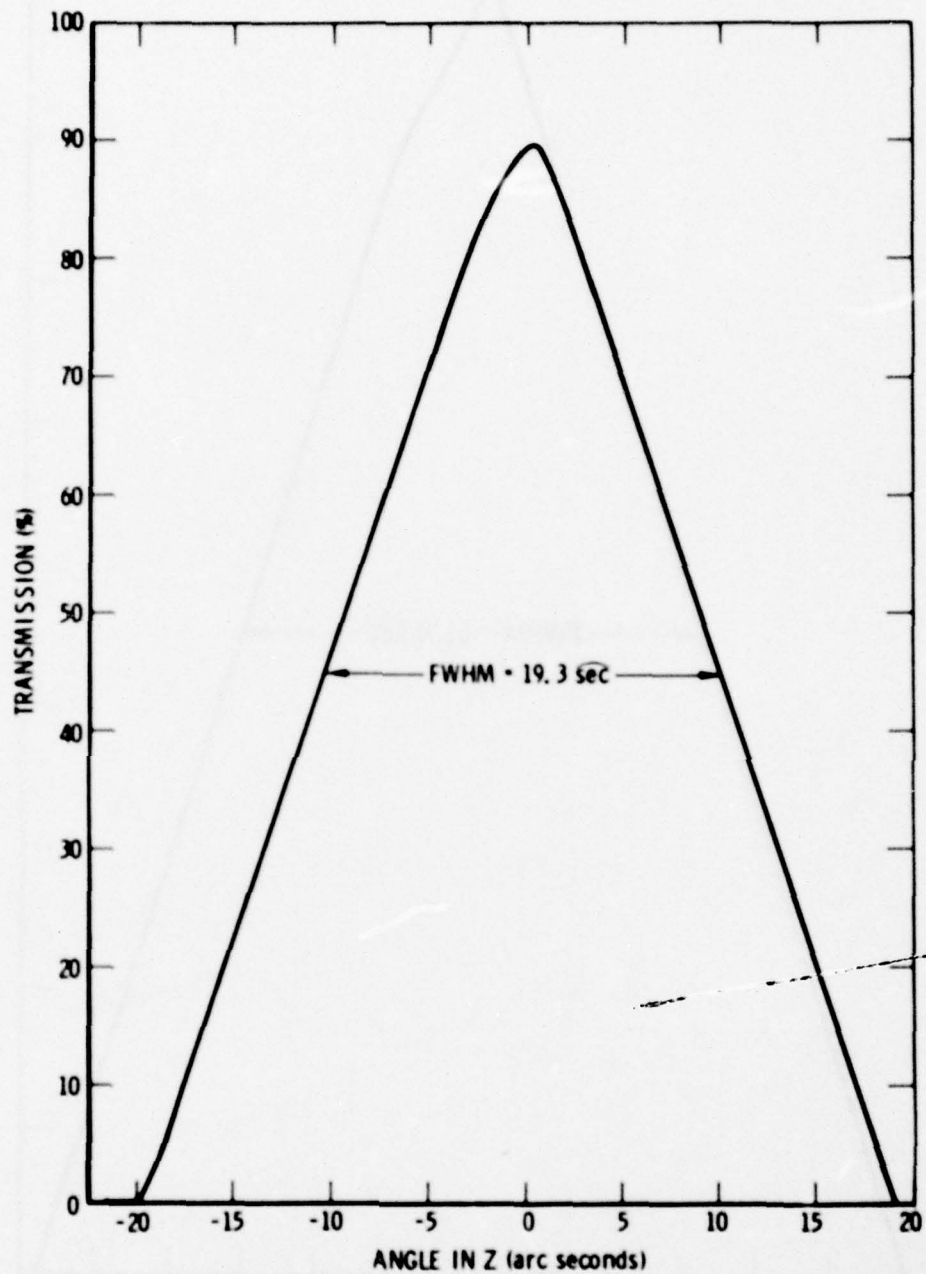
Figure 2.10. CRLS-229 20 arc sec Collimator Efficiency
in the Horizontal XZ Plane.

2-23
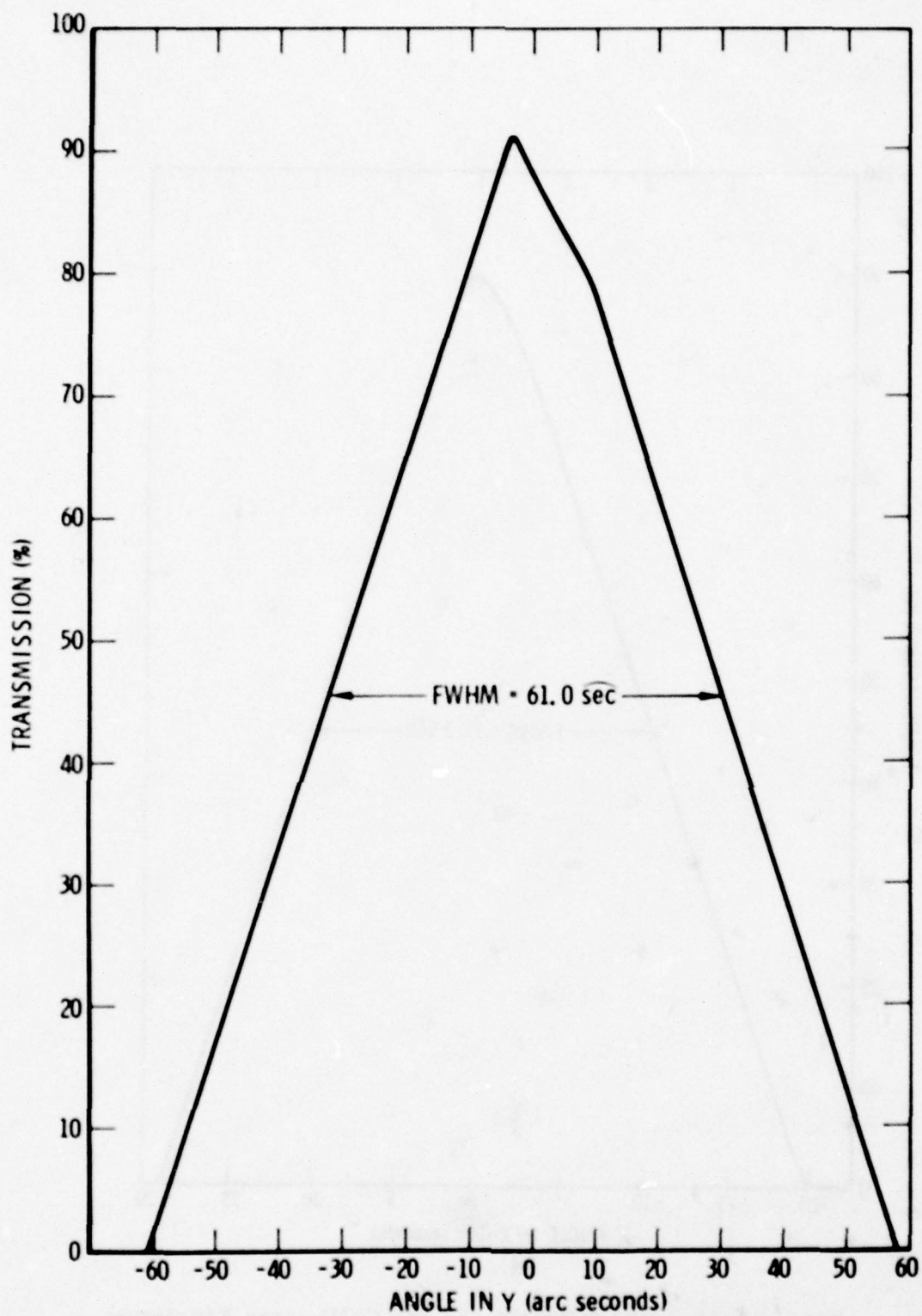
Figure 2.11. CRIS-229 1 arc min Collimator
Efficiency in the Vertical X Y Plane.

2-24
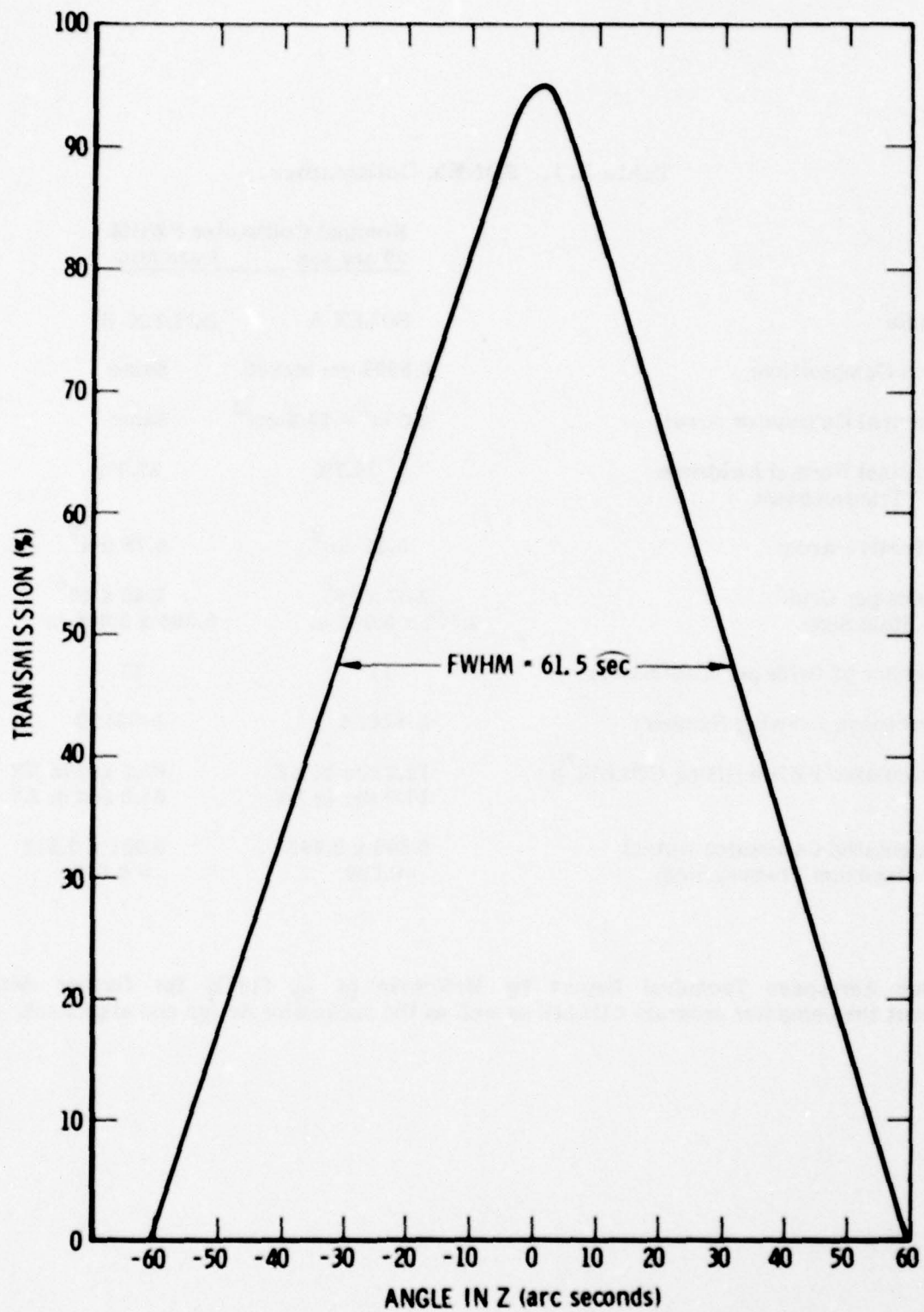
Figure 2.12.   CRLS-229 1 arc min Collimator Efficiency
in the Horizontal XZ Plane.

Table 2.1. SOLEX Collimators.

| | Nominal Collimator FWHM | |
	20 arc sec	1 arc min
Name	SOLEX A	SOLEX B
Grid Composition:	0.0023 cm nickel	Same
Nominal Collimator Area:	4.0 in^2 = 25.8 cm^2	Same
Nominal Normal Incidence Transmission:	23.7%	22.3%
Effective Area:	6.11 cm^2	5.76 cm^2
Holes per Grid: Hole Size:	2.37 x 10^5 0.002 x 0.002 in	2.48 x 10^4 0.006 x 0.006 in
Number of Grids per Collimator:	11	11
Aerospace Drawing Number:	L-5301A	L-5317B
Calculated FWHM (Using COLLIE[*]):	19.3 sec in XZ 20.0 sec in XY	61.5 sec in XZ 61.0 sec in XY
Calculated Collimator Actual Maximum Transmission:	0.896 x 0.893 =0.800	0.951 x 0.912 = 0.867

[*]See Aerospace Technical Report by McKenzie et al. (1978) for further details about the computer program COLLIE as well as the collimator design and alignment.

2.3.6 Alignment

The alignment of SOLEX is described in detail by Howey and McKenzie (1978). The 20 arc second and 1 arc minute collimators are coaligned to ± 7 arc sec. In the XY plane, the BBRC control eye is +14 arc sec clockwise from the mirror on the 20 arc sec SOLEX A collimator while looking towards the experiment. In the XZ plane, the BBRC control eye is +4 arc sec clockwise from the mirror on the 20 arc sec SOLEX collimator while looking towards the experiment. Refractosyn boresight sun detectors, manufactured by H. H. Controls under U. S. Patent 3,137,794, combine internal reflection in a triangular prism with balanced photodetectors, and are mounted on the collimators to indicate the location of the center of the solar disk. A solar calibration at Ball found that the relative alignment of the raster readout eye on NRL-401 (see Section 2.1) and the boresight Refractosyns on the 20 arc sec SOLEX collimator was about 90 arc sec in the XY plane and 20 arc sec in the XZ plane. The raster readout eye on NRL-401 is closely aligned to the control eye on CRLS-229, but it should be noted that the final coalignment of these two eyes had not been performed at the time of the sun test. The data above are illustrated in Figure 2.13. The SOLFLEX experiment is rotated counter-clockwise by 1 ± 1 arc min from the BBRC control eye as viewed from the +Y direction. More accurate alignment measurements will be performed after launch.

2.4 MONEX LEM

The MONEX Low Energy Monitor (LEM) package is described by Drawing L-5511. This module is a proportional counter system, described in Section 5 of this report, which is mounted in a forward location on the bottom panel of the chassis tube. There is a 0.25 inch diameter aperture in the front face. The detector itself is stopped down further by
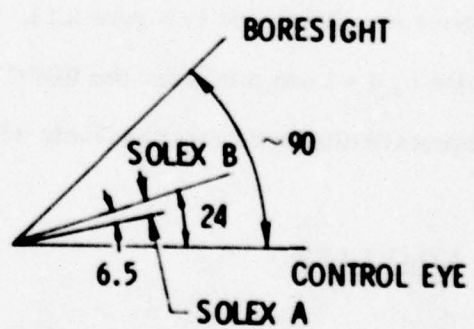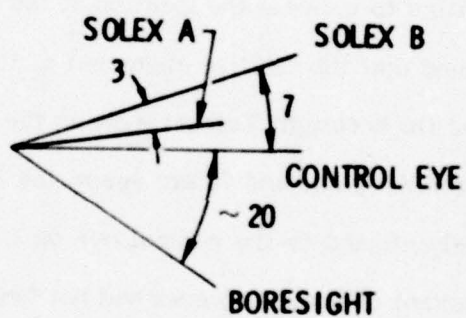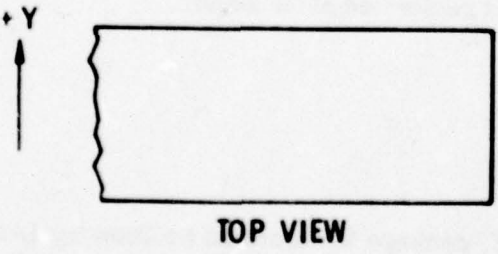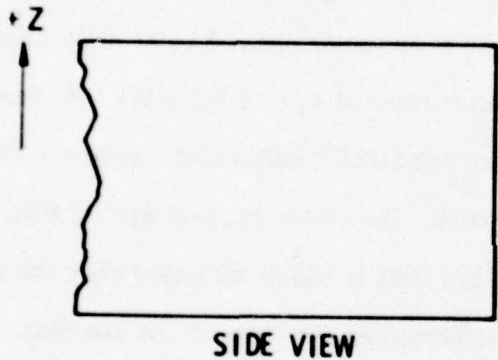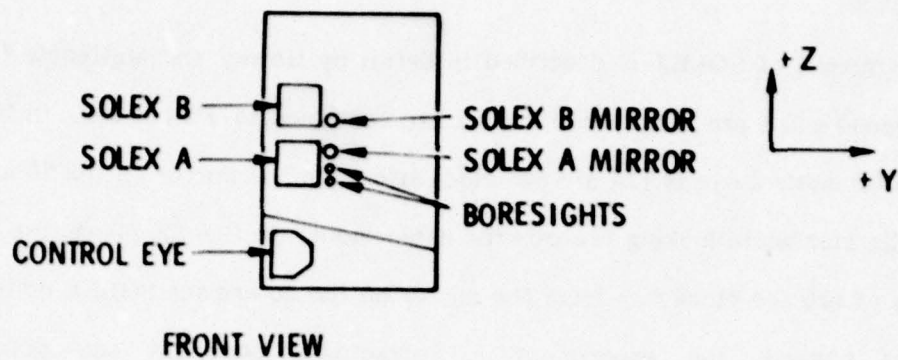
Figure 2.13. CRLS-229 Alignment Summary.

a 0.040 inch diameter aperture through which radiation reaches the detector window.

The LEM is a free standing 2.25 lb package which is complete in itself. It is connector coupled into the payload wiring harness. The LEM requires only coarsely regulated power from the payload bus and returns data to the payload command box. Other than having a chassis machined from a billet, in the interest of high strength and low weight, the LEM has no special mechanical features.

2.5   MONEX HEM

The MONEX High Energy Monitor (HEM) module is described by Drawing L-5565. This package is also a proportional counter system described in Section 6 of this report.

The package weighs 4.31 lb and is mounted to the main chassis cover. It also is connector coupled, free standing and complete in itself. The HEM uses a large 3.75 x 1.375 in. aperture. Radiation enters through a coarse "egg crate" collimator (18° from on-axis to cutoff). As with the LEM, the three HEM chassis elements are machined from a billet in order to meet weight and strength criteria. The major geometrical problem was to package the very large detector (2 x 2 x 6 in) in an envelope small enough to avoid occulting other apertures.

2.6   SOLFLEX

The SOLFLEX module is a 6.10 lb free standing package which, with its 5.40 lb electronics package, is mounted on the top side chassis panel. This instrument views the sun through a large aperture in the front panel. Other than the space it occupies it does not interact with SOLEX or MONEX. With the exception of the high voltage power

supplies, which were built by The Aerospace Corporation, the SOLFLEX module was supplied by NRL tested and ready for installation.

2.7   MAGMAP

MAGMAP is the second of two instrument modules supplied by NRL. This 3.43 lb package is mounted on the aft end of the payload, behind SOLEX. The aft location is dictated by the MAGMAP requirement to view the sun through the SOLEX one arc minute collimator (built by Aerospace). This is accomplished by so positioning the SOLEX crystal panel and detector assembly that the two MAGMAP apertures are illuminated by radiation passing through the SOLEX one arc minute collimator (see Section 2.3).

MAGMAP interacts electrically only with SOLFLEX. It was supplied by NRL checked out and ready for installation. Aerospace also built the high voltage power supply for this experiment.

3. SOLEX SOLAR X-RAY SPECTROMETERS

3.1 Scientific Objectives

The SOLEX part of the CRLS-229 experiment is used to obtain X-ray spectra from 3 to 25Å of the quiet and active solar corona as well as of flares. These data are required to determine the thermodynamic properties of different solar regions as well as for the determination of coronal abundances. In addition, SOLEX will provide daily maps of the solar disk in the emission lines of various coronal ion species. These maps provide information on the coronal temperature and density of the entire sun. Finally, the small raster capability of the P78-1 satellite allows SOLEX to map individual centers of activity to 20 arc sec resolution on a rapid time scale. This capacity presents an unprecedented opportunity to observe the events leading up to a solar flare with high spectral and spatial resolution. The ATM/Skylab photographs have shown that flares are centered in very small regions, so that high spatial resolution is essential. In addition, the development of active regions will be followed by periodic observations over long intervals.

3.2 Collimator Design and Test Results

The experimental objectives of the SOLEX and MAGMAP instruments demanded relatively small and lightweight collimators of 20 arc sec and 1 arc min (FWHM) fields of view. McKenzie et al. (1978) describe in detail the design, construction and testing of the multigrid collimators which meet this need. Figure 3.1 is a photograph of a completed unit.

Figure 3.2 illustrates a system for placing the grids to provide collimation free of leaks out to a maximum angle θ_M. The FWHM collimator resolution is W/L for square
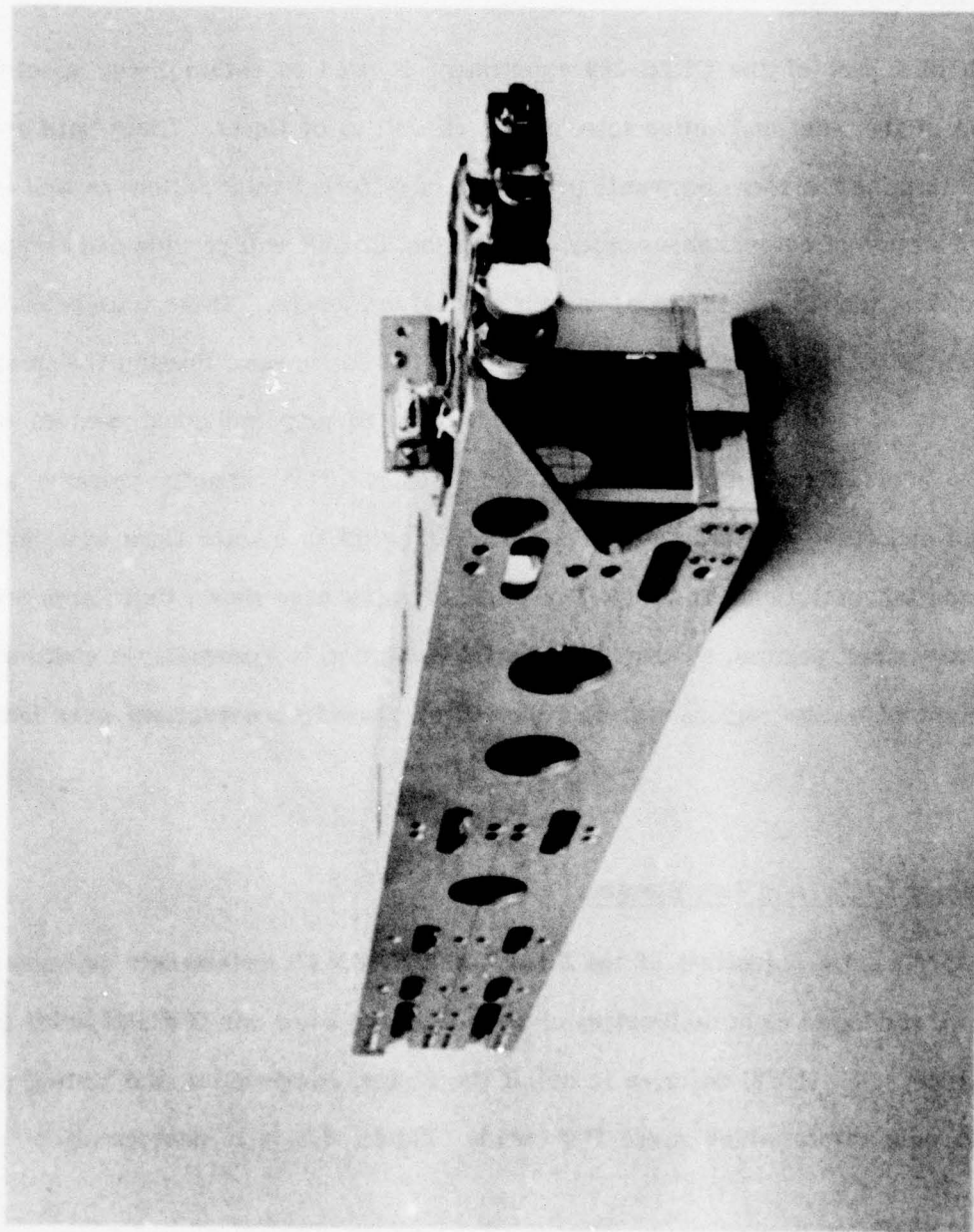
Figure 3.1. Flight Spare Collimator. This collimator has one arc minute resolution but is configured like the flight 20 arc second unit. On the front are the refrac- tosyns and alignment mirror.
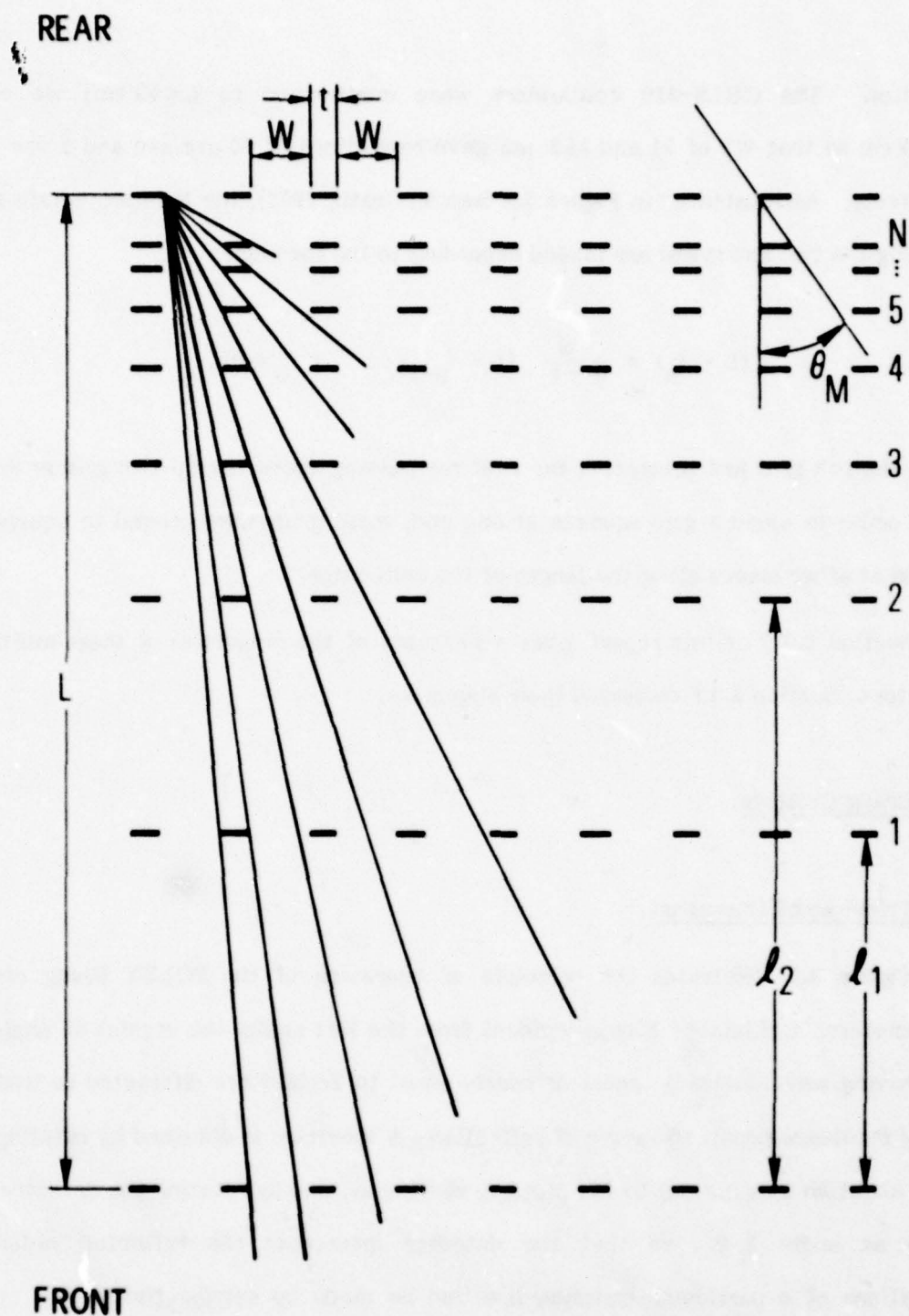
Figure 3.2. Optimum Procedure for Placing Collimator Grids. Each grid just blocks radiation passing through the grid below it.

grid holes. The CRLS-229 collimators were constrained to $L \leq 53$ cm; we chose L = 52.4 cm so that W's of 51 and 152 μm gave resolutions of 20 arc sec and 1 arc min, respectively. As illustrated in Figure 3.2 (see McGrath, 1968), the N intermediate grids (excluding the two end grids) are placed according to the formula,

$$(L - \ell_n) = \frac{W}{W + t} \ (L - \ell_{n-1}) \qquad (\ell_o = 0) ,$$

so that the nth grid just intercepts the first ray passing above the (n-1)th grid in Figure 3.2. In order to avoid a grid squeeze at one end, some grids were moved to equivalent positions at other places along the length of the collimator.

Section 2.3.5 of this report gives a summary of the properties of these multigrid collimators. Section 2.3.6 discussed their alignment.

3.3   Bragg Crystals

3.3.1   Principle of Operation

Figure 3.3 illustrates the principle of operation of the SOLEX Bragg crystal spectrometers. Collimated X-rays incident from the left strike the crystal at angle θ. Those having wavelengths λ equal or nearly equal to 2dsin θ are diffracted so that the angle of incidence equals the angle of reflection. A spectrum is obtained by rotating the crystal about an axis normal to the picture, varying θ, and by rotating the detector arm through an angle 2 θ, so that the detector intercepts the reflected radiation. Observations of a particular emission line can be made by setting the crystal at the appropriate angle to pick out the desired wavelength.

3-4

DETECTOR

DIFFRACTED BEAM
(n λ = 2 d sin θ)

2θ

θ

θ

CRYSTAL
(plane spacing = d,

INCOMING
X-RAY
BEAM
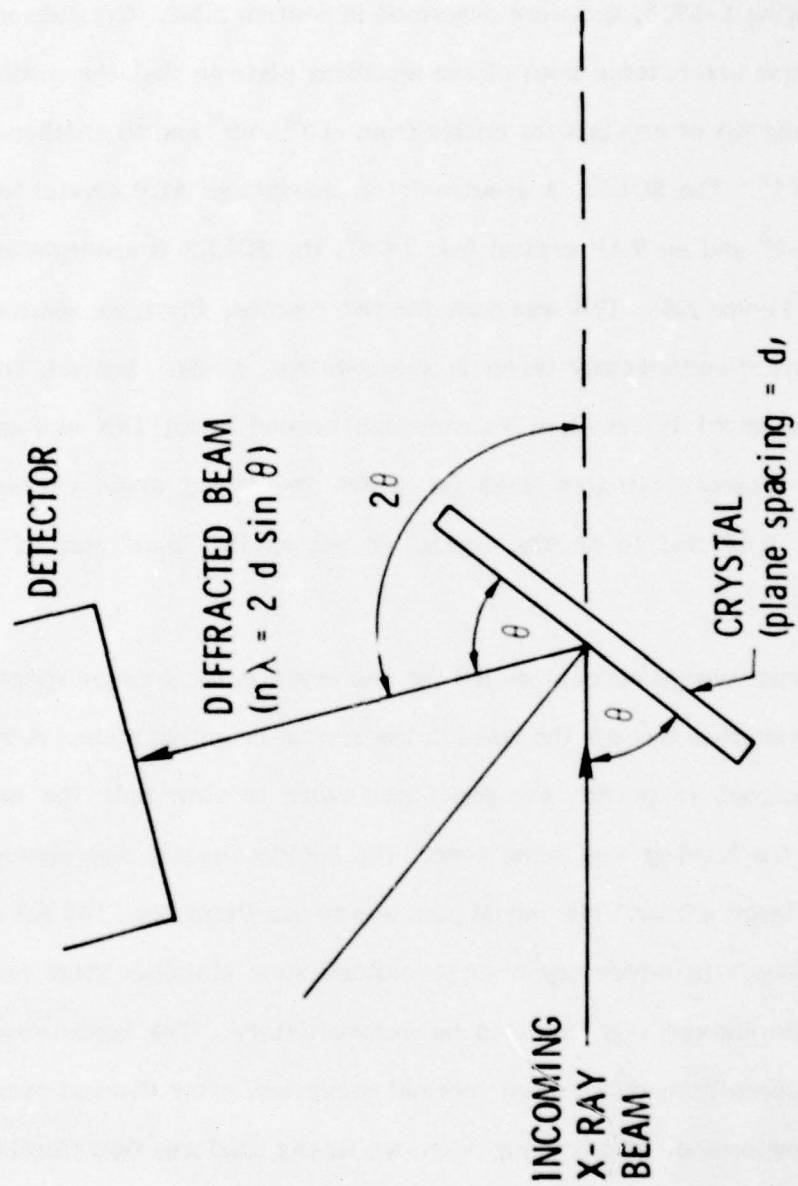
Figure 3.3. Principle of Operation of SOLEX and SOLFLEX
Crystal Spectrometers.

3.3.2 Crystal Mounts

The crystals for the two SOLEX spectrometers are mounted on the mounting plate shown in Drawing L-5733, and were described in Section 2.3.3. Crystals are mounted on both the obverse and reverse sides of the mounting plate so that the collimators present radiation to one set of crystals for angles from -60° to 0° and to another set for angles from 0° to -75°. The SOLEX A spectrometer presents an ADP crystal to the incoming beam for $\theta > 0^{\circ}$ and an RAP crystal for $\theta < 0^{\circ}$; the SOLEX B spectrometer is just the opposite (see Figure 2.6). This was done for two reasons. First, we wanted to have ADP and RAP scans simultaneously taken in the spectrum mode. Second, only the CEMA (SOLEX B detector) is sensitive to radiation beyond about 14Å and we wanted the capability to measure nitrogen lines for which the Bragg angle exceeds 60°. This dictated that RAP had to be the crystal in use on the "plus" side of the SOLEX B spectrometer.

The initial design concept called for the crystals for a single spectrometer to be bonded to one another through the holes in the crystal mounting plate. A crystal bonding stand was designed to permit the panel assembler to view both the top and bottom crystal while the bonding was being done. The bottom crystal was viewed through the stand using a large mirror. The initial plan was to use Delta Bond 152 KA as the bonding agent, but tests with laboratory crystals bonded to a stainless steel mock-up of the mounting plane showed this agent to be unsatisfactory. The bonds were found to be weakened, apparently by differential thermal expansion, after thermal cycles of the test pieces were performed. The bonding agent we finally used was Dow Corning No. 6-1104, a rubbery material that cures in a few hours at room temperature.

The SOLEX B crystals were bonded by the technique described above. While the bonding agent cured, the assembly was weighted down by a granite straight edge. Examining the glued panels with an autocollimator after the bonding agent had cured

revealed that each crystal had suffered some distortion. The RAP crystal had two zones with the dividing line between them going across the crystal about one-third of the distance from one end. The zones were separated in such a way as to cause the Bragg angle to differ between them by about two arc min. The ADP crystal zones were separated by a lengthwise line down the middle of the crystal. The Bragg angles for the two zones would differ by 1-2 arc min.

Since the first set of crystals suffered significant distortion in bonding we changed the technique for the second set (SOLEX A). The RAP was bonded directly to the mounting plate and pressed down with a plastic "dummy crystal", the same size as the crystal itself. This pressing introduced distortion, so about 45 minutes later the crystal was pulled loose from the plate, it and the plate were cleaned, and the crystal was reglued. The bond was allowed to cure under the weight of the crystal only, and this introduced no significant increase in distortion. The Bragg angle was estimated to change by only 40 arc sec over the crystal surface. The final ADP crystal was then bonded using this same technique. The crystal chosen was zoned with the dividing line running across the crystal about 40 percent of the distance from one end with an angular spread of about 1 arc min. The gluing process did not change this significantly.

3.3.3 Crystals

The SOLEX spectrometers consist of pairs of crystals mounted side-by-side on a common plate behind collimators, providing 20 arc sec and one arc min resolution, respectively. A crystal pair is comprised of one ADP (ammonium dihydrogen phosphate, $2d = 10.64\text{Å}$) and one RAP (rubidium acid phthalate, $2d = 26.12\text{Å}$) crystal. So that observations can be made with each crystal having 20 arc sec and one arc min spatial resolution, an ADP crystal is mounted in back of the RAP crystal and vice versa. A

summary of SOLEX crystal properties is given in Table 3.1.

Let $R(\theta, \lambda)$ be the coefficient of reflection of X-rays at wavelength λ incident on the crystal at angle θ. The crystal integrated reflectivity is defined as

$$R_c(\lambda) = \int R(\theta, \lambda)\, d\theta \ \text{radians}.$$

The number of diffracted photons is then given by

$$I_D(\lambda) = \frac{R_c(\lambda)}{\omega}\, I_o(\lambda)$$

where $I_o(\lambda)$ is the incident flux in photons sec^{-1} and ω is the crystal rotation rate in radians sec^{-1}. On the crystal integrated reflectivity curve, shown in Figure 3.4, the dots and crosses are experimental points for the two flight CRLS-229 ADP and RAP crystals, respectively. The error bars show the range of values measured at each wavelength for each crystal. The solid lines are the unpublished Darwin-Prins curves calculated by Burek (1977) over the wavelength ranges of the two SOLEX spectrometers. The theoretical curve for RAP has been normalized by dividing by the factor 1.32 for values below 20.91Å to better fit the experimental Aerospace data. Points at 20.91, 23.62 and 24.78Å are from Burek's latest unpublished 1977 calculations. Note there is an overlap in crystal wavelength ranges between 7.63 and 10.27Å.

Peak reflectivities for ADP and RAP shown in Figures 3.5 and 3.6 were determined assuming a Lorentzian rocking curve. For this case, it can be shown that

$$\bar{R}_p = \frac{2 \bar{R}_c}{\pi\, \Gamma}$$

where $\bar{R}_p$ is the crystal peak reflectivity, R_c is the crystal integrated reflectivity, and Γ is the crystal FWHM rocking curve width for monochromatic and perfectly collimated

3-8

Table 3.1. SOLEX Crystals.

Dimensions of Each Crystal: 2.00 in x 4.00 in x 0.125 in

Crystal Type:	ADP (101)	RAP (001)
Crystal 2d Spacing:	10.64Å	26.12Å ± 0.01Å

Flight Crystals Serial Numbers	20 arc sec	1 arc min
Reference Zero Side ($\theta_B < 0°$)	R5-B[&]	A2-B
Maximum Angle Side ($\theta_B > 0°$)	A3-F	R7-F

Crystal[&]	(Å)	Measured FWHM (sec)[•]	$R_c(\lambda)$(radians)[@] Mosaic[+]	$R_c(\lambda)$(radians)[@] Ideal[x]
A2-B	8.34	32 (110)[#]		6.6×10^{-5}
	6.07	15		4.5×10^{-5}
	2.75	6.6		3.3×10^{-5}
A3-F	8.34	38 (110)		6.1×10^{-5}
	6.07	21		4.4×10^{-5}
	2.75	13		3.7×10^{-5}
R5-B	9.89	50	1.0×10^{-4}	
	13.34	89 (340)	8.4×10^{-5}	
	17.56	184	9.1×10^{-5}	
	8.34	(40)		
R7-F	9.89	47	1.0×10^{-4}	
	13.34	90 (380)	9.5×10^{-5}	
	17.56	176	7.4×10^{-5}	
	8.34	(50)		

[&] R for RAP (A for ADP), 5 is the 5th crystal tested, B stands for back in the original nomenclature (and now the crystal front surface).

[•] Listed deconvoluted value is half the former measured rocking curve width.

$$^+R_c(\lambda) = R_{uncorrected}(\lambda) \frac{(1 + \cos^2 2\theta)^2}{2(1 + \cos^4 2\theta)}$$

$$^xR_c(\lambda) = R_{uncorrected}(\lambda) \frac{(1 + |\cos 2\theta|)^2}{2(1 + \cos^2 2\theta)}$$

[#] Experimentally measured system values in arc seconds in parenthesis (corrected for divergence through the collimators and line profiles).

[@] Best estimate of inflight values (experimentally measured with theoretical corrections).
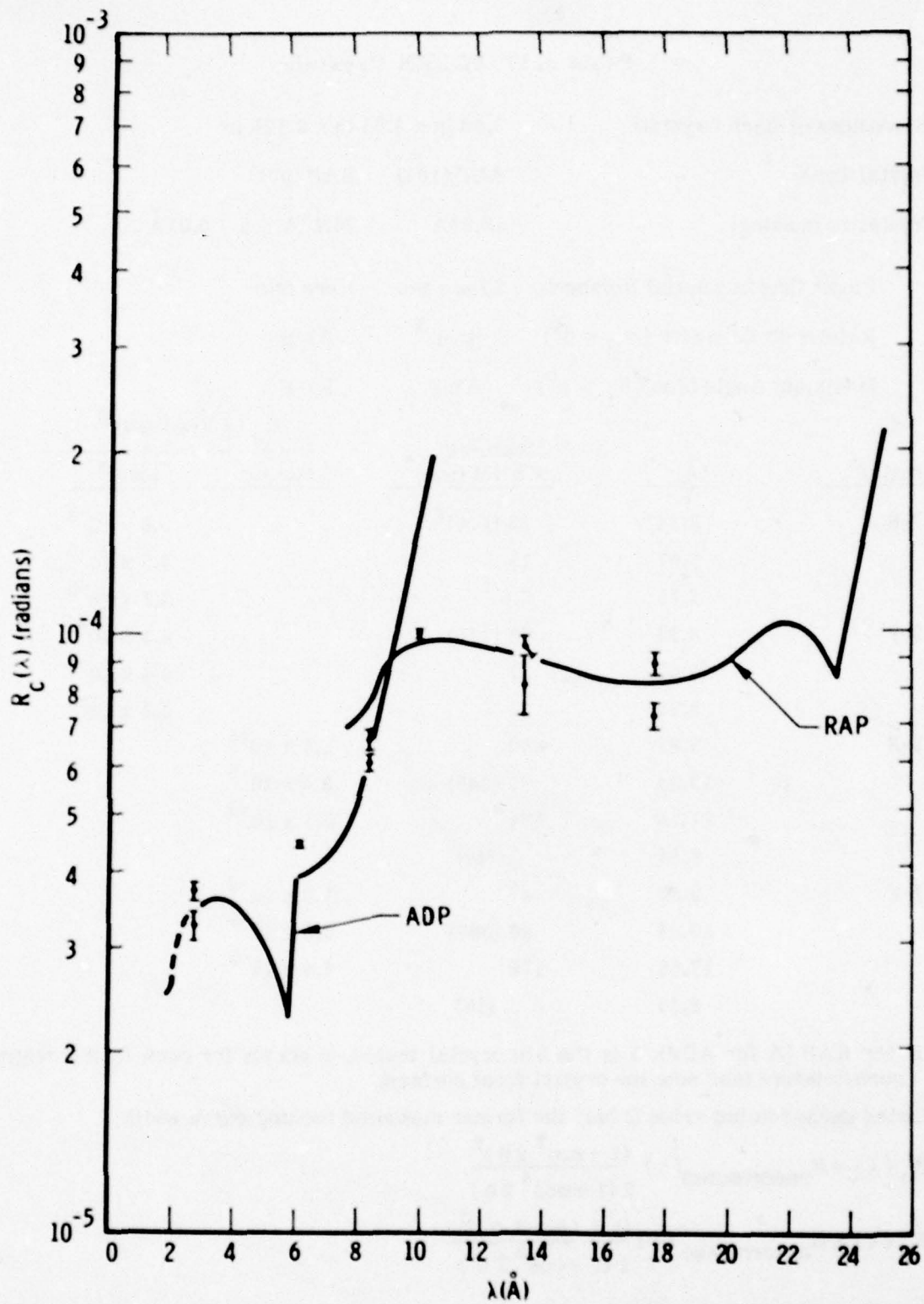
Figure 3.4.   CRLS-229 Crystal Integrated Reflectivity as a
Function of Wavelength.
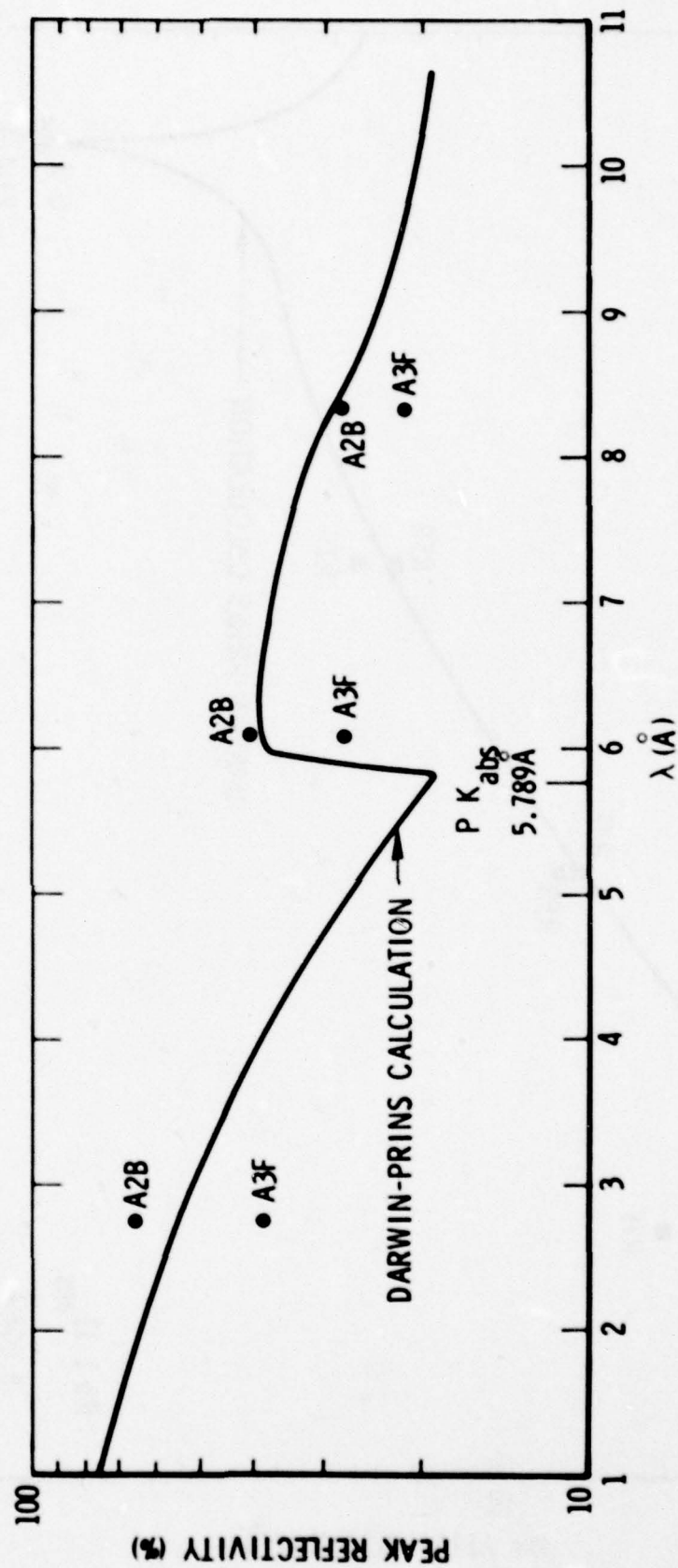
Figure 3.5. ADP Peak Reflectivity as a Function of Wavelength.
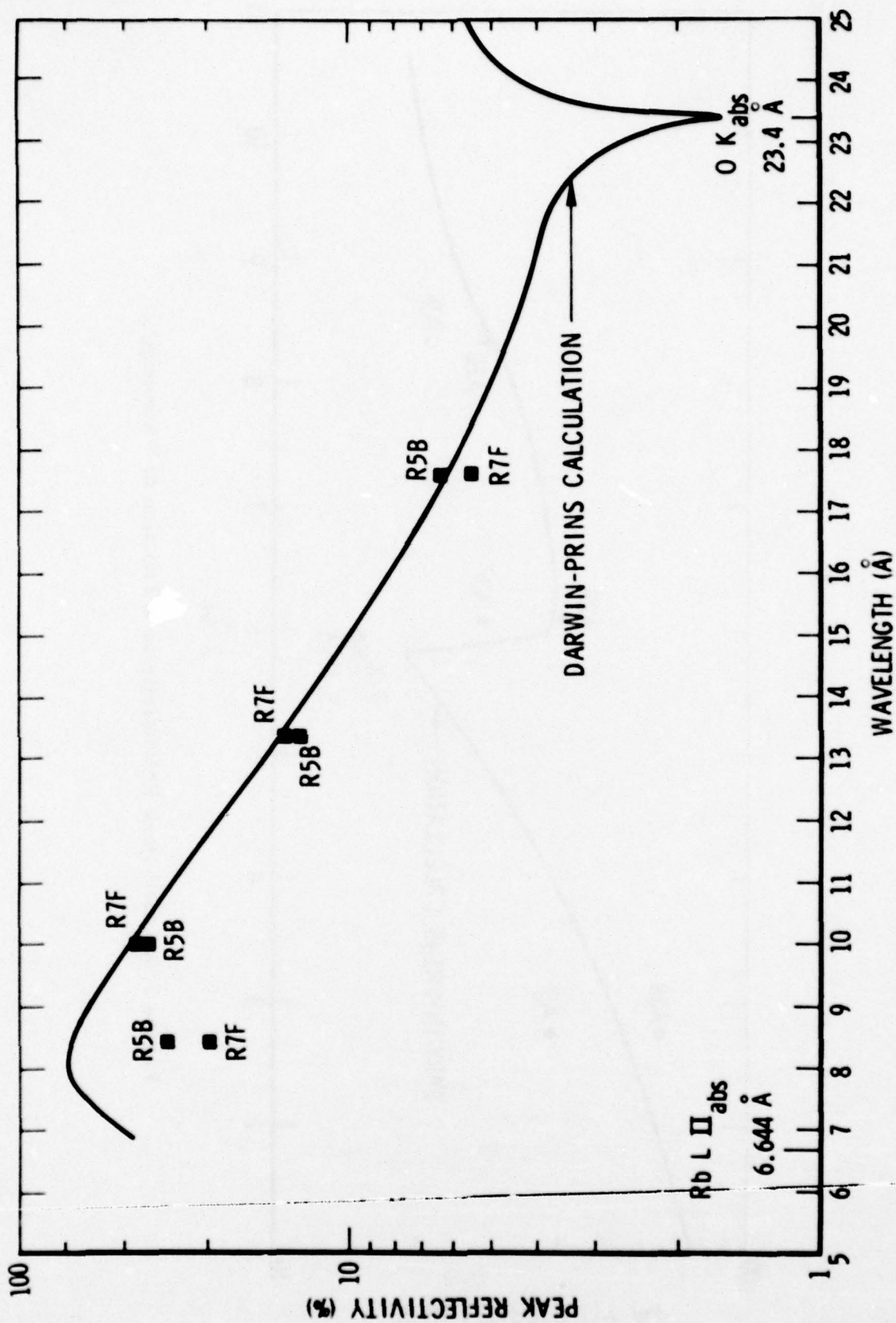
Figure 3.6. RAP Reflectivity as a Function of Wavelength.

incident radiation. Corrections for Al K α_1 and K α_2 were performed using a computer program (LOREN2). In Table 3.1, A2B stands for the side B of ADP crystal #2. Larger values of Γ (and hence smaller values of R_p) could be inferred from the single crystal spectrometer system tests. However, a subsequent study by Eng (1978) showed that the flight crystals almost certainly had not degraded. The most reasonable assumption is therefore that the values derived from the double crystal measurements are correct. Preliminary analysis of post-launch data corroborates this assumption. Therefore these are plotted in these figures. Theoretical peak reflectivity curves by Burek (1977, 1978) derived using Darwin-Prins theory have been included. These calculated values are in excellent agreement with the measurements at Aerospace.

Dispersion produces small changes in the effective crystal 2d spacing (Burek, 1977). The effect of the Kallman-Mark theory of dispersion in the case of RAP is to vary the apparent 2d spacing in the range 26.115-26.127Å for wavelengths between 1 and 26Å; this is shown in Figure 3.7. In the SOLEX wavelength range, it is greater than 26.120 only above 20Å near the O K$_{abs}$ edge. The two error bars correspond to an estimated ± 5% uncertainty in the index of refraction theoretical corrections calculated by Burek (1977, 1978). Similar calculations of dispersion effects in ADP yielded apparent 2d spacing changes of at most 0.0001Å in the wavelength range 1-10Å.

3.4   Crystal and Detector Drives

In order to obtain proper Bragg motion, the crystals rotate through the range θ = -60 degrees to +75 degrees while the detector rotates through twice the angle of the crystal as described in Sections 2.3.1 to 2.3.4.

Detailed calibration information about these drives is given in Table 3.2 and Figure 3.8. The correspondence between crystal step number (from Reference Zero position) and wavelength is given in Table 3.3.
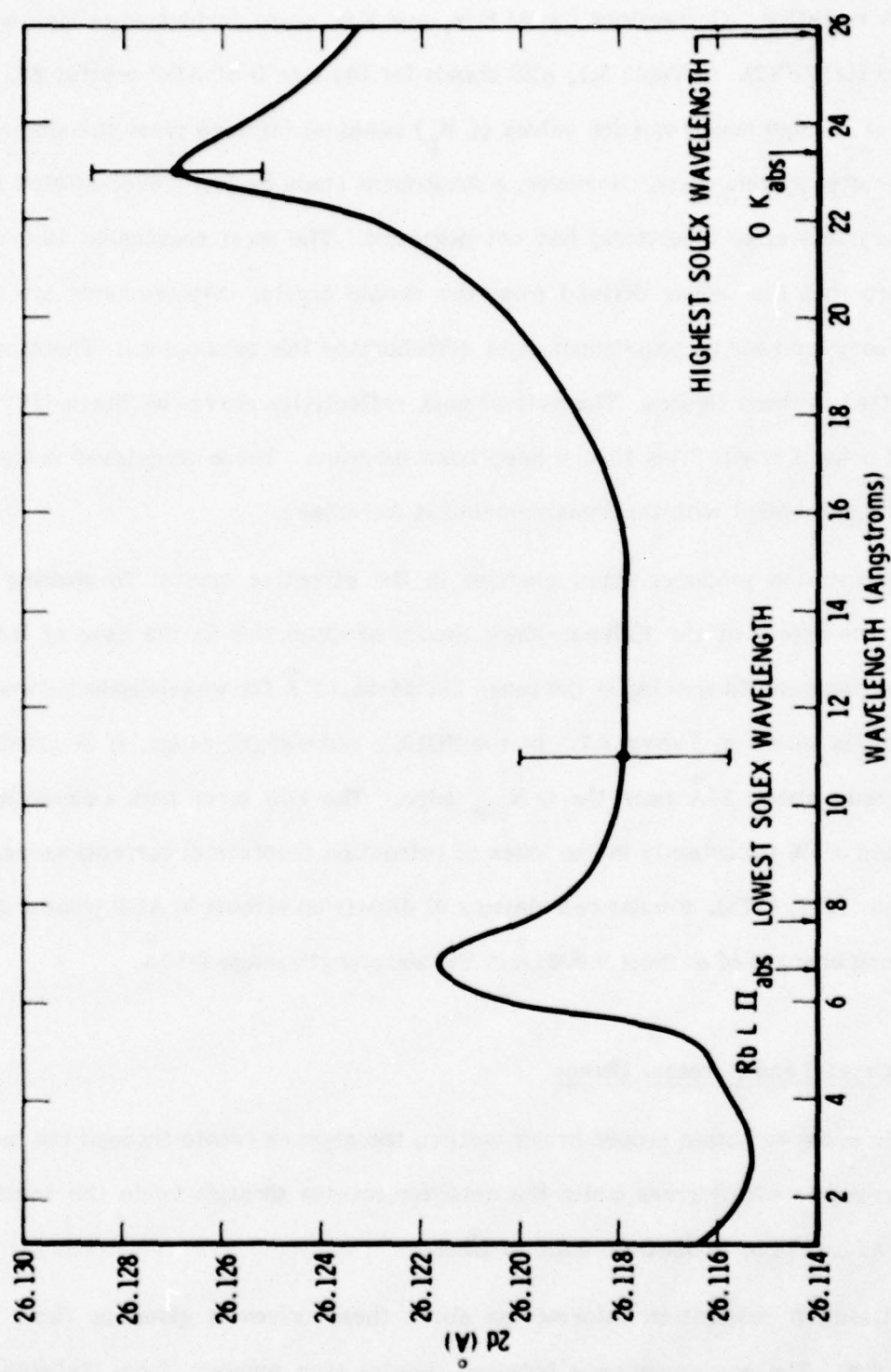
Figure 3.7. Theoretical Calculation of the RAP 2d Spacing as a Function of Wavelength.

Table 3.2. SOLEX Crystal Drive.

Step Size: $\theta_1 = 0.008393185$ degrees $= 30.21547$ arc sec

Angular Range: ≈ 16055 steps $= 134.75$ degrees

Time for Full Scan: 4.3 min to go 16055 steps at 32 msec per step

Potentiometer No. 1 Voltage: $0.97 + (0.0001763)$ (No. steps from Ref. Zero)

Repeatability of Microswitches: 1 step

Gear Backlash: 20 arc sec

The number of steps to a line is given by $n = \dfrac{\theta_B - \theta_{RZ} + \Delta}{\theta_1}$

where θ_B is the Bragg angle ($\lambda = 2d \sin \theta_B$) in the range $-60.015°$ to $+74.879°$

θ_{RZ} is the Reference Zero angle:

PC	RAP	$-59.956°$
	ADP	$-60.016°$
CEMA	RAP	$-60.050°$
	ADP	$-60.015°$

Δ is the angle correction given in Figure 3.6.2 (in degrees)

θ_1 is the crystal single step angular size given above (in degrees)

λ is the wavelength of the line (in Angstroms)

2d is twice the crystal lattice spacing (10.648Å for ADP and 26.121Å for RAP).

Scan Rate: 4.5778×10^{-3} rad sec^{-1} at 31.25 steps sec^{-1}

9.1555×10^{-3} rad sec^{-1} at 62.50 steps sec^{-1}

Table 3.3. SOLEX Key Angles and Wavelengths.

		ADP			RAP	
	Step Number	Bragg Angle (deg)	Wavelength (Å)	Detector	Bragg Angle (deg)	Wavelength (Å)	Detector
Reference Zero	0	60.015	9.22	CEMA	59.956	22.61	PC
Lower Limit Auto Shutoff	5120	17.042	3.12	CEMA	16.983	7.63	PC
MAGMAP†	7168	≤ 0.2	—	—	≤ 0.2	—	—
Upper Limit Auto Shutoff	9216	17.336	3.17	PC	17.301	7.77	CEMA
Max Excursion from Ref. Zero*	16055*	74.737	10.27	PC	74.703	25.19	CEMA
Energy Range (keV)		1.21 - 3.97 (ADP)			0.49 - 1.63 (RAP)		

† In the MAGMAP position, SOLEX POT 1 = 2.2 V and SOLEX POT 2 = 4.5 V.

* Do not command to a step number greater than 16040 ($3EA8_{16}$).
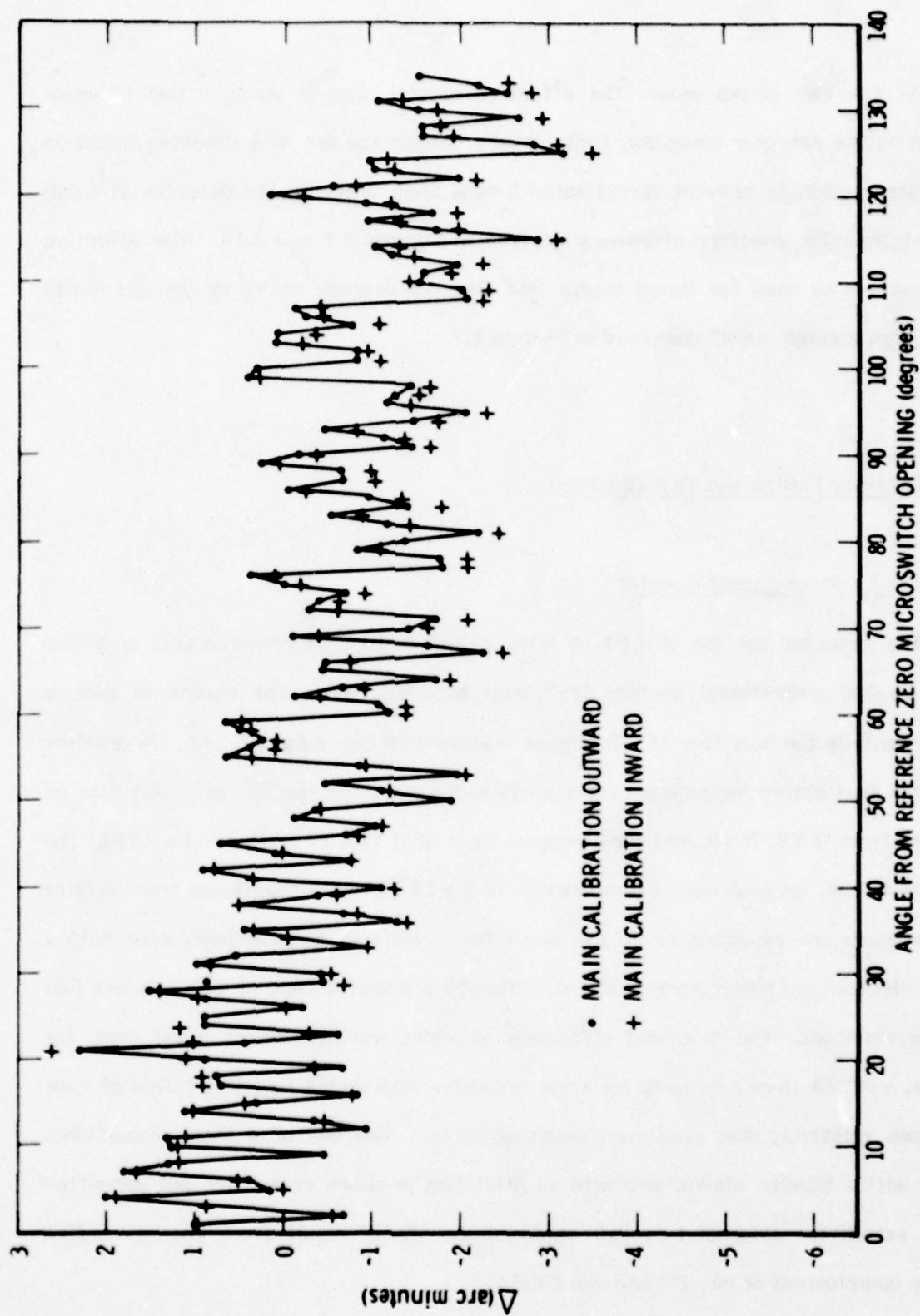
Figure 3.8. SOLEX Crystal Drive Calibration Curve.

3-17

As the two drives move, the effective crystal area is changed due to beam blocking by the detector assembly, finite crystal length and use of a detector shield on the crystal panels to prevent direct solar X-rays from entering the detector at small Bragg angles. The aperture efficiency is given in Figures 3.9 and 3.10. The effective area is shown as zero for Bragg angles less than 17 degrees owing to the automatic angular high voltage cutoff discussed in Section 4.7.

3.5   Detector Design and Test Results

3.5.1   SOLEX Proportional Counter

The detector for the SOLEX A (also called SOLEX 1) spectrometer is a thin window sealed proportional counter (PC) built by LND, Inc. The choice of such a detector entails the sacrifice of all data at wavelengths beyond about 14Å. In practice this means that active region observations will lack 20 arc sec spatial resolution data on emissions from O VII, N VII, and the strongest lines of O VIII, Fe XVII, and Fe XVIII. The O VII line intensities peak near a temperature of 2×10^6K. Solar line fluxes from outside active regions are expected to be too weak for significant observations, even with a channel electron multiplier array (CEMA), with a 20 arc second field of view. It was felt that the reliability and enhanced efficiency at short wavelengths of a PC over, for example, a CEMA were necessary for a spectrometer with such a restricted field of view and hence relatively low predicted counting rates. The use of a flow proportional counter with a thinner window and with an attendant pressure vessel was not permitted on this satellite. Enhanced overall performance should result from the diversified detector complement of one PC and one CEMA.
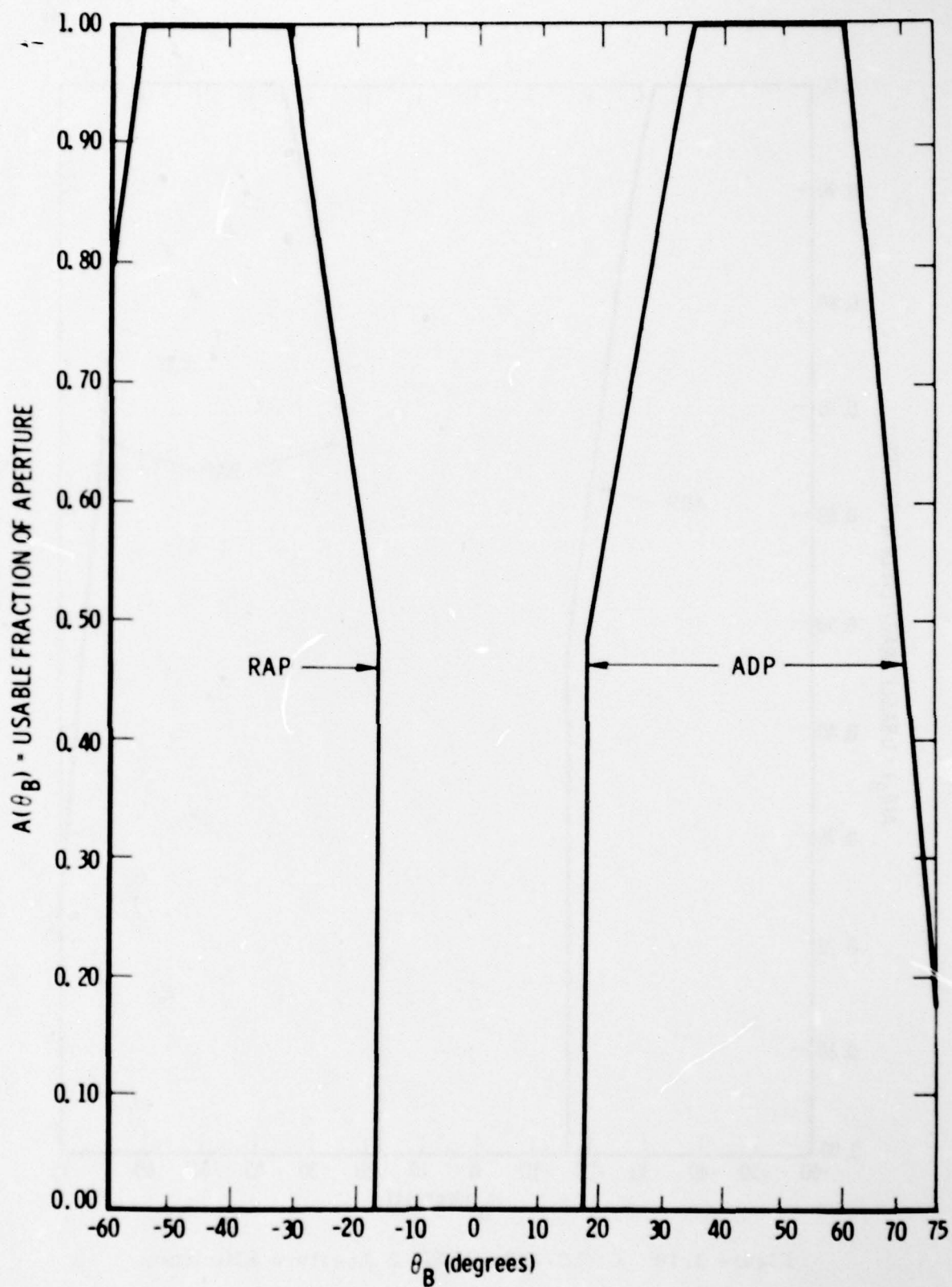
Figure 3.9   CRLS-229 SOLEX A Aperture Efficiency as a Function
of Bragg Angle.
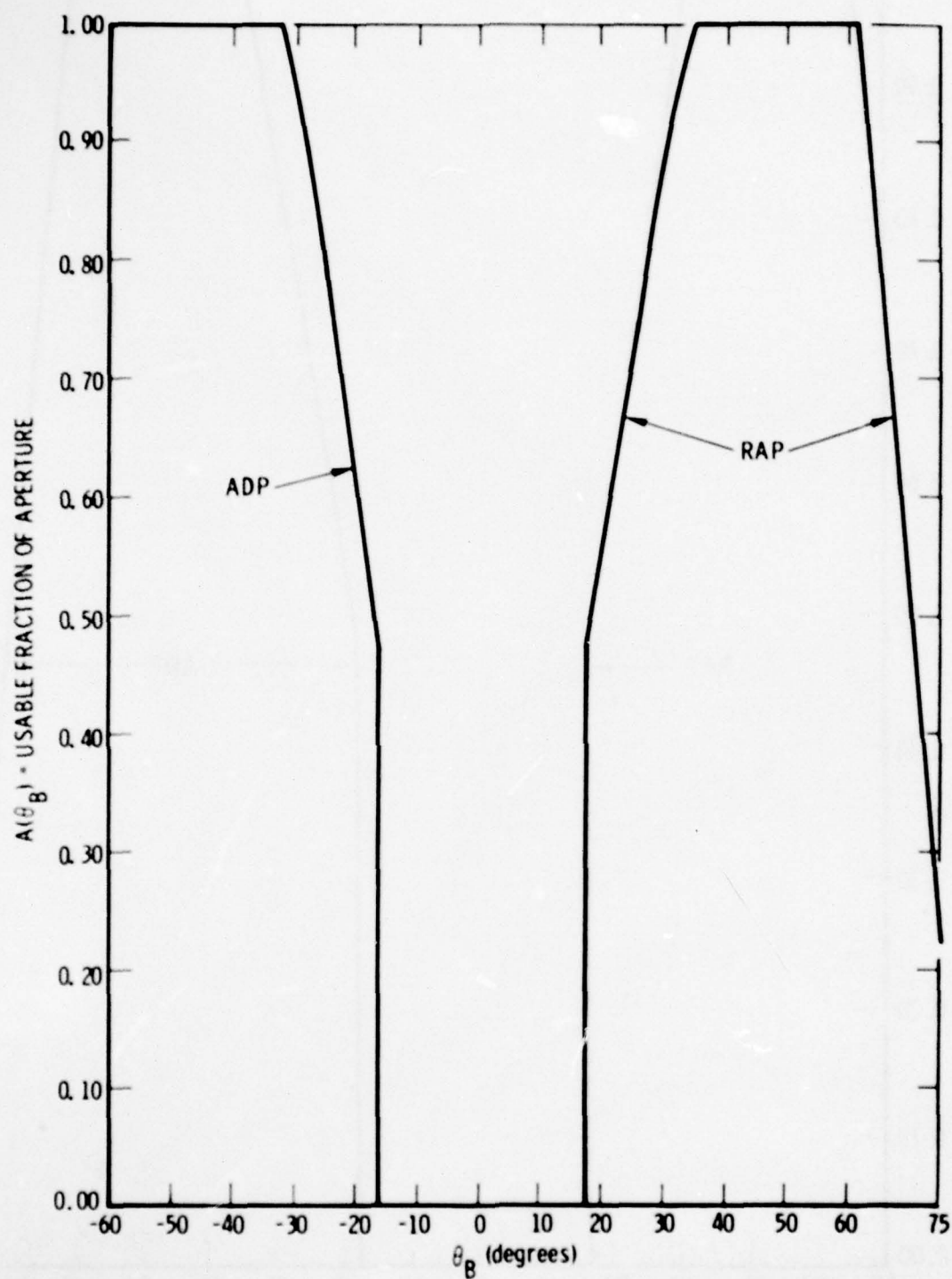
Figure 3.10.   CRLS-229 SOLEX B Aperture Efficiency.

The SOLEX A proportional counter (as well as the SOLEX B CEMA) is shown in Drawing L-5811. The high voltage feed-through for the three anodes in the PC detector volume can be seen in this drawing as well as in Figure 3.11. Flanking the center anode on each side are three grounded cathode wires. These serve to divide the PC into three separate detectors. The anodes are, however, connected together so that one set of front-end electronics processes all PC signals. Because the three detectors in the case are not geometrically identical, degraded energy resolution is a consequence of the anode interconnection. Since the Bragg crystals provide very good spectral resolution, the small degradation in counter resolution is not important. The nominal detector window is 4.7×10^{-3} gm^{-2} cm^2 of beryllium and the nominal gas fill is 1.2 atmospheres of 90 percent argon and 10 percent carbon dioxide. The gas maintains an outward pressure on the window at all times, barring exposure to very low temperature and abnormally high pressure ambient atmospheric conditions, thus avoiding potentially destructive "oil-canning".

The efficiency of the SOLEX PC was calibrated by comparison with a standard detector. Four detectors were available from which to choose. As a preliminary survey, window thicknesses were determined for two of the window panels in each counter. Al K and Mg K X-rays were used for this measurement; the expected gas efficiencies for these X-rays are 0.99 and 1.00, respectively. The gas density was then determined from measurements of Fe^{55} (Mn K) X-rays, using the window thickness determination results. For two counters having thin windows and about the right gas density, surveys of window thickness over eight additional panels were made with Al K radiation only. The counter chosen for flight was found to have a window thickness of $(5.3 \pm 0.6) \times 10^{-3} gm\ cm^{-2}$ of beryllium, where the quoted error is the standard deviation of ten measurements. The gas pressure was measured to be 1.11 atmospheres. Various PC parameters are

3-21
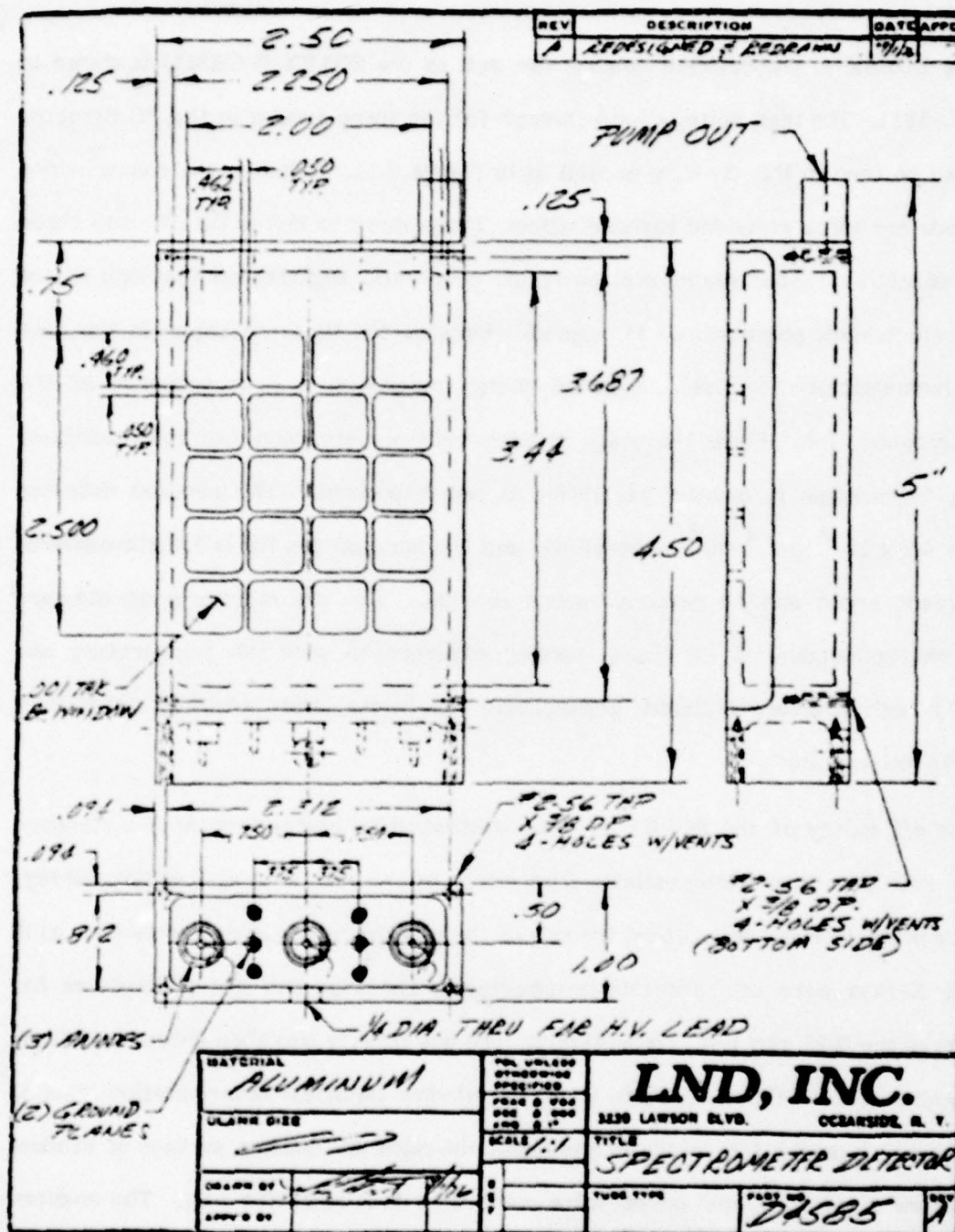
Figure 3.11. SOLEX A Proportional Counter Detector Drawing.

summarized in Table 3.4. Results of an efficiency calculation are also given in this table and plotted in Figure 3.12.

Cosmic rays are expected to dominate the SOLEX A PC background on orbit. About 40 cosmic ray events per second will occur in the detector. For a relativistic proton normally incident on either of the large-area sides of the detector, the energy loss will be about 8 keV in the detector gas. This is above the nominal upper level discriminator setting of 6.6 ± 0.5 keV, so most events will be rejected because of pulse height. Taking a conservative estimate of 20 events per second with acceptable pulse height and risetime rejections (see Sections 3.7.2 and 3.7.3) of 50 to 75 percent we arrive at a conservative background counting rate estimate of 5-10 $\sec^{-1}$. At high latitudes where lower energy cosmic rays can penetrate the Earth's magnetic field, the background could be three times as high as this estimate.

3.5.2 SOLEX Channel Electron Multiplier Array

The Channel Electron Multiplier Array (CEMA) detector is used in SOLEX B in conjunction with the 1 arc min collimator. The sensitive 2.7 in by 2.3 in area of the detector consists of approximately 1.4×10^6 individual channels in which X-rays are detected and an electrical signal generated. A photograph of the flight detector assembly is given in Figure 3.13. Detailed information about this detector is given in Table 3.5. The "cathode" has been coated with magnesium fluoride to increase the quantum efficiency. Measurements of the efficiency of the flight CEMA detector (attached to the flight filters described in the next section) were performed using collimated monochromatic X-ray beams and a flow proportional counter monitor of known efficiency. Efficiency measurements over a wider wavelength range were

Table 3.4.   SOLEX Proportional Counter.

Detector Dimensions:	1.00 in x 2.50 in x 4.50 in
Cathode Material:	aluminum
Window Thickness:	0.0011 in = 0.0052 gm cm^{-2} ± 10%
Window Material:	beryllium
Unobstructed Window Area:	20 x 0.460 x 0.462 = 4.25 in^2 = 27.4 cm^2
Gas Thickness:	0.75 in = 1.90 cm
Gas Mixture:	90.0% Argon, 10.0% CO_2
Gas Total Pressure:	1.20 atmospheres = 921 Torr
Collimation:	1 arc min FWHM
Counter Serial Number:	63534
Time Resolution:	Main SOLEX Data = 32.0 msec Rise time rejects = 1.024 sec
Efficiency Calculation:	Cross sections from Henke and Tester (1975) and Storm and Israel (1970)

SAMPLE CALCULATED EFFICIENCY

(Å)	E (keV)	Efficiency
1.24	10.000	0.1905
1.55	8.000	0.3270
2.07	6.000	0.5810
2.28	5.445	0.6892
2.43	5.102	0.7420
2.48	5.000	0.7519
2.59	4.782	0.7835
3.10	4.000	0.8898
3.87-	3.203+	0.9139
3.87+	3.203-	0.3849
4.13	3.000	0.4290
6.20	2.000	0.5877
7.95	1.560	0.4383
8.27	1.500	0.3931
10.85	1.143	0.1265
12.40	1.000	0.0461
13.34	0.930	0.0213
14.56	0.852	0.00688
15.97	0.776	0.00142
17.59	0.705	0.00017
18.32	0.677	0.00006
19.45	0.638	0.00001
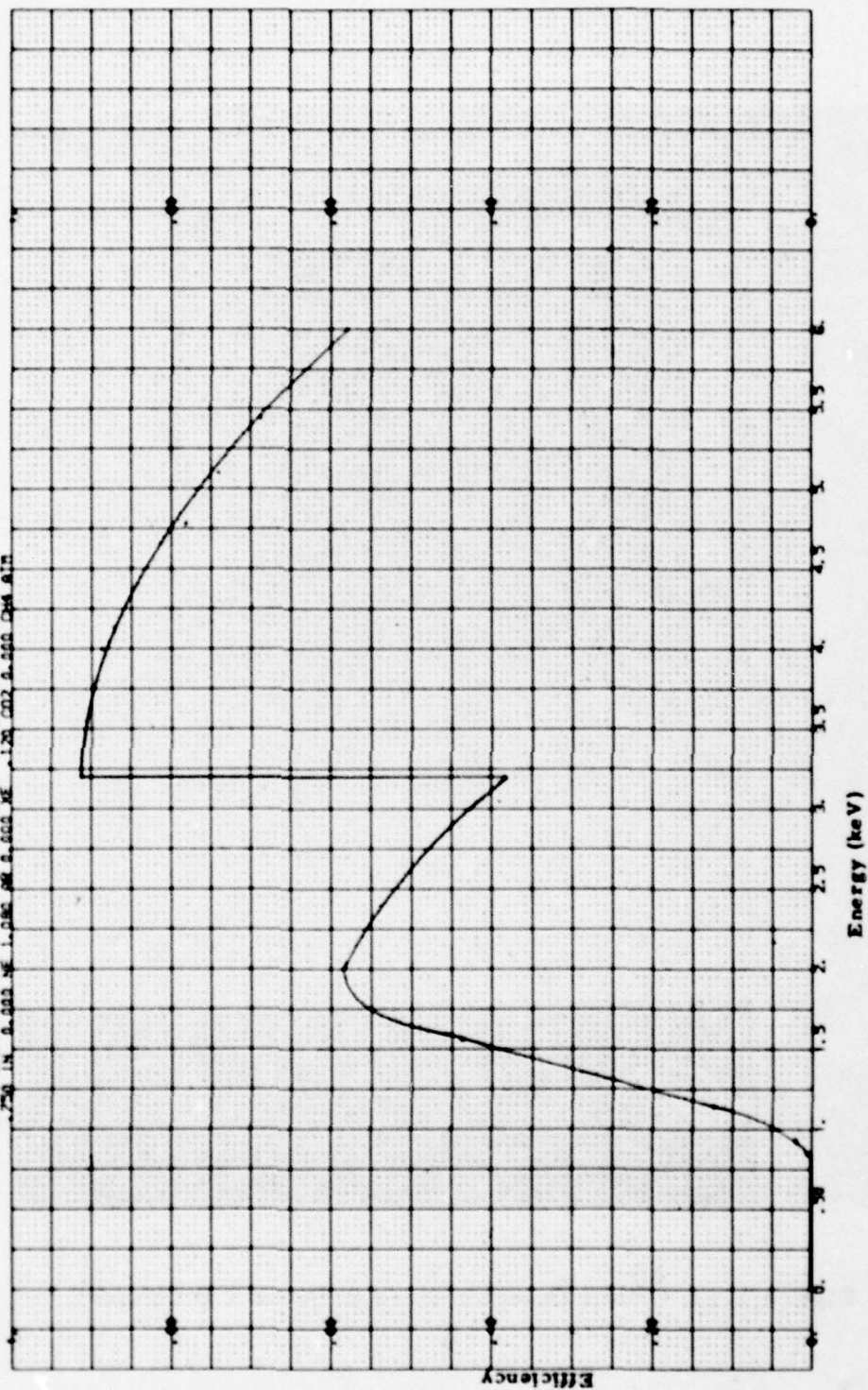
Figure 3.12.   Calculated Efficiency of the CRLS-229 Proportional Counter.
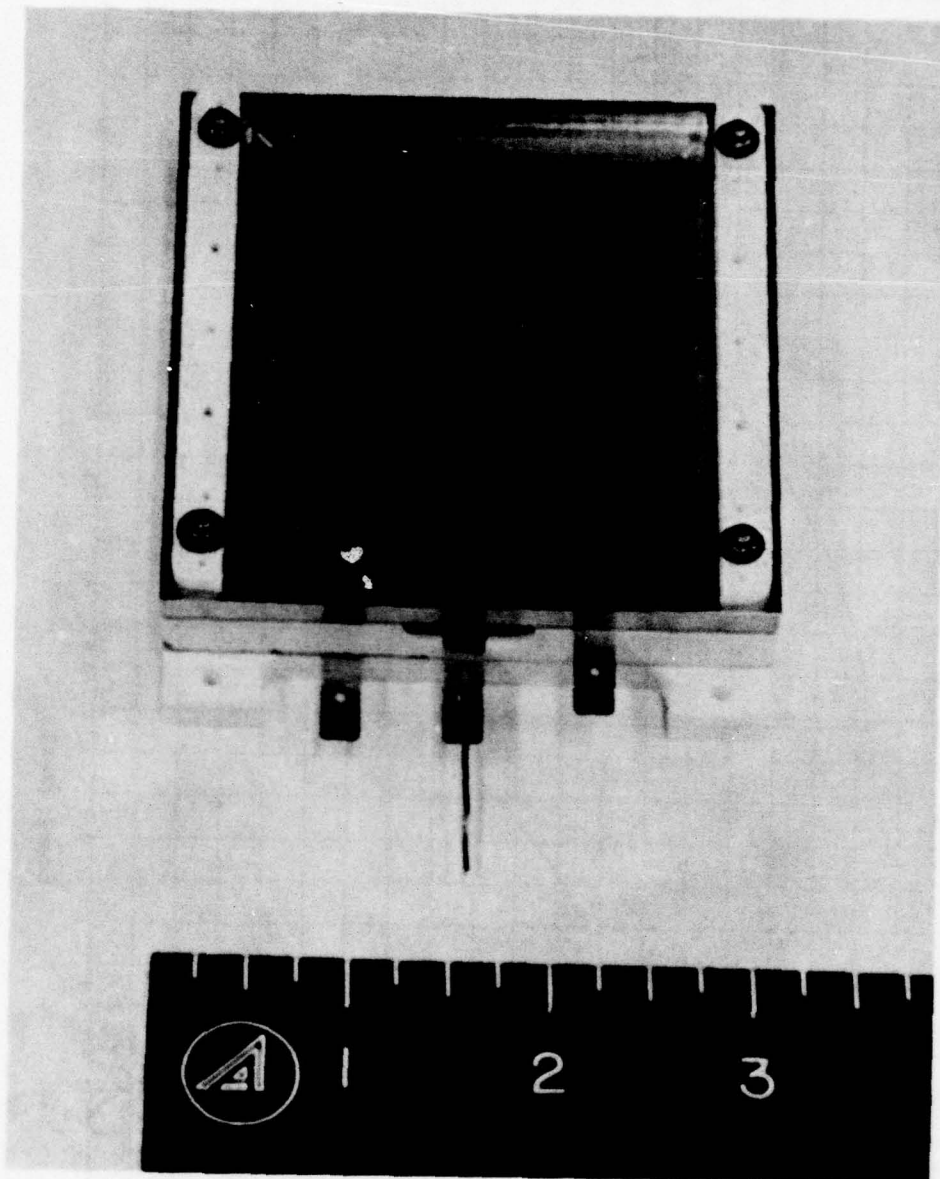
Figure 3.13. CEMA Detector Used in SOLEX B Channel.

Table 3.5. SOLEX CEMA Detector.

Faraday Shield Dimensions:	0.9 in x 3.2 in x 4.4 in
Photocathode Material:	4000 Å magnesium fluoride
Bias of Plates:	4° for front, 11° for rear, 15° relative bias
Plate Serial Numbers:	M3050-010 for front, M3069-006 for rear
Chevron Serial Number:	101
Size of Front Mask:	2.05 in x 2.60 in
Active Area:	5.33 in^2 = 34.4 cm^2
Plate Thickness:	0.130 in = 0.330 cm
Channel Diameter:	3.8×10^{-3} cm
Channel L/D:	87
Channel Center Spacing:	5.3×10^{-3} cm
Number Channels per Plate:	1.4×10^6
Interplate Spacing:	0.002 in = 5.1×10^{-3} cm

SOLEX CEMA EUV Shield

Polypropylene Thickness:	$(1.89 \pm 0.05) \times 10^{-4}$ cm
Aluminum Thickness:	(2450 ± 70) Å
Serial Number:	10-12

Aerospace Corp. Technical Memorandum ATM-78 (3960-01)-2 by Landecker and Eng contains additional details.

Cross Sections from Storm and Israel (1970) and Henke and Tester (1975).

performed on the flight spare and supposedly identical CEMA (Serial number 102); it was assumed that relative K-edge effects and estimated uncertainties for both detectors were similar. A plot of this efficiency as a function of incident photon wavelength is given in Figure 3.14. The reduction in efficiency near 25Å is due to the filters discussed in Section 3.5.3.

Prior to the determination of the flight configuration, many measurements were made. It was found that a length-to-channel width ratio of about 80 gave better resolution than the standard ratio of about 40. The optimum angle of about 4 degrees between the incident photon beam and the channels resulted in a reasonable compromise between quantum efficiency and resolution. Details about this testing effort as well as that of the calibration of the flight detector are given by Landecker and Eng (1979).

3.5.3 CEMA Filter

The CEMA is sensitive to EUV and UV radiation as well as to X-rays. Experience with similar detectors on OV1-10 and OV1-17 (Rugge and Walker, 1968; Walker and Rugge, 1969) indicated to us that high counting rates could be expected at Bragg angles below 30° due to specular reflection of EUV radiation by the crystal. To determine what filtering is necessary to eliminate this unwanted background requires knowledge of the solar EUV spectrum, the crystal reflectivity for EUV, and the filter transmission; the first two are not well known. Therefore, we examined the performance of past experiments to define a filter that would reduce the EUV to an acceptable level while still transmitting X-rays having wavelengths as long as 24.8 Å (N VII 1s-2p). The results obtained by the OSO-3 Bragg spectrometer using a KAP crystal (Neupert, et al. 1969) were degraded below about 12 Å by scattered EUV. Since the OSO-3 detector viewed the entire sun and ours views only a small region, we decided that the 2 μm

3-28

Q.E. w/FILTERS No. 10 AND No. 12
ON CEMA No. 101 vs λ
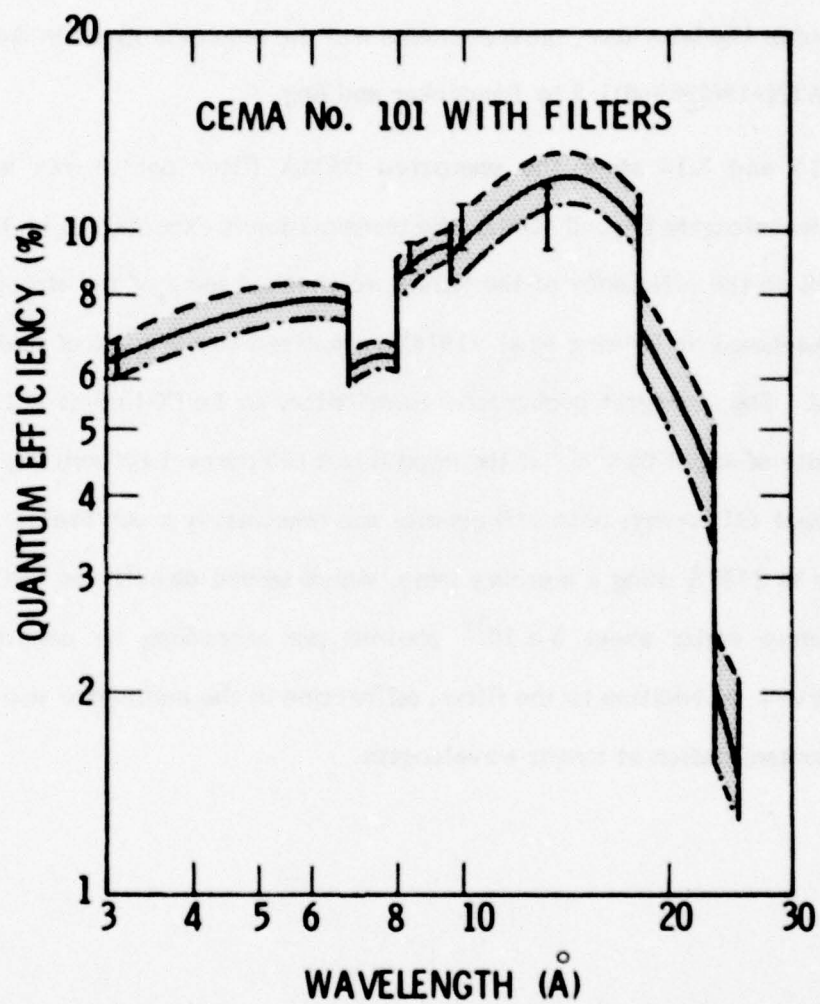
Figure 3.14.   CEMA Quantum Efficiency in SOLEX B Wavelength
Range (with EUV filter).

polypropylene, 2000Å aluminum filter used on that mission would be a minimum for our CEMA. The SOLEX B spectrometer has two filters with a total of $1.89 \pm .05$ μm of polypropylene and 2450 ± 70Å of aluminum (see Table 3.5). A complete description of the techniques used in the laboratory measurements and the results is given in Aerospace Technical Memo ATM-78(3960-01)-2 by Landecker and Eng.

Figures 3.15 and 3.16 show the computed CEMA filter pair X-ray and EUV transmission. At wavelengths beyond 1000Å, the transmission is expected to be less than 10^{-10}. As a check on the efficiency of the filters we checked some of the stronger lines in the spectrum discussed by Behring et al. (1976) normalized to the data of Malinowsky and Heroux (1973). The strongest background contributor, an Fe IX line at 171Å, would yield a counting rate of about 25 sec^{-1} if the crystal had 100 percent reflectivity and the detector 100 percent efficiency; both efficiencies are presumably much lower. We also checked the filter at 2537Å using a mercury lamp, which shined directly on the filtered detector. The lamp emits about 5×10^{16} photons per steradian; no counting rate increase was observed. In addition to the filter, diffraction in the collimator will provide protection from contamination at longer wavelengths.

LAMBDA	2450 A
2.00	.9916
2.48	.9854
3.10	.9725
4.00	.9417
4.13	.9384
6.00	.8328
6.20	.8160
7.95	.6587
7.95	.8492
8.00	.8807
8.34	.8764
9.89	.8071
11.90	.6967
12.30	.6765
13.32	.610?
14.60	.5??2
16.00	.4450
17.60	.349?
18.35	.314?
19.40	.2552
21.60	.164?
22.30	.1422
23.60	.104?
27.40	.037?

TRANSMISSION (%)

λ(Å)
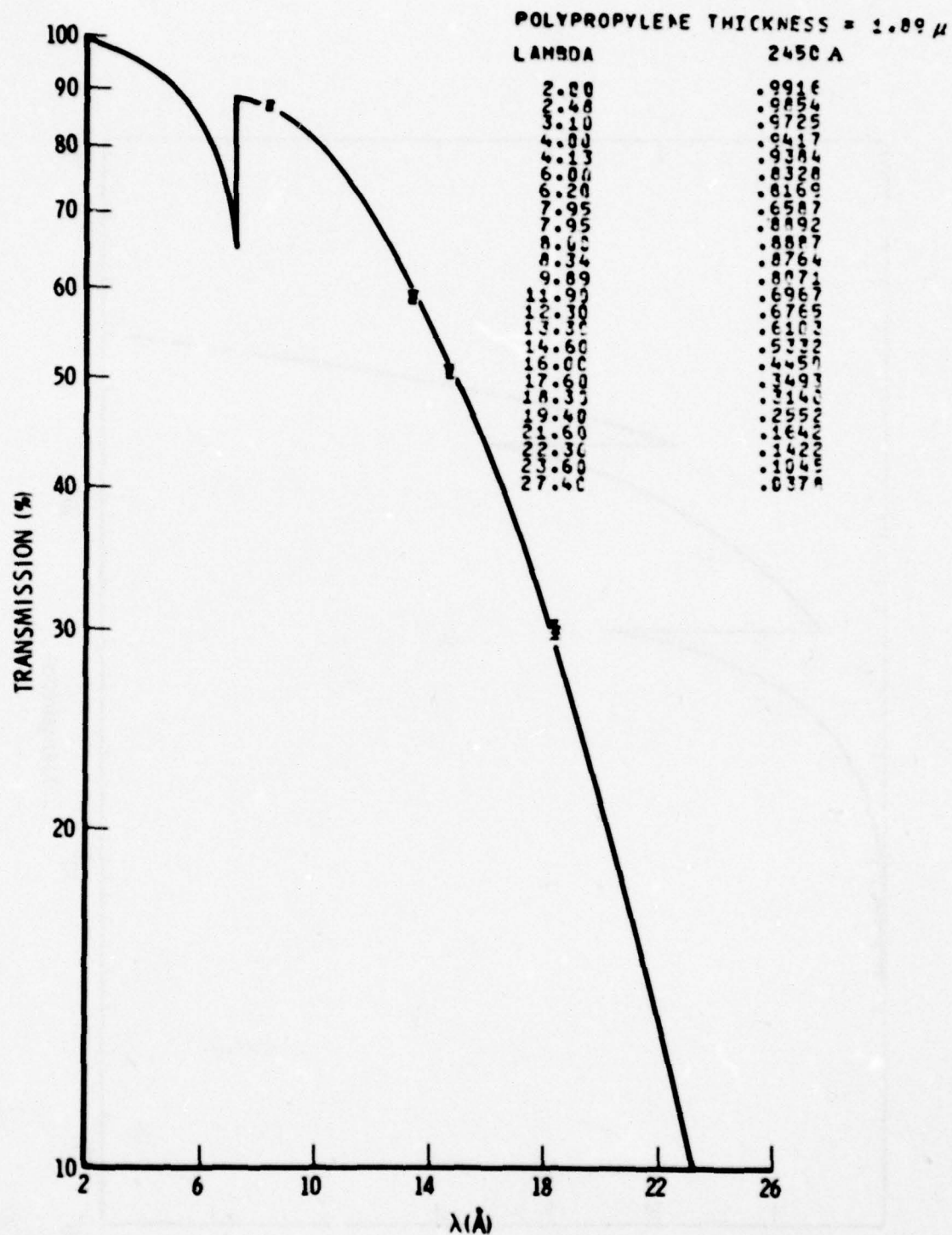
Figure 3.15. Combined Transmission of the Two SOLEX Filters (Flight Unit). The theoretical transmission of a shield consisting of 1.89 μm of polypropylene and 2450 Å of aluminum is given by the solid curve and the table insert. Experimental values are also noted.

3-31
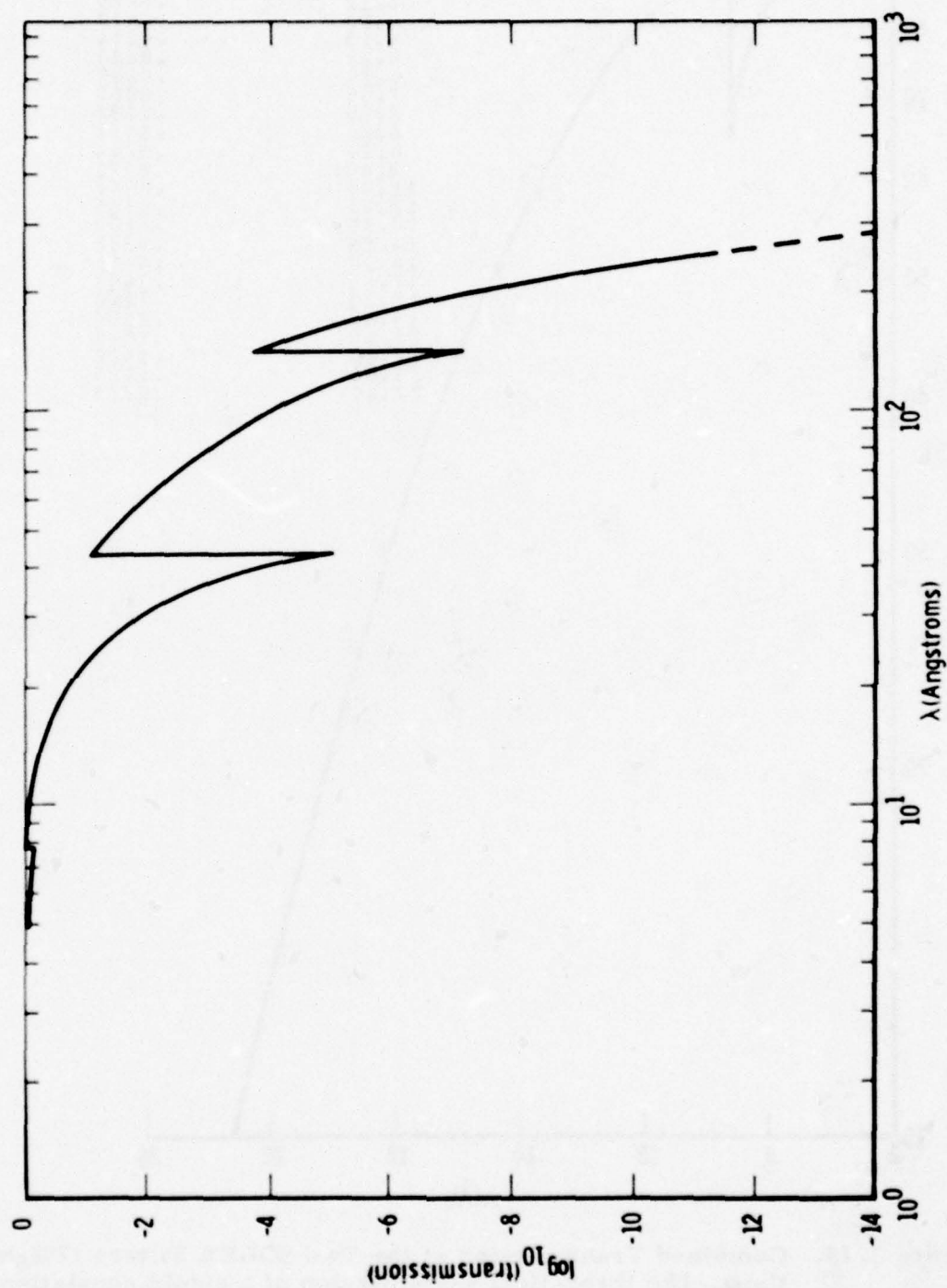
Figure 3.16. Calculated Transmission of Flight CEMA Filters as a Function of Wavelength.

3.6 SOLEX Motor Drive Electronics

The SOLEX motor drive utilizes stepping motors to position both the crystal and detector. For a particular angle of incidence of X-rays on the crystal surface, the detector is moved to a unique angular position to accept diffracted X-rays (see Figure 3.3).

The Bragg angle is determined from the angular step size and the number of steps that the drives have moved away from the Reference Zero position ($\theta \simeq -60^{\circ}$). If synchronism is lost between the crystal and detector, it is necessary for both crystal and detector drives to return to the Reference Zero position. These drives are automatically commanded to the Reference Zero position when standby power is turned on. No other activity can take place until both the crystal and detector mechanisms are in the Reference Zero position. Step direction and step rate are derived from the command box. A coarse analog readout of the angular positions of the drives is given in Figure 7.4.

3.6.1 Block Diagram Description

The power amplifier and its control logic form the basis of the SOLEX motor drive subsystem. It is also necessary to interface the power amplifier and control logic with both the spacecraft and other parts of the CRLS-229 experiment. The motor drive power amplifier and its control logic interacts directly with the motors. This flow is shown in Figure 3.17. The step rate, step direction, and end of travel blocks interface with the command box. Potentiometer readouts of the angular position of the shafts are buffered by the SOLEX detector electronics and sent to the spacecraft telemetry interface. The step rate, step direction, and end of travel signals are logic levels or transitions. The end of travel logic state is controlled by microswitch closures.

3-33
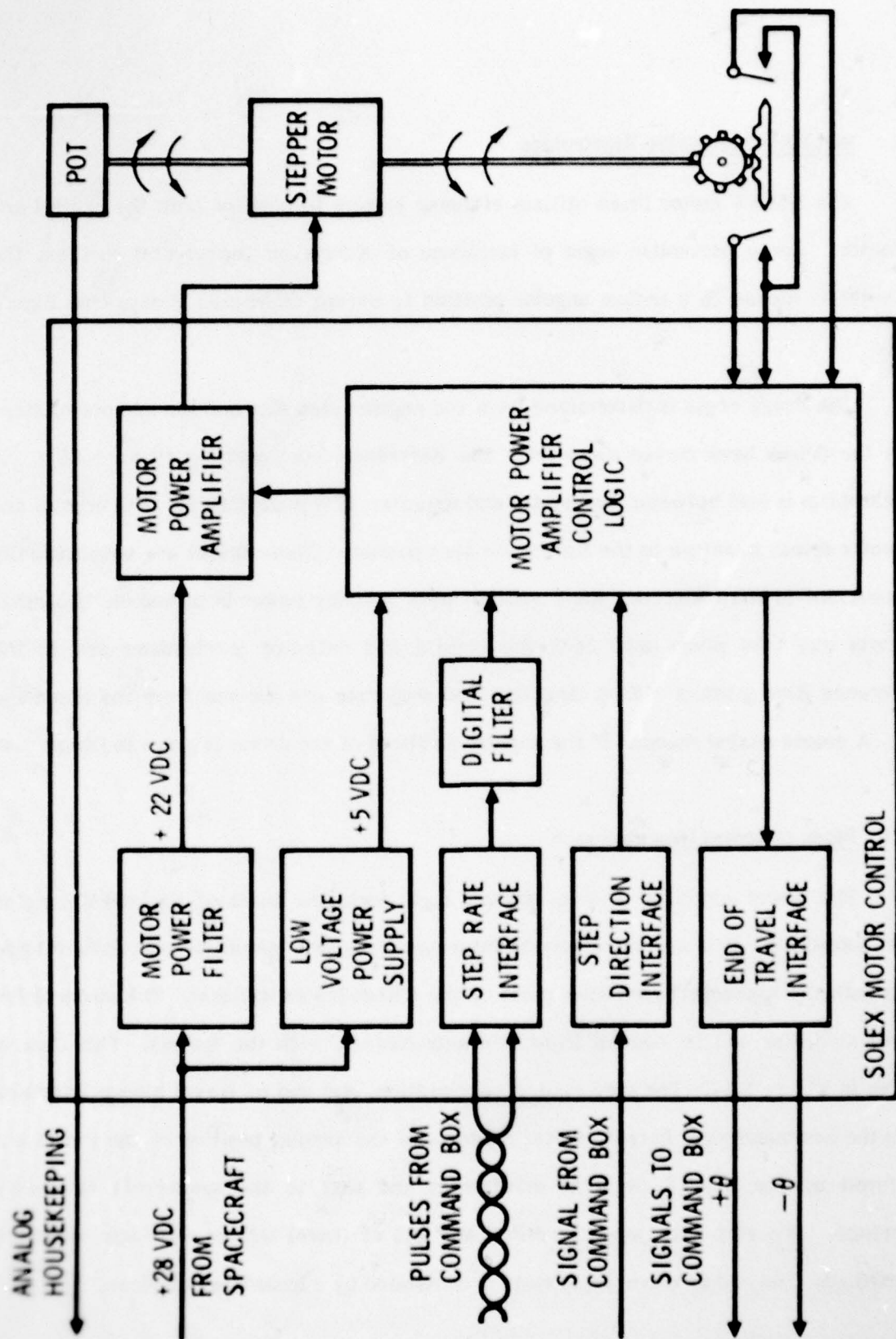
Figure 3.17. CRLS-229 SOLEX Motor Control Block Diagram.

The angular positions of the detector and crystal assemblies are independently controllable. Duplicate circuits are used for both; this circuitry is shown in Aerospace Drawing L-5283.

3.6.2 Stepper Motor Parameters

The stepper motor is a permanent magnet type. It has two quadrature center-tapped windings. The motors were manufactured by Kearfott (Part Number 05088-CM40191048). The winding resistance to each center tap is about 500 ohms.

3.6.3 Motor Direction Terminology

A switch closure at Reference Zero results in a logic zero to the motor drive subsystem and causes the motor to move in a positive angular direction away from Reference Zero. The following table defines the detector and crystal angular positions at Reference Zero and the upper end.

	Reference Zero	Upper End
Crystal	A_x at -60°	B_x at $+75^{\circ}$
Detector	A_D at -120°	B_D at $+150^{\circ}$

A_x, B_x, A_D and B_D equal 0 when the respective microswitch is closed and this information is supplied in telemetry word known as DFORM2 (discrete format number 2 listed in the glossary in Section 10).

3.6.4 Angular Rate

The motor steps in 90° increments. The step rate is keyed to the spacecraft's main frame (MF) telemetry rate. Two rates are available, 62.5 Hz and 31.25 Hz. Motor steps

occur at the beginning of main frame word 1 for the case of 31.25 Hz. For the 62.5 Hz rate this transition occurs at the beginning of MF words 1 and 65.

3.6.5 Motor Power

The power consumption of the SOLEX motor drives is essentially constant. The motor amplifiers are always on when the motor drive subsystems are energized. There is a slight reduction of power when the stepper motors are in motion. Power consumption for both motors is 4.8 W.

Spacecraft power to the SOLEX motor drive is interrupted by execution of the SOLEX/MONEX +28V OFF command. Power is restored by execution of the SOLEX +28V ON command.

3.6.6 Electrical Description

In order to minimize the effects of stepper motor operation on the spectrometer's detection system, the stepper motor's power amplifier and associated logic were not operated at telemetry ground. In addition, the stepper motor itself was dielectrically isolated from the spacecraft chassis. Control signals from the command box are isolated by relay switches. The step rate pulses are transformer coupled into the power amplifier's control logic. The control logic's power supply (5VDC) ground is connected to spacecraft power return.

The main objective of the power amplifier's control logic is to cause the stepper motor to turn 90 degrees for each pulse. If the direction of the motor is changed, the logic circuitry must cause the power amplifier to reverse the stepper motor's angular motion and still maintain a 90 degree step for each pulse.

3-36

3.6.7 Motor Power Filter

The motor power filter serves two purposes. First, it attenuates stepper motor current surges on the spacecraft power lines. Second, turn-on current surges are limited and short circuit protection for the spacecraft power line is provided. The windings of the stepper motor form the filter's electrical load. When the motor is at rest the load is the winding resistance of the motor, approximately 250 ohms. When the motor is in motion the load obeys Lenz's law and a slight reduction in load current is experienced.

The motor power filter is a series regulator. Its output is nominally 22 VDC. The motor current changes only slightly as a function of step rate and temperature. The ripple current as seen by the spacecraft is approximately 2 mA peak-to-peak.

3.6.8 Step Rate Interface

The spectrometer stepper motors undergo a 90 degree step upon receipt of each pulse from the command box. The minimum pulse to cause a step motor response is 5 V for at least one μsec whereas the minimum pulse generated by the command box is 12 V for 300 μsec. Upon receipt of each pulse, the interface circuit is disabled for approximately 8 msec. This input circuit deadtime feature is compatible with the maximum input pulse rate of 62.5 Hz. A transformer is used at the input to isolate the two subsystem grounds.

Within microseconds of receipt of the leading edge of the driver pulse, stepper motor action is initiated. The period of time for completion of the 90 degree motor step is about 10 msec. Creation of an 8 msec input circuit disable deadtime serves the same purpose as establishing the upper frequency in a bandpass filter.

3.6.9 Step Direction Interface

As mentioned previously, a switch closure in the command box results in a logic zero at the step direction interface and receipt of step pulses will cause the motors to drive the spectrometer away from Reference Zero (see Section 3.6.3). Switch closure is accomplished in a few milliseconds. The command box inhibits step pulses during the switch closure transition period.

3.6.10 Electrical End-of-Travel Interface

The spectrometer motion is bounded both electrically and mechanically. The electrical bound is implemented by actuation of microswitches. Microswitch actuation disables the input step rate circuit. No further spectrometer motion can occur until the motor direction logic is changed. The states of the microswitches are duplicated via relays, whose contacts transfer the microswitch information to the command box. Thus, independence of subsystem grounding is maintained.

3.6.11 Motor Power Amplifier and Control Logic

The method of motor excitation implemented in SOLEX is called two-phase drive. This is accomplished by driving the four windings two at a time. The four windings form two quadrature pairs. A set of two windings forming a quadrature pair upon excitation generate opposing magnetic fields. To cause stepping action, only one winding from a quadrature pair is excited for a particular motor position. For two-phase operation one winding from each quadrature pair is excited for each motor position. The control logic circuitry creates the power amplifier signals from motor direction and step rate signals to implement the proper excitation of the quadrature windings. The logic circuitry retains the information concerning the current windings excitation, and upon receipt of

3-38

step rate pulse takes on a new state which results in a 90 degree step. Let the two quadrature pairs be defined as A and B, and further let the windings of each pair be defined by subscripts 1 and 2. The four motor positions can then be defined by the following Table.

Position	Windings		Excitation	
1	A_1	$\bar{A}_2$	B_1	$\bar{B}_2$
2	A_1	$\bar{A}_2$	$\bar{B}_1$	B_2
3	$\bar{A}_1$	A_2	$\bar{B}_1$	B_2
4	$\bar{A}_1$	A_2	B_1	$\bar{B}_2$

where a bar over a letter signifies a non-excited winding.

A motor winding may be considered as an inductor in series with a resistor. The time constant (L/R) is of the order of 10 msec. The function of the power amplifier is to impress a voltage across the winding. For the current in a winding to reach 95 percent of its full value requires about 3 time constants. A voltage is impressed across a winding at 1/4 the input step rate, so that each winding receives 95 percent of full current at an input step rate of $4/0.032 = 125$ steps sec^{-1}. A description of both the control logic and power amplifier circuitry is shown in Aerospace Drawing L-5283.

3-39

3.7   SOLEX Detector Electronics

The SOLEX experiment has two independent detectors: a sealed gas-filled proportional counter (PC) and a channeltron electron multiplier array (CEMA). Outputs from both detectors are sensed in a similar fashion. For each X-ray photon sensed by the detectors, a single detector output pulse occurs. The amplitude of the output signal from the PC is proportional to the energy of the X-ray whereas the output from the CEMA is essentially independent of energy.

The basic signal acceptance criterion is determined by the minimum and maximum signal amplitude selected thresholds. In the case of the PC, another criterion related to the signal collection time is also included. The PC signal collection time is used to allow some reduction of background events which on the average have a longer collection time. If the output signal from a detector satisfies the amplitude and risetime criteria, a digital accumulator is incremented by one. The main data outputs (SOLEX A and SOLEX B) give the number of detector pulses which satisfy these electrical constraints per telemetry main frame (32 msec).

In addition to X-ray detection electronics there are commandable controls and housekeeping monitor outputs. The commandable controls turn the power supplies on and off, and set the programmable high voltages. Monitors provide an indication of the output magnitude of the high and low voltage power supplies. The angular position potentiometers (described in Section 3.6) are also analog outputs.

A block diagram for a typical SOLEX detector is shown in Figure 3.18.

The high voltage power supplies used in CRLS-229 use a standard Cockroft-Walton design. In these supplies, the spacecraft day power (+ 28 V) drives a blocking oscillator from which a 25 kHz sinusoidal output is derived. This output in turn drives the voltage
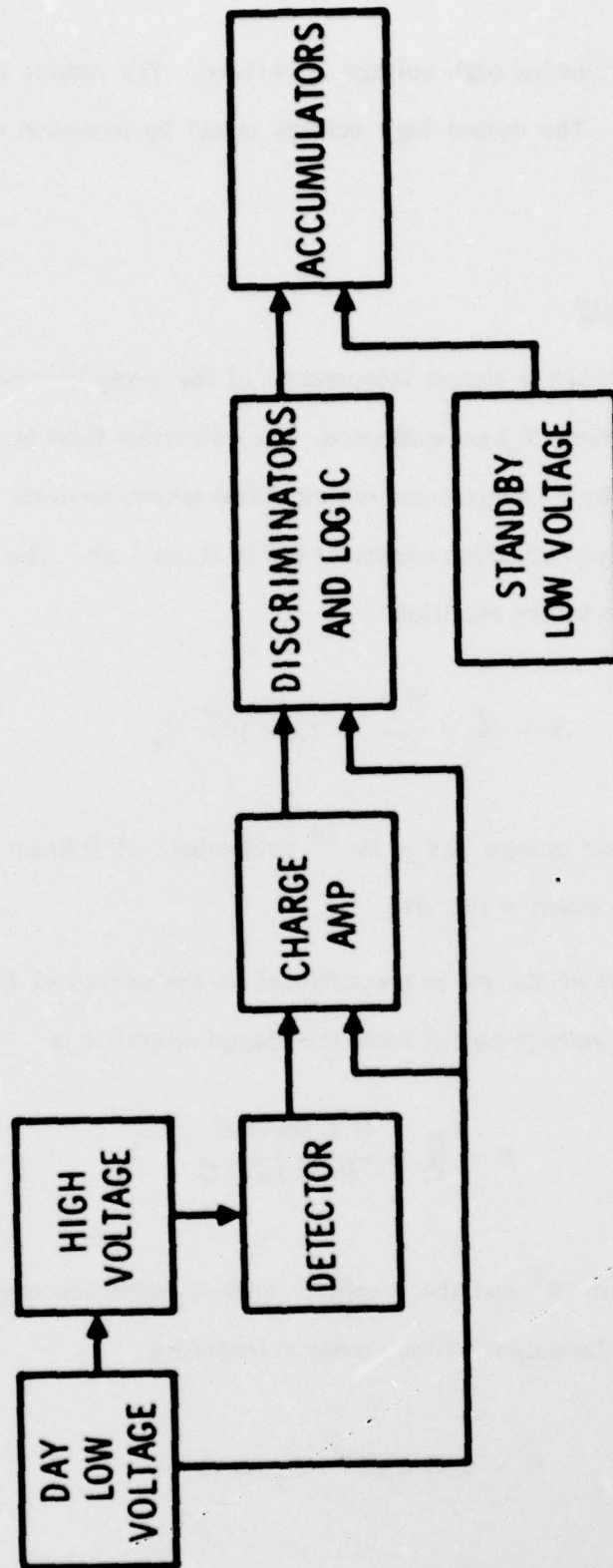
Figure 3.18. CRLS-229 Front End Electrical Block Diagram.

multiplying circuit from which high voltage is derived. The output is variable over a range $V_{max}/2$ to V_{max}. The output high voltage is set by inclusion of an appropriate resistor.

3.7.1 Detector Sensitivity

The gain of the CEMA is almost independent of the X-ray energy. For each X-ray approximately 10^6 electrons (N_e) are collected. The collection time is about 10-20 nsec. The charge is collected by a charge sensitive amplifier which converts this charge into a voltage pulse. The charge collection capacitor (C) is about 1 pF. The amplitude of the voltage pulse out is given by the equation

$$V = \frac{Q}{C} = \frac{N_e e}{C} = 1.6 \times 10^{-7} N_e$$

where e is the electronic charge (1.6×10^{-19} coulombs). It follows that the nominal amplitude of each X-ray event is 160 mV.

The charge output of the PC is proportional to the energy of the incident X-ray (E_x). The corresponding voltage output from the charge amplifier is

$$V = \frac{Q}{C} = \frac{G\, E_x(keV)\, e}{(0.03\ keV)\, C}$$

The PC gain (G) is about 10^4 and the amplifier charge collection capacitor (C) is also 1 pF. The amplitude of the output voltage pulse is therefore

$$V = 5.33 \times 10^{-2}\ E_x\,(keV) \ .$$

The nominal output for a 1 keV X-ray is 53 mV.

3-42

3.7.2 Amplitude Detection Thresholds

The electronic dynamic range of the SOLEX electronics is ≈ 150, from 10 mV to 1.5 V. The lower and upper level discriminator voltage fixed thresholds are 15 mV and 300 mV for the PC and 35 mV and 1.5 V for the CEMA. Adjustment of the magnitude of the high voltage power supply outputs changes the detector gain and thus is used to match the desired X-ray energy ranges with those of the electronics. As shown in Table 3.6, the nominal electronic energy range for the PC corresponds to 0.4 - 6.6 keV. X-ray events which deposit this energy are candidates for primary data events. Any event with an amplitude less than the lower level discriminator (LLD) threshold is ignored.   Any event with an amplitude greater than the upper level discriminator (ULD) threshold is excluded from the SOLEX A or B event scalers.

3.7.3 Risetime Criteria

The proportional counter is equipped with a risetime discrimination (RTD) network as a background reducing device. When an energetic charged particle or a gamma ray interacts in a proportional counter, it almost always leaves a long ionization track and, since the electrons from these ion pairs are collected relatively slowly by the counter anode, the pulse has a relatively slow risetime. On the other hand, an X-ray is absorbed in a photoelectric event (at these energies of interest) at a very localized region in the counter. Since in this case the electrons all migrate to the anode together, a more rapid pulse risetime results. Hence, by eliminating the events with long risetime, the RTD increases the signal-to-noise ratio.

The risetime discriminator uses a tapped, shorted delay line to generate an output signal which is sampled at a specific time after the pulse height passes a lower level threshold. If the risetime of an input signal is longer than a specified value, the sampled

3-43

Table 3.6. SOLEX Spectral Information.

	Proportional Counter					CEMA Detector		
		Nominal SHV1=1.95 HV="00" (or "10")	SHV1=1.99 HV="11"	SHV1=2.04 HV="01"		SHV2=1.39 HV="00" (or "10") Gain wrt N	SHV2=2.70 HV="11" Nominal=N	SHV2=2.77 HV="01" Gain wrt N
	mV	keV	keV	keV	mV			
Lower Level Discriminator	15	0.4	0.3	0.2	35	+	+	+
Upper Level Discriminator	300	6.6±0.5	5.1±0.4	3.1±0.2	1500*	+	+	+
Gain with respect to Nominal	—	1.0	1.3	2.1	—	0.0	1.0	1.9±0.1

Data above taken at about 22°C
SHV1 and SHV2 are the monitor outputs for the high voltage power supplies (see Table 7.2).

+ CEMA run in saturated mode

* CEMA circuit incapable of producing a pulse above the ULD

	Proportional Counter	CEMA
X-ray Counting Efficiency of Risetime Circuitry	97%	100%
Y-ray Counting Efficiency of Risetime Circuitry	54%	100%
Counter Resolution = $\frac{FWHM}{MAX}$	$(0.9\pm0.1)/\sqrt{E}$ (keV)	1.4 ± 0.2
Background Counting Rate at Sea Level	1 sec^{-1}	30 sec^{-1}
Gain Changes (between -4°C and 41°C)	-0.4 %/°C	N/A

signal is rejected. The limiting risetime was set by adjusting the delay period. An RTD pulse is generated for acceptable events.

The RTD circuit was adjusted until a large fraction of the charged particle events was rejected while most legitimate X-ray events were not. The detector was irradiated with low energy X-rays. This test was then repeated using a Co^{60} gamma ray source. The delay was set so that 97 percent of the X-rays were accepted; 46 percent of the Co^{60} gamma rays are rejected at this setting.

3.7.4 X-Ray Event Accumulation

The SOLEX A PC processes a signal output consisting of the number of legitimate X-ray events between the LLD and ULD with acceptable risetime and a background output comprised of the number of events between the LLD and ULD with excessive risetime. The SOLEX B CEMA accumulates a signal output consisting of the number of events between the LLD and ULD as well as a background estimate composed of the number of events above the ULD. Signal events are accumulated for 32 msec in 13-bit registers whereas background events are added for 1.024 sec in 16-bit registers (see Figure 7.3).

3.7.5 Commands

There are five discrete commands which affect the power status of SOLEX. These commands and their effects are described by the following matrix.

3-45

	Command	Low Voltage Circuitry Active	Detector Active
(a)	SOLEX +28V On	Yes	No(unless(b)or(c)alsoon)
(b)	SOLEX HVPS 1 On	Yes (only if (a) also on)	Yes (only if (a) also on)
(c)	SOLEX HVPS 2 On	Yes (only if (a) also on)	Yes (only if (a) also on)
(d)	SOLEX/MONEX + 28V Off	No	No
(e)	SOLEX/MONEX HVPS Off	Yes (only if (a) also on)	No

The command state is maintained by use of latching relays. If the spacecraft power is turned off and then on, the SOLEX circuitry state will return to its original configuration.

There are four bits V1-V4 received by the Command Box (see Section 4.5). These signals control the output voltage of the high voltage power supplies (HVPS). The following matrix describes the output value of the HVPS as a function of the input logic level of these signals applying to the PC and CEMA, respectively.

Bit V1	0	1	1	0
Bit V2	0	0	1	1
HV1 R_{adj}	98 k ohm	98 k ohm	103 k ohm	111 k ohm
HV1 Output	Low (1940V)	Low (1940V)	Medium (1990V)	High (2040V)
HV1 Monitor	1.94 V	1.94 V	1.99 V	2.04 V

PC Nominal Voltage

3-46

Bit V3	0	1	1	0
Bit V4	0	0	1	1

HV2 R_{adj}	322 k ohm	322 k ohm	805 k ohm	855 k ohm
HV 2 Output	Low (1340V)	Low (1340V)	Medium (2620V)	High (2770V)
HV2 Monitor	1.34 V	1.34 V	2.62 V	2.77 V
	CEMA Conditioning Voltage		CEMA Nominal Voltage	

3.7.6 Detector Power

The power required to turn on all the SOLEX detector low and high voltages is 1.0 W.

3.7.7 Analog Monitors

There are six SOLEX analog monitors. These are used to indicate the health of the SOLEX electronics. These include LV and HV monitors as well as the crystal and detector potentiometers and correspond to the first six entries in Table 7.3. The SOLEX potentiometer calibration curves are given in Figure 7.4.

3.8 System Efficiency

The SOLEX system efficiency can be calc il ted from a product of the efficiencies given earlier in this section as follows.

1·0

2·8   2·5

3·15   2·2

3·5
1·1   4·0   2·0

1·8

1·25   1·4   1·6
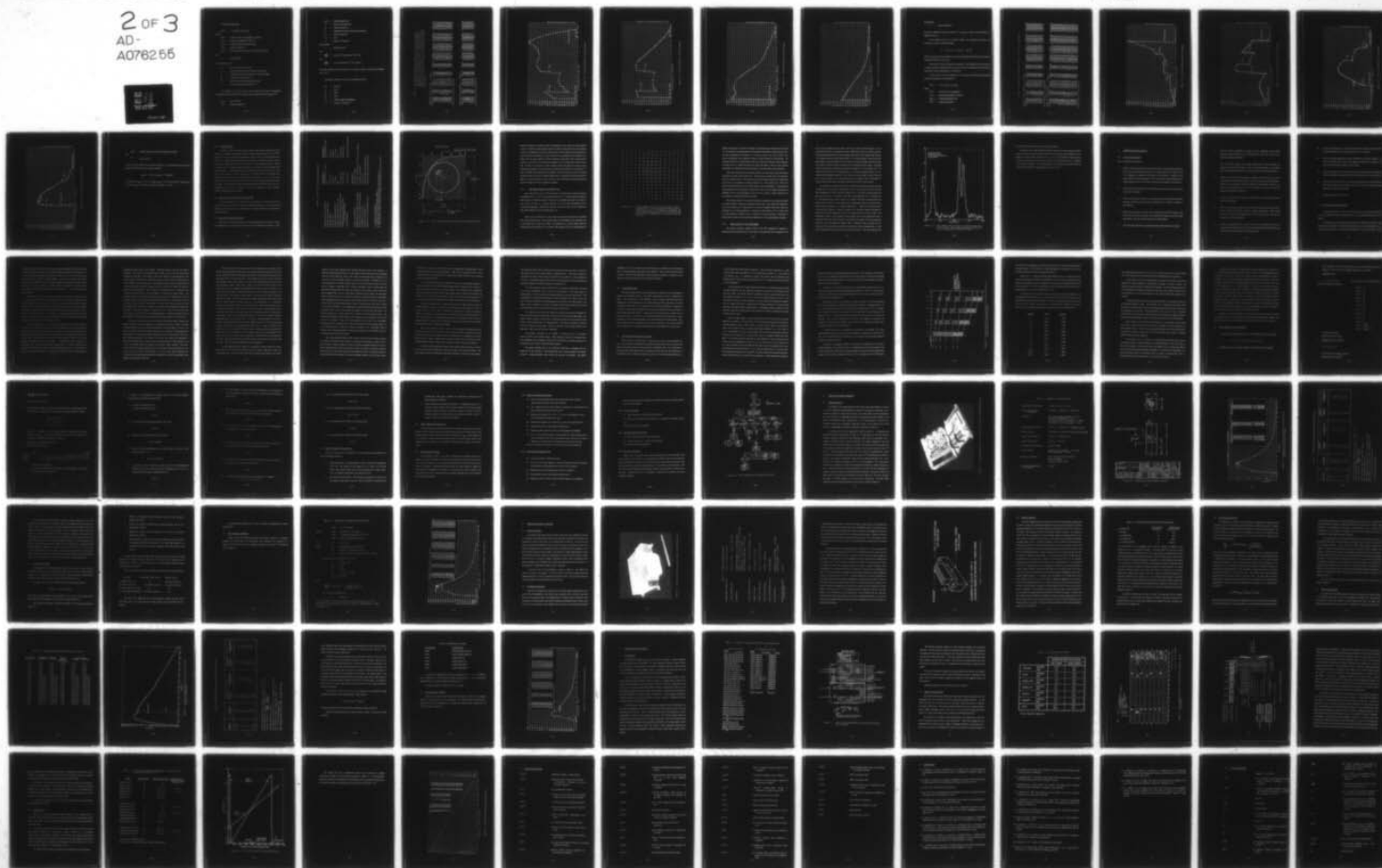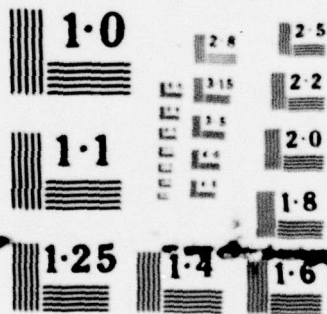
NATIONAL BUREAU OF STANDARDS
MICROCOPY RESOLUTION TEST CHART

In the SOLEX Scan Mode,

$$N(\lambda) = C\ F(\lambda)\ R_c(\lambda)\ A(\lambda)\ E_d(\lambda)$$

where

$N(\lambda)$ = Counts in a line at wavelength λ, per scan

$F(\lambda)$ = Incident flux (photons $cm^{-2}sec^{-1}$)

$R_c(\lambda)$ = Crystal integrated reflectivity (rad)

$A(\lambda)$ = Aperture efficiency

$E_d(\lambda)$ = Detector quantum efficiency (including EUV shield)

and

$$C = \frac{A_o\ t_e\ e_{rt}\ f_d\ t_a}{\omega}\ .$$

In the expression for C,

A_o = Nominal collimator area (cm^2)

t_a = Nominal normal incidence collimator transmission

t_e = Calculated collimator efficiency as a function of angle

e_{rt} = Efficiency of risetime circuit

f_d = Fraction of detector aperture that is open

ω = Crystal angular velocity (rad sec^{-1}).

For example, at 3.2Å into the ADP side of SOLEX A (20 arc sec collimator, proportional counter detector) at the faster crystal rotation rate (62.5 steps sec^{-1}),

$R_c(\lambda)$ = 3.56×10^{-5} rad

$A(\lambda)$ = 0.49 (see Figure 3.9)

$$E_d(\lambda) \quad = \quad 0.89 \text{ (see Figure 3.12)}$$

$$A_o \quad = \quad 25.8 \text{ cm}^2 \text{ (see Table 2.1)}$$

$$t_a \quad = \quad 0.237 \text{ (see Table 2.1)}$$

$$t_e \quad = \quad 0.800 \text{ (for maximum collimator transmission)}$$

$$e_{rt} \quad = \quad 0.97 \text{ (see Table 3.6)}$$

$$f_d \quad = \quad 0.83$$

$$\omega \quad = \quad 9.1555 \times 10^{-3} \text{ rad sec}^{-1}$$

and therefore

$$C \quad = \quad 430 \text{ cm}^2 \text{rad sec}^{-1}$$

and

$$\frac{N(\lambda)}{F(\lambda)} \quad = \quad 6.68 \times 10^{-3} \text{ counts photon}^{-1} \text{ cm}^2 \text{ sec}$$

and

$$\frac{F(\lambda)}{N(\lambda)} \quad = \quad 1.50 \times 10^2 \text{ photons cm}^{-2} \text{ sec}^{-1} \text{ count.}^{-1}$$

The system calibration results for SOLEX A are given in Table 3.7 and plotted in Figures 3.19 - 3.22.

In the case of SOLEX B for the same conditions as above,

$$A_o \quad = \quad 25.8 \text{ cm}^2$$

$$t_a \quad = \quad 0.223$$

$$t_e \quad = \quad 0.867$$

$$e_{rt} \quad = \quad 1.00$$

$$f_d \quad = \quad 1.00 \text{ (no counter strongback)}$$

$$\omega \quad = \quad 9.1555 \times 10^{-3} \text{ rad sec}^{-1}$$

Table 3.7. Calculation of SOLEX A Sensitivity as a Function of Wavelength. The conversion numbers are for the case of maximum collimator transmission. To convert from counts in a line to flux, divide the number of counts in the line by the y-coordinate factor (counts photon^{-1} cm^2 sec at 62.5 steps sec^{-1}). At the slower crystal stepping rate (31.25 steps sec^{-1}), multiply the numbers on the y-axis by the factor 2.

CONVERSION FACTOR CONSTANT = 4.10E+02

WAVELENGTH	APERTURE	XTAL RC	XTAL PK	DETECTOR	CTS/FLUX	FLUX/CT	CTS/MF/FLUX	FLUX/CTS/MF

CRLS-223 SOLEX A ADP CALCULATION

CONVERSION FACTOR CONSTANT = 4.30E+02

WAVELENGTH	APERTURE	XTAL PC	XTAL PK	DETECTOR	CTS/FLUX	FLUX/CT	CTS/MF/FLUX	FLUX/CTS/MF

CRLS-223 SOLEX A KAP CALCULATION

Figure 3.19. CRLS-229 SOLEX A ADP Calculation.
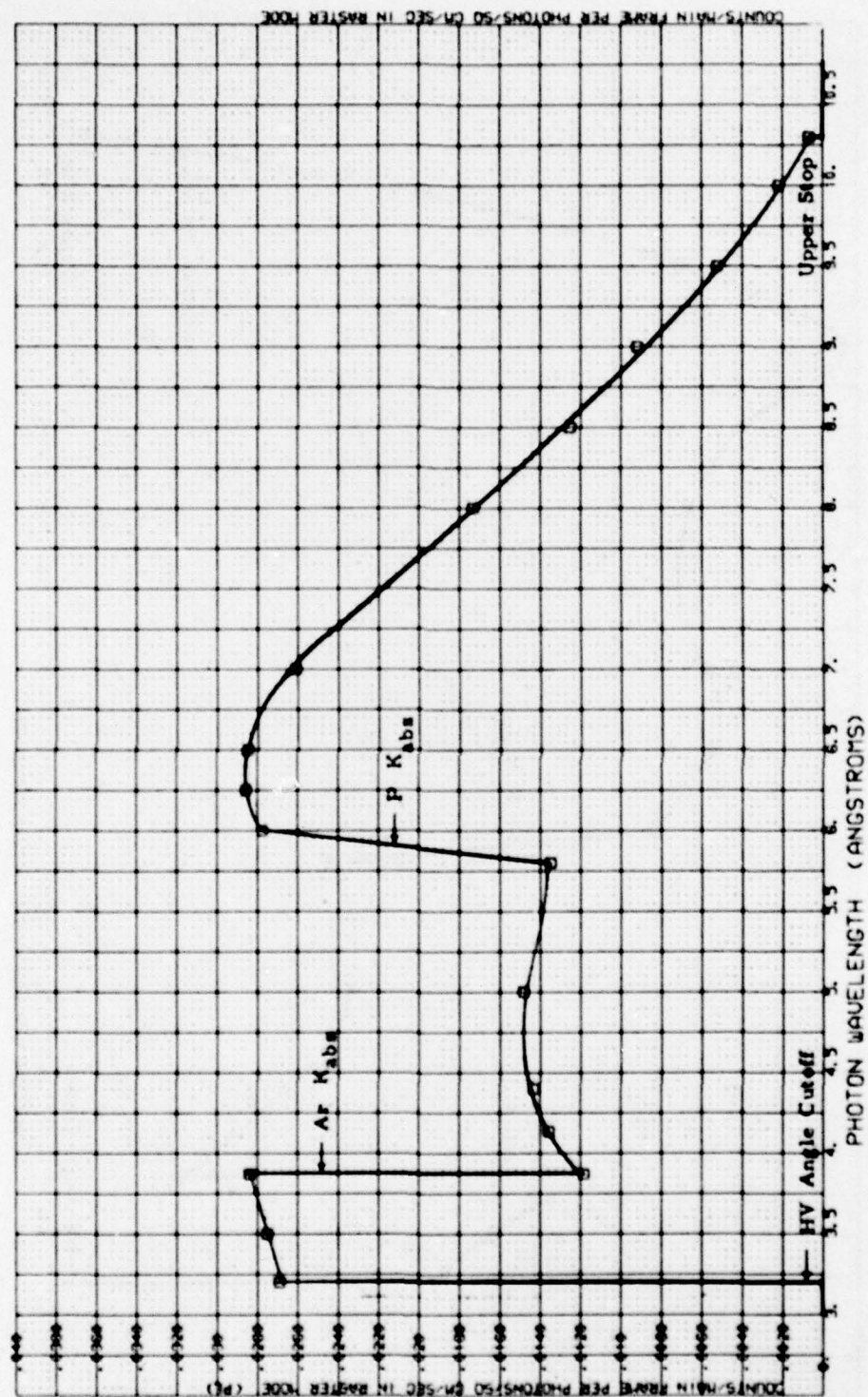
Figure 3.20. CRLS-229 SOLEX A ADP Calculation.
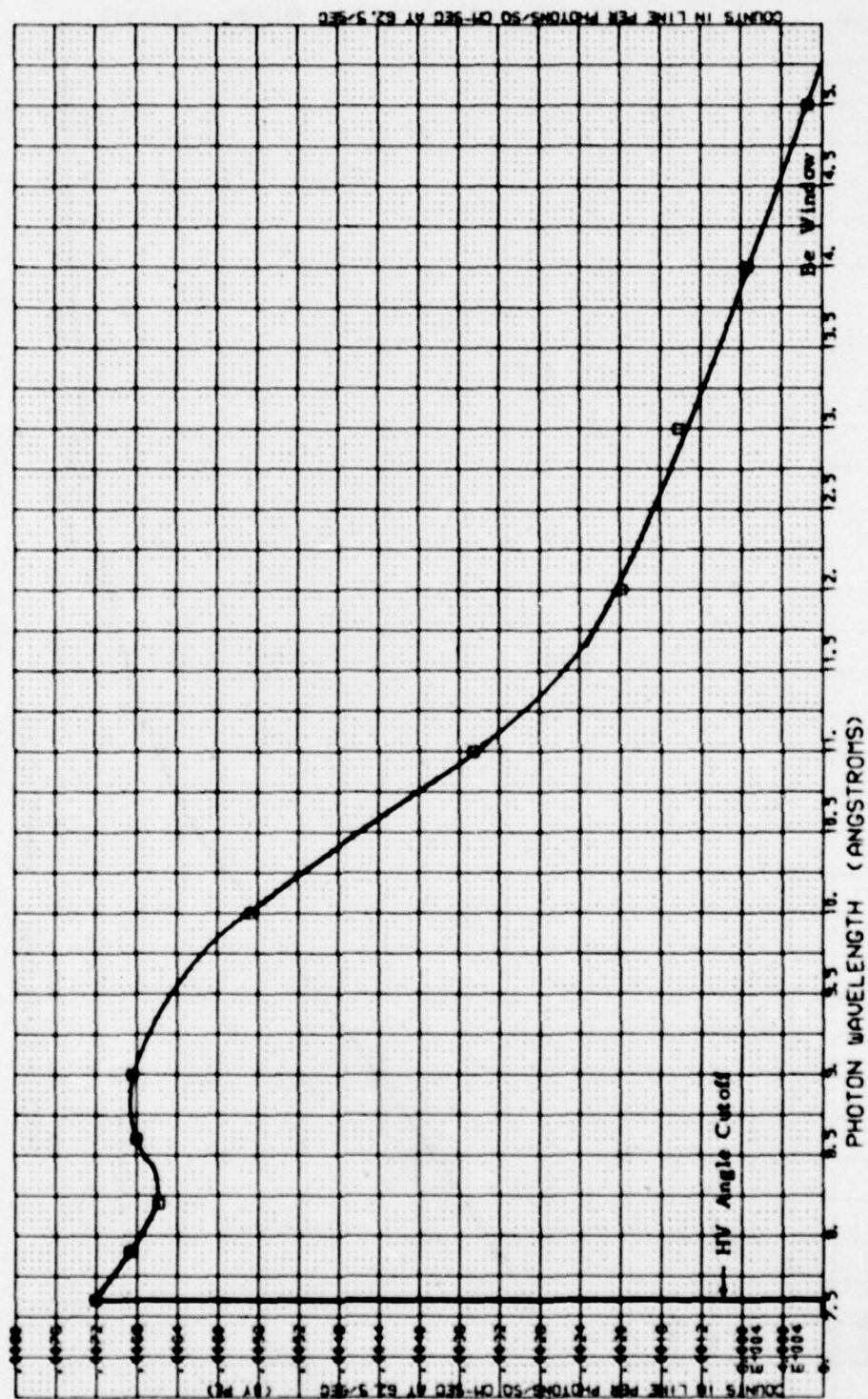
Figure 3.21. CRLS-229 SOLEX A RAP Calculation.

3-53
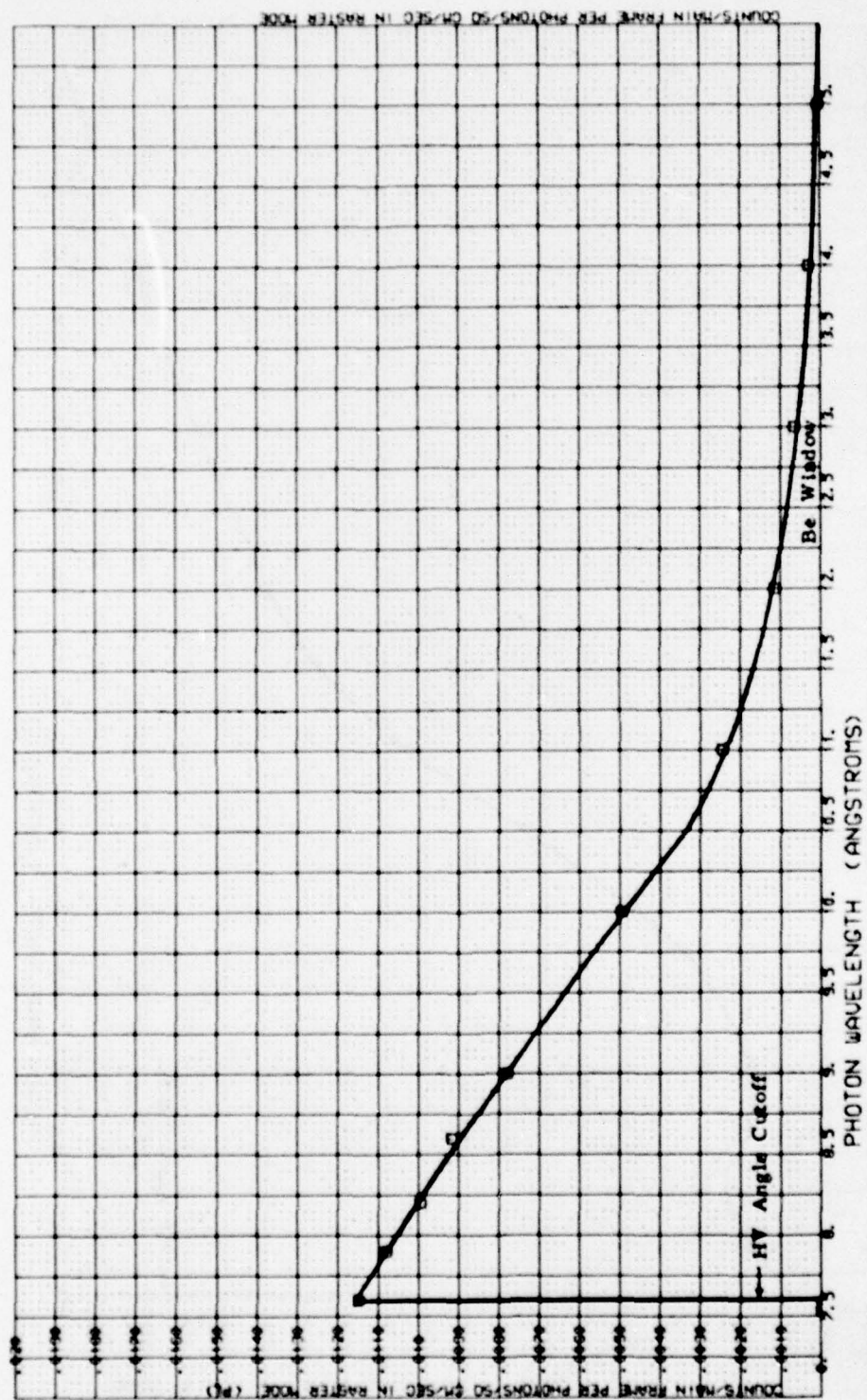
Figure 3.22. CRLS-229 SOLEX A RAP Calculation.

and therefore

$$C = 539.4 \text{ cm}^2 \text{rad sec.}^{-1}$$

The system calibration results for SOLEX B are given in Table 3.8 and illustrated in Figures 3.23-3.26.

If the incident beam is at a different angle to the collimator axis, then it is necessary to make t_e a function of angle

$$t_e = t_e(\theta_z, \theta_y) = t_{xz}(\theta_z) \quad t_{xy}(\theta_y)$$

where t_{xz} and t_{xy} are the collimator efficiency transmission for the XZ and XY planes, respectively, plotted in this report.

The curves of system efficiency (flux/count) in this report are for the case of maximum collimator transmission (an on-axis point source) and include a "photon barrier" (see Section 3.4) for both SOLEX A and SOLEX B.

For the case of the SOLEX experiment in the raster mode where the crystal and detector are stationary, the counting rate

$$N^1(\lambda) = C^1 F(\lambda) R_p(\lambda) A(\lambda) E_d(\lambda)$$

where

$N^1(\lambda)$ = Counts sec^{-1} at wavelength λ

$F(\lambda)$ = Incident flux (photons $\text{cm}^{-2}\text{sec}^{-1}$)

$R_p(\lambda)$ = Crystal peak reflectivity

$A(\lambda)$ = Aperture efficiency

Table 3.8 Calculation of SOLEX B Sensitivity as a Function of Wavelength.
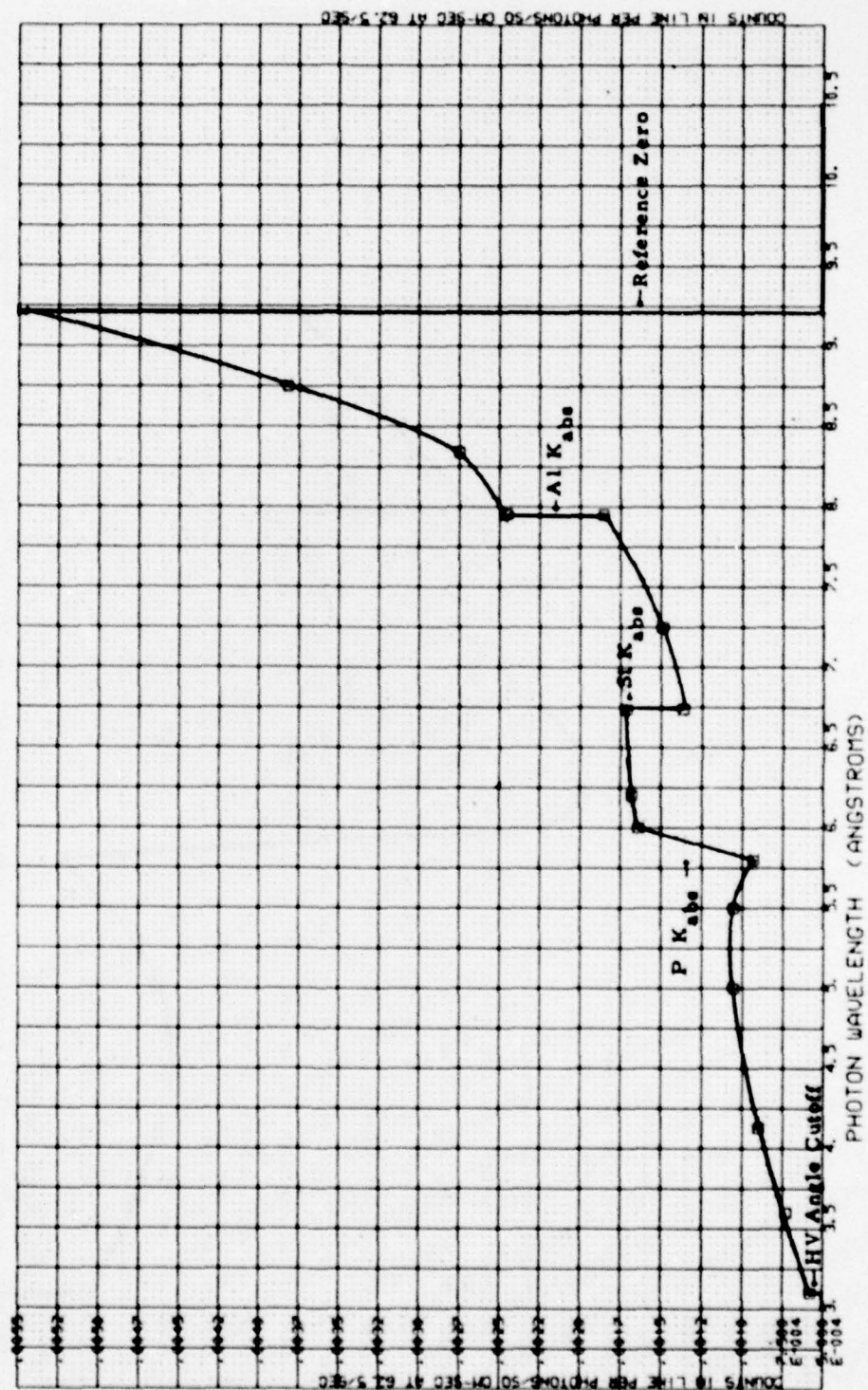
Figure 3.23. CRLS-229 SOLEX B ADP Calculation

3-57
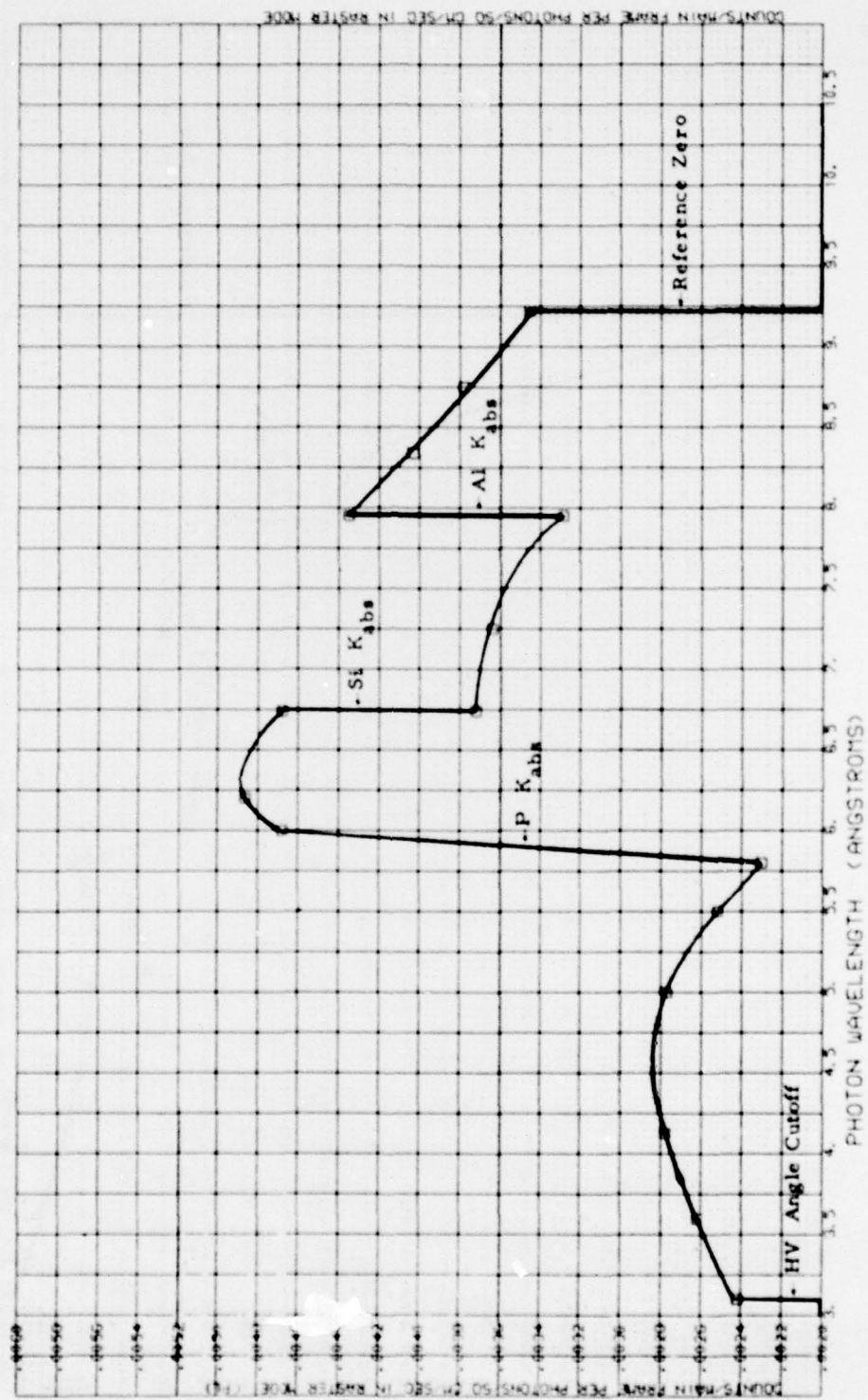
Figure 3.24. CRLS-229 SOLEX B ADP Calculation.

3-58
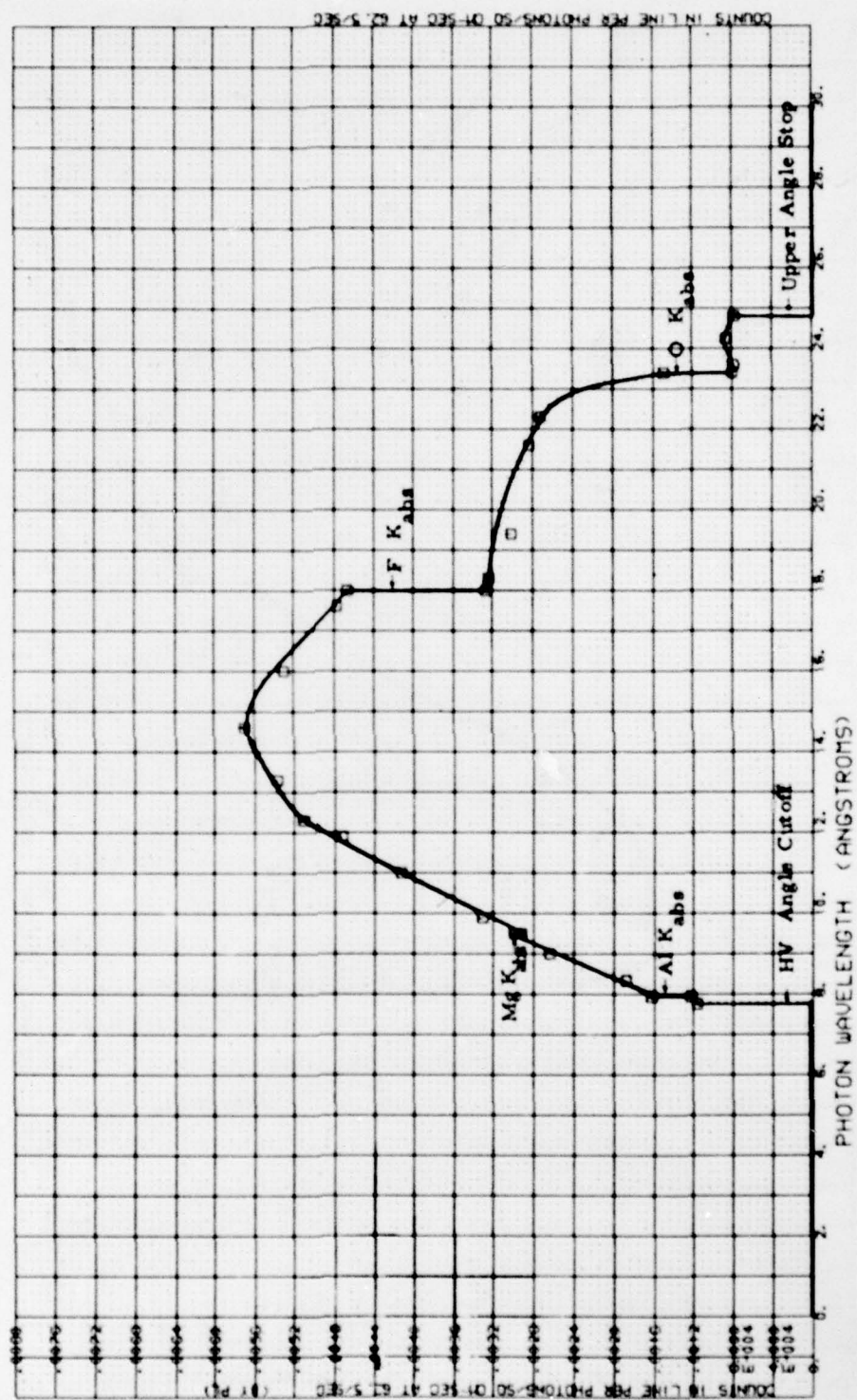
Figure 3.25. CRLS-229 SOLEX B RAP Calculation.
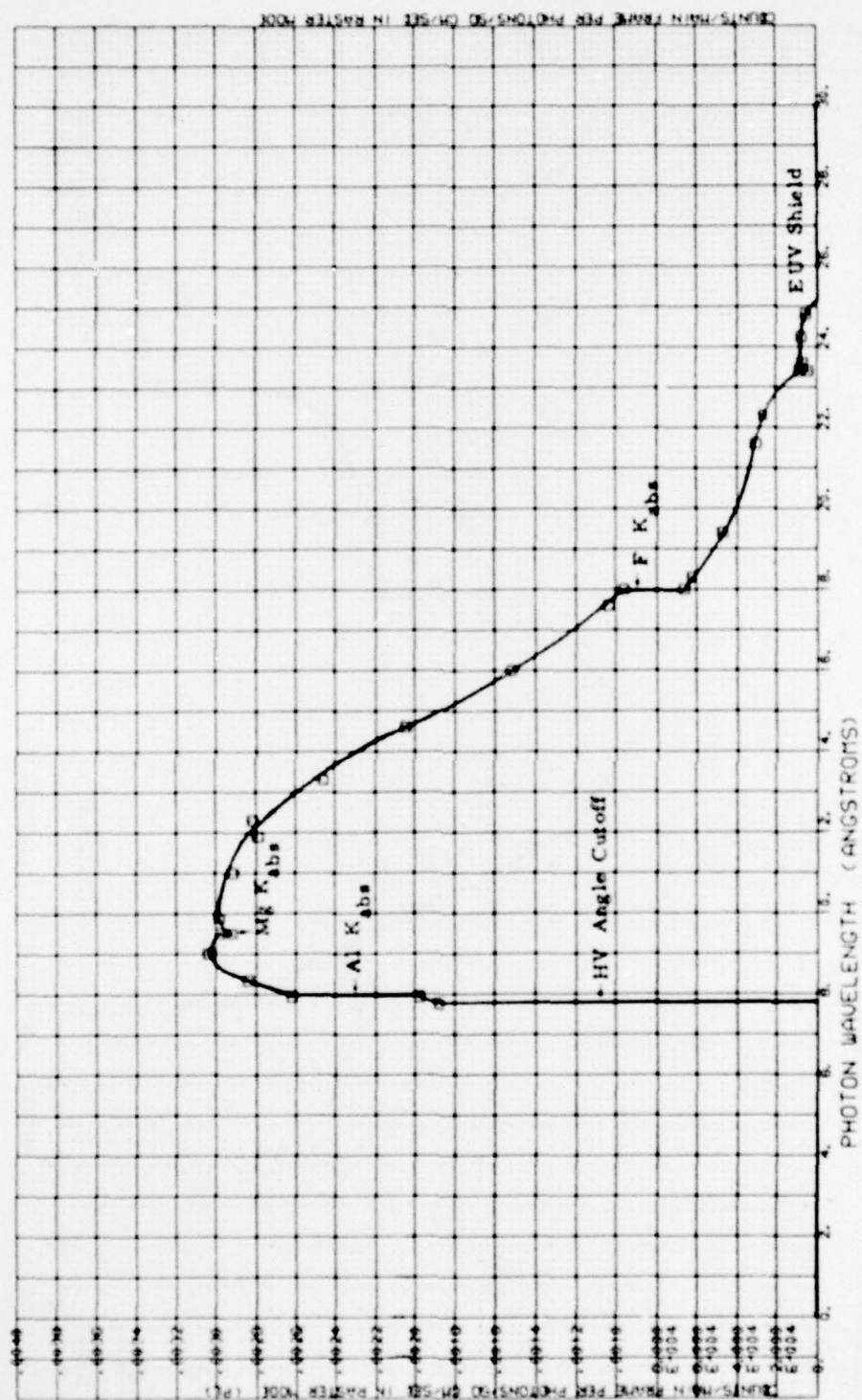
Figure 3.26. CRLS-229 SOLEX B RAP Calculation.

$$E_d(\lambda) \quad = \quad \text{Detector quantum efficiency (including EUV shield)}$$

and

$$C^1 \quad = \quad A_o \, t_a \, t_e \, e_{rt} \, f_d$$

where the above symbols were previously defined. In one spacecraft telemetry main frame (32 msec), the number of counts recorded is

$$N_{MF}(\lambda) = [N^1(\lambda) \text{ counts sec}^{-1}] [0.032 \text{ sec}].$$

To convert from $N_{MF}(\lambda)$ to $F(\lambda)$, multiply $N_{MF}(\lambda)$ by "FLUX/CTS/MF" in Tables 3.7 or 3.8 or divide N_{MF} by "CTS/MF/FLUX" given in Figures 3.19-3.26.

3.9 Calibration Source

In order to check the health of the SOLEX proportional counter and CEMA detectors, a magnesium fluorescence source excited by alpha particles from Cm^{244} is included. This Curium-244 source (Aerospace number 217) had a measured activity of 0.98 mCi on 1 January 1977 and a half-life of 17.6 years. A magnesium target is used to convert the alpha particles from this source to X-rays characteristic of excited magnesium atoms. Mg $K\alpha$ emission at 9.89Å is in the middle of the wavelength range for both detectors. The collimated source is located on the crystal panel in such a way that the two detectors view it only near the MAGMAP position (see Section 4.4). Collimation is such that most of each detector is illuminated. A 1.5×10^{-2} cm thick beryllium foil is used to shield the CEMA from most of the alpha particles emitted by the source. Counting rates in the MAGMAP position are 410 sec^{-1} for SOLEX A (1 sec^{-1} background) and 105 sec^{-1} for SOLEX B (35 sec^{-1} background), in the laboratory. Different backgrounds prevail in space.

3.10 Spacecraft Pointed Instrument Assembly (PIA)

Using the spacecraft PIA, CRLS-229 has the capability of being pointed at any part of the solar disk as well as forming a two dimensional solar map. A summary of PIA features is given in Table 3.9. An illustration of the spacecraft offset mode patterns is given in Figure 3.27.

3.11 Sample SOLEX Instrument Results

Data from all of the instruments in the CRLS-229 payload are recorded, whenever the instruments are on and can view the sun, on a P78-1 satellite tape recorder. These

Table 3.9. P78-1 Pointed Instrument Assembly.

	Large Raster	Small Raster
Map Size (azimuth x elevation)	43.92 min x 41.29 min @	4.88 min x 4.69 min
Number of Horizontal Lines +	64 @	16
Time per Raster	8.192 min @	61.44 sec
Time per Line	7.68 sec	3.84 sec
Time per Data Sample (MF)	32.0 msec	32.0 msec
Number of Data Samples per Line	240	120
Azimuth Displacement per Sample (MF)	10.98 arc sec	2.44 arc sec
Displacement in Elevation between Lines of Single Raster	39.33 arc sec *	18.76 arc sec
Center of Raster	Center of sun x	Offset Point Coordinates

	Offset Point
Number of Coordinates	128 x 128 = 16384
Angular Spacing of Adjacent Coordinates	20.75 arc sec azimuth, 19.66 arc sec elevation
Number of Bits in Offset Point Generator	7 azimuth, 7 elevation
Coordinate of Sun Center	(63.5, 63.5)
Location of Coordinate (0, 0)	Extreme upper left looking at sun
Effect of LSB in Large Raster Mode	Move down and right looking at sun

+ First line never scanned
* 19.66 arc sec between interlace rasters
x Could be offset by least significant azimuth bit and elevation bit.
@ 128 lines and 16.384 min for case of regular raster followed by interlace raster.

OFFSET MODE PATTERNS
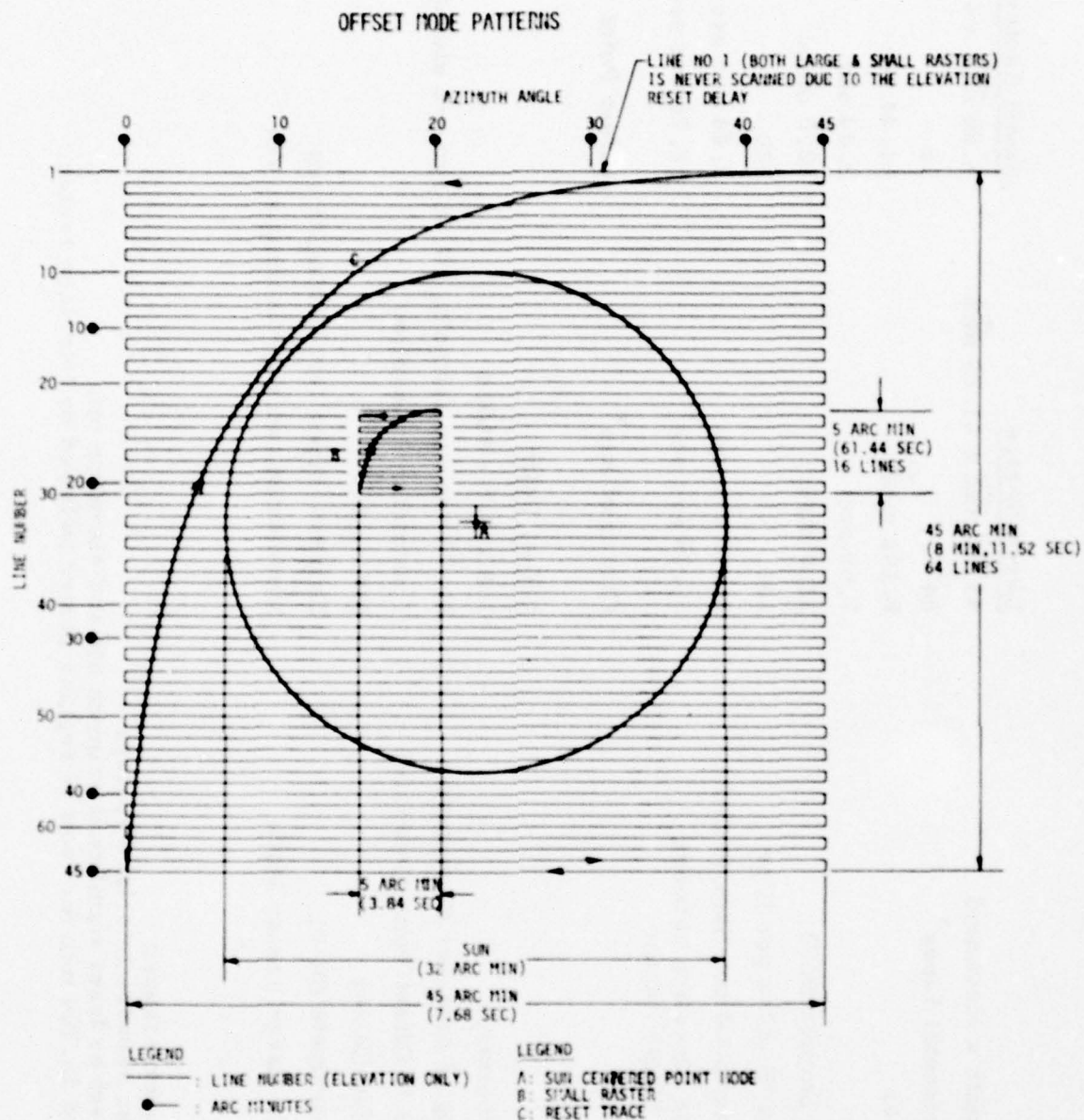
Figure 3.27. P78-1 Pointed Instrument Assembly Offset Mode Patterns.

3-64

data are transmitted to ground stations, at appropriate times, before the tape recorders are full. In addition, during satellite passes over ground stations data from the satellite and all of the payloads on board are transmitted to check satellite and payload health. Only limited data, typically for a few minutes from any payload, can be obtained on a single real time pass because of data transmission restrictions from remote ground stations. At the time of the writing of this paper we have received only such real time data. Further, we obtain only a single software mode which allows us to look at solar rastering maps (large or small), spectrometer spectral scans (SOLEX A or SOLEX B, not both) or MONEX data during real time passes. In the near future we will be receiving production tapes of all of the CRLS-229 payload data. The purpose of this section of this paper is to provide samples of data received to date showing the excellent spatial and spectral resolution of which the payload is capable.

3.11.1 Solar Maps in Single X-ray Emission Lines

Solar maps with 20 arc sec or 60 arc sec spatial resolution at command selectable wavelengths from 3 to 25Å are routinely generated. In a typical observing sequence SOLEX makes a selectable number of maps at one wavelength, then goes on to make the same number of maps at a number (typically 4 to 6) of other preprogrammed (by command) wavelengths. Small raster maps (5 x 5 arc min) take 61.4 sec to generate; large raster maps (45 x 45 arc min) take 491.5 sec.

Figure 3.28 is an example of a small raster map made with the 20 arc sec FWHM field of view spectrometer. This map was made at the wavelength of the resonance line of the helium-like ion Mg XI at 9.169Å. The observation is of active region 1638 (AR 1638) and was made at 0049 UT on 25 March 1979 during an M2 (x-ray classification) B

3	2	2	4	2	7	6	22	6	4	4	1	2	4	1
2	5	2	3	5	10	10	22	15	5	6	0	3	1	2
2	6	4	6	18	31	52	58	27	14	5	2	0	1	2
4	2	5	7	21	63	104	109	80	42	6	3	1	1	4
5	4	4	8	41	114	184	189	161	82	16	5	5	4	3
8	4	4	16	47	146	421	795	547	192	26	16	6	8	2
11	16	21	26	59	200	1003	3767	1360	159	30	9	19	11	5
4	10	16	11	24	96	237	605	324	102	23	10	8	5	1
12	8	10	6	18	54	112	135	152	63	16	8	9	4	5
7	9	6	6	8	21	59	121	89	37	15	8	7	2	4
4	5	10	11	12	18	24	40	26	11	12	3	5	8	6
6	6	8	6	17	8	13	16	11	7	11	17	13	13	11
2	7	11	10	9	11	14	19	9	9	7	12	17	12	8
4	2	6	5	11	4	7	8	10	5	7	6	3	11	12
3	1	5	6	4	1	5	5	10	6	1	1	4	6	10

Figure 3.28.   M2 B Subflare in AR 1638 observed at 0049 UT on 25 March 1979. The flare maximum was at 0040 UT. The SOLEX Å 20 arc sec FWHM FOV collimator was used to generate this map at 9.169 Å in Mg XI 1s-2p. Each number corresponds to the number of counts in 0.256 sec.

subflare that peaked in intensity (according to Hα ground-based observations) near 0040 UT. In the figure the spacing between the numbers corresponds to approximately 20 arc sec both horizontally and vertically, i.e., the map is about 5 arc min on a side. Each number corresponds to the integrated number of counts obtained in 0.256 seconds. The temporal resolution is actually eight times better than that; however, eight successive counting values on a single horizontal line have been added to allow a more compact presentation at a spatial resolution about equal to that determined by the collimator.

These data represent the first satellite-based x-ray solar maps made at this spatial resolution in a single x-ray emission line. As can be seen, the flare core is of small size (but not consistent with a point source) as has been reported earlier from observations made from x-ray telescopes on Skylab (Vorpahl et al., 1975; Kahler et al., 1975) with better spatial resolution, but over a broad range of x-ray wavelengths. A quick analysis of data presently on hand appears to indicate the sizes of active regions and flares are dependent on the x-ray wavelength in which they are viewed, a result consistent with most theories of solar flares and active regions.

The pointing stability of the pointed instrument assembly is very good and results in excellent spatial registration of successive raster maps. This means the development of an active region over a long period of time can be analyzed using raster data with confidence in the image registration. Furthermore, when activity is low or weak lines are being observed, statistics may be improved by simply summing a succession of rasters point by point, if the region under observation is not varying rapidly in intensity.

3.11.2 Spectral Scans of a Small Solar Region

The pointed instrument assembly (PIA) of the P78-1 spacecraft is capable of pointing the SOLEX spectrometers to any point on the solar disk with a resolution of 20

arc sec and a stability of better than 1 arc sec for a time of several minutes. At the times when the PIA is commanded into this "offset point mode," the SOLEX spectrometers perform spectral scans over a programmable series of wavelength ranges (usually 2 to 3 ranges are used for each spectrometer). In a typical sequence the spectrometers each perform a selected number (1 to 13) of scans over one wavelength range and then go on to perform the same number of scans over the remaining selected ranges. The Bragg crystal scan rate can be selected to be either 0.26 degree sec^{-1} or 0.52 degree sec^{-1}. By limiting the total scan of the spectrometer to a narrow wavelength range (by commanding the wavelength registers in the CRLS-229 memory) high temporal resolution over a limited region of the x-ray spectrum can be obtained while maintaining the excellent spatial and spectral resolution afforded by the SOLEX spectrometers.

An example of a single scan taken over a relatively narrow spectral region is shown in Figure 3.29. The data were taken using the 60 arc sec spectrometer with the RAP crystal scanning in the fast mode (0.52 degree sec^{-1}). The three strong emission lines seen are from the 2p - 3s multiplet of Fe XVII at wavelengths of 16.77, 17.05 and 17.10 Å. The observation was made at 1343 UT on 22 March 1979 while the spectrometer was pointed near the center of active region 1638. Ground-based observers reported that a Class 2N flare, observed in Hα, reached a maximum at $\simeq$ 1400 UT in this active region. This particular spectrum is shown to illustrate the excellent spectral resolution as indicated by the clean separation of the two emission lines at 17.05 and 17.10Å. This separation is equal to that achieved by any previous solar x-ray spectrometer and is somewhat better than that achieved by the previous best satellite-based measurements (Walker et al., 1974; Rugge and Walker, 1978). Somewhat better resolution may be anticipated when spectra are obtained in the slow step crystal scanning mode. In that mode integrated counts are read out after each motor step. In the fast scanning mode
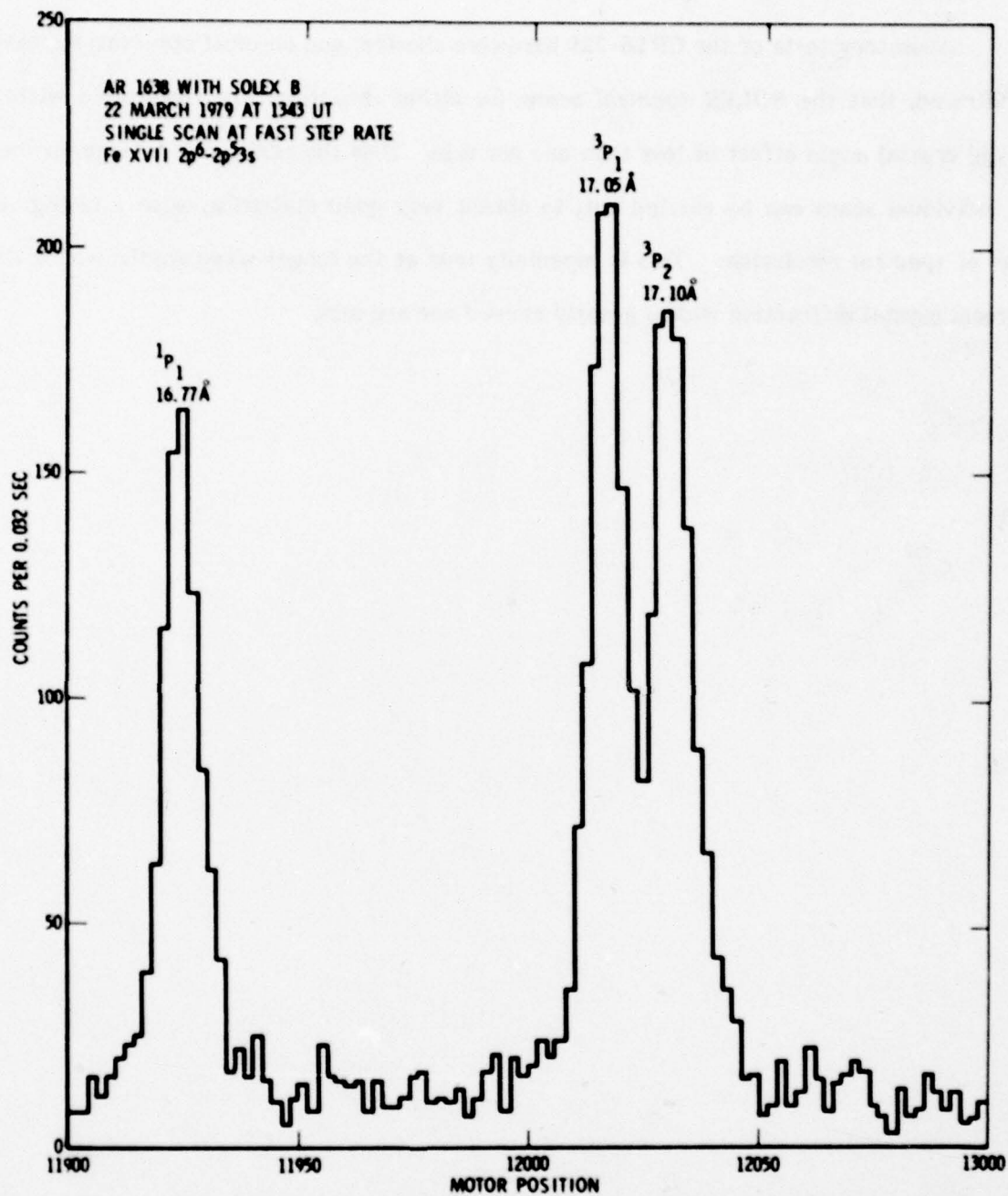
Figure 3.29. Short Spectral Scan of 60 arc sec Spectrometer Using RAP Crystal. The strongest lines seen are those of the 2p-3s transition in neon-like Fe XVII.

the counts from two consecutive motor steps are summed.

Laboratory tests of the CRLS-229 hardware showed, and on-orbit observations have confirmed, that the SOLEX spectral scans (in either direction) are repeatable with a Bragg crystal angle offset of less than one arc min. Thus the addition of a large number of individual scans can be carried out, to obtain very good statistics, with a negligible loss of spectral resolution. This is especially true at the longer wavelengths where the natural crystal diffraction widths greatly exceed one arc min.

4. COMMAND BOX ELECTRONICS

4.1 Command Box Functions

The Command Box is required to:

1. provide a memory consisting of twelve 16-bit words. These groups are required to reset into a pre-wired pattern whenever the standby power bus is turned on, and to be changable by spacecraft command to new patterns as required by the current SOLEX observation program. Ten of the words are used as SOLEX wave-length registers and two of the words are used as control registers (16 bits each).

2. receive and decode spacecraft serial magnitude commands so that the experiment memory can be changed.

3. receive and accumulate 4 inputs (13 bits each) from the main SOLEX and MONEX data lines. These are called the priority A signals SOLEX A, SOLEX B, MONEX A and MONEX B.

4. receive and accumulate 18 inputs from the SOLEX and MONEX auxiliary data lines (such as risetime and upper level discriminator rejects, and pulse height information). These are called the priority B or BSUB signals.

5. form the accumulated data into appropriate serial digital telemetry bit groups.

6. form the memory play-back bit groups into the appropriate serial digital telemetry signal, and format this with the priority B data into a 32 deep sub-commutated signal called BSUB.

7. form the SOLEX stepper motor position register into a format suitable for inclusion into the telemetry signal. This is the XMOTOR signal, a 16 bit group which is partially entered into the telemetry format in any one telemetry frame.

8. include in the telemetry digital signal a playback of the command box counter which indexes the 32-point commutator. This minor frame count (MFCT) signal is included in the instrument output for easing the data reduction burden in the group data handling process, as well as to facilitate the use of the lab test equipment during test and check-out.

9. receive and distribute internally to the command box the spacecraft telemetry clock and sync signals.

10. receive and distribute internally to the command box the spacecraft Raster Mode, Pattern Generator Disconnect, and Start of Raster (SOR) signals. These signals are used to control the operating mode of the command box, and thus the operating mode of the experiment.

11. receive the spacecraft Master Frame, Main Frame (not used) and the 31.25 Hz square wave sync signals, and to make up from these signals all timing pulses and levels required for the operation of the command box.

12. receive and distribute the 5 SOLEX orientation relay discrete commands which are needed internal to the command box (e.g., "Go to $\lambda 1$ Position").

13. receive the analog signals from the two refractosyn sun sensors mounted the SOLEX collimators, and convert these signals into digital bits included in the telemetry output shown in Figure 7.3 as B_1 and B_2.

14. receive the analog levels from three thermistors mounted in the main body of the CRLS-229 hardware, and supply these levels, suitably buffered, to the spacecraft.

15. receive 28 Volt DC power from the standby (launch) power bus in the spacecraft. This power operates the command box via an internal free-running inverter operating at approximately 25 kHz.

16. operate reliably for 1 year in orbit.

4.2 Command Box Circuit Description

A detailed description of the CRLS-229 command box is included in this section; it may be skipped by readers interested only in a more general description of this payload.

All digital logic is performed using Cosmos (RCA's CMOS) logic elements. These elements were purchased to a radiation hardened high relability specification from the vendor, and are rated at 1×10^5 rads (Si), equivalent to a one year mission in orbit.

Considerable use in the command box is made of digital comparators (a dual-in-line quad of these comparators) purchased to a MIL-STD-38510 specification. Occasional use is made of the analog operational amplifier type LM124, and of some discrete transistors, types 2N2222 and 2N2907A (MIL-STD-38510). One pair of junction field effect transitors, type 2N4091 and one pair of analog regulator microcircuits MIL-STD-38510) are also used in the power system. MIL-STD resistors, capacitors to the lowest failure rate available, and Spec 44 radiation cross-linked hookup wire 'ere used in the assembly of the circuitry.

The interface circuits are recorded in the Electrical Interface Control Drawing, Ball Document Number 49328. These circuits make use of the LM139 comparator, with internal reference levels of either +2 or +4 Volts, as required by the nature of the signal being received. All logic signals except the digital telemetry and command data signals (two lines) are negative TRUE, with the positive (FALSE) level being supplied by a pull-up resistor in the command box. This establishes compatibility of signal levels between systems. The two digital data signals are positive TRUE, with the positive level being supplied by a pull-up resistor in the receiver circuit.

The circuit descriptions are given in the following pages. The memory section of the command box is formed with an array of 24 type CD4034 registers. These chips each contain 8 bits of the required 16 per word. The power-on memory of pre-wired form is provided in the hard-wired jumpers on the cards, which force the register contents to the desired values. New data groups are loaded into these registers serially by the serial magnitude command clock and data signals. To address the desired register, an addressing word is first sent, containing a leading flag bit to define the group as an address, not a data group. Any number of such address groups can be sent, with the final one sent being the one acted on. A data group is then sent, with a leading flag bit

4-4

defining the group as data, not an address. This group serially enters only the register addressed. Any number of such groups can be sent, with the last two such groups defining the final value of the register. Since these address and data groups are 9 bits long, inclusive of the flag bit, it is necesary to send a minimum of one for addressing and two for filling a 16 bit memory word. After filling a memory word, the address pointer remains at this word, so that the address need not be present at a later time unless to change the word addressed. This memory of the addressed word is included in the telemetry read-out format so that the address of the pointer is always known. The complete contents of all memory words are also read out in the telemetry at a rate of once per 1.024 sec in the sub-commutated priority B information. In this entry and read-out scheme, the so-called control words in memory are treated the same as the wavelength words. All memory is entered and read as 16 bits, although the wavelength accuracy of the SOLEX hardware is restricted to 14, so that the top two bits must remain zeros in the case of the ten wavelength registers. Additional information about the structure of the CRLS-229 serial magnitude commands appears in the next section.

The raster control circuits receive the Offset Mode Status, Start of Raster, and Pattern Generator Disconnect signals from the spacecraft, and act on these to develop an indexing signal to step the wavelength pointer from one wavelength to the next. This serves to cause the SOLEX instrument to take data at a succession of wavelengths while the spacecraft is in a rastering mode of operation, with one or more rasters of the sun at each selected wavelength. The option of how many such rasters per wavelength is formed by predetermining a constant in one of the control words. This constant is used to limit the number counted in a register in the raster control circuitry. The raster control circuit also develops signals for use in other parts of the command box so as to control the way in which the instrument is ca ed to reset various registers and constants when the wavelength sequences are compeleted, or when the spacecraft mode changes from rastering to pointing.

4-5

The frame sync circuit receives the 31.25 Hz square wave sync signal, and the Master Frame signal (and the Main Frame sync signal, although this signal is not used in the command box), and from these signals develops the timing waveforms required by the telemetry system of the command box. These signals are used to load the telemetry shift registers at the correct times, and to index the counter which drives the 32 point sub-commutator circuit. This counter is kept in sync with the frame format of the spacecraft so that one complete cycle through the 32 items is done in 1.024 sec (i.e., in one half of a master frame). In the event of a start-up from a random condition, or loss of count state in the counter, this lost phase is corrected by the arrival of the next Master Frame pulse. Since the command box telemetry includes the actual state of this sub-com counter (MFCT), the data read out is still interpretable. It is sometimes possible for the telemetry system in the command box to clash with the fetch cycle of the wavelength registers in the memory: in case this occurs, a priority governs so that the SOLEX motor reference is loaded first, then the telemetry read-out of that memory word follows. Thus with a small probability (about 10^{-7}) there can be a load of incorrect wavelength data in the telemetry frame. This will be correctly loaded the next time. Similarly, during the transmission of a serial magnitude command or SMC (9 msec long), a clash can occur with the wavelength fetch from memory. Again, a priority circuit gives the time to the completion of the command (it cannot wait), and then allows the fetch from memory to take place (a 9 msec delay is less than the time assigned to the motor step time). In this case, there might also be an interference with the telemetry load cycle, with the result that the telemetry sub-com value could be zeros from that one frame. This will be correctly loaded on the following frame.

The wavelength reference register and associated circuitry receive the wavelength value from memory and compare this with a counter which indexes from the motor pulse train. In this way, the motor position counter keeps track of the current

position of the motor, assuming these registers have been reset to zero together. In spacecraft rastering modes, when the motor position counter agrees with the wavelength value, the motor pulses are stopped until either the wavelength value changes (say by command to that wavelength register), the called wavelength is changed (say by an indexing pulse from the raster control circuit), or the motor position counter is cleared (say by a change in operating mode). The same hardware is used to accommodate the spacecraft pointing modes, but in that case, when the motor position counter agrees with the wavelength value, then an output pulse is generated which indexes the wavelength called to the next one so as to develop a continuous scanning ('rocking') in wavelength. This wavelength reference circuitry also drives 60 μsec pulses at the 31.25 or 62.5 sec^{-1} rate to both SOLEX crystal and detector motors. These pulses are transformer coupled in the SOLEX hardware to avoid generating a ground loop problem between the two instrument boxes. Also, motor up/down information is formed and transmitted to the SOLEX hardware via a relay, again for the purpose of avoiding ground loops. The mechanical hardware is protected from hard running into the mechanical limits by the use of limit switches: these limit switch signals are also used in the wavelength reference circuits in the generation of end-to-end rocking of the wavelength range, and in the determination of where the electrical end-point of the wavelength range is located. The motor position counter is zeroed at the Reference Zero endpoint each time it is reached by the motor drive system.

The memory address counter circuit is used to keep track of the number of cycles of 'rocking' (TCOUNT), and the number of the selected wavelengths in 'rasters' (N) so that a pointer is always available to locate the desired wavelength register in memory. Binary comparisons are made in this circuit to determine when the reference constants (how many 'rocks', how many rasters per wavelength) are equal to the present conditions. Another feature, the sub-division of the ten wavelength registers into two types, is also

controlled. In this way, it is possible to vary the assignment of wavelengths to either 'rocking' end-points or to rastering locations. Thus, from ten assignments there can be eight end-points or 4 scan pairs ($N=1$), or eight raster points ($N=4$), with even numbered choices between these limits.

The control word formats are assigned to the two non-wavelength registers in memory, and consist of two 16 bit reference words, used as explained above as well as in the next section, to control the various options in the behavior of the instrument. Control is available over the detector high voltage values in SOLEX and MONEX and selection of one of the two motor rates is made. In the event of loss of power to the command box, the fall-back values of these constants given later in this section govern.

Telemetry accumulators are included, consisting of CD4040 binary counters and CD4034 registers, with two of each for each of the priority B data inputs (32 in all). A binary count up to $2^{16}-1 = 65535$ is available for each of the 18 inputs from SOLEX/ MONEX. This action, as explained above, is interleaved with the telemetry read-out of all 12 memory words. The remaining two assignments in the sub-com total of 32 are two words containing 32 discrete binary values from various points within the Command Box. These words are called DFORM1 and DFORM2.

The B priority (BSUB) circuit is used to load the digital housekeeping sub-com data at the correct time in a telemetry frame, and to steer the two eight-bit halves of these data into the correct telemetry frames (a single eight-bit assignment in the main digital format is used to transmit the 32 sub-com values, each of 16 bits, by time-multiplexing these halves). Each of these 32 values is read out once every 1.024 sec.

A memory read timing circuit, based on the internal sub-com counter, is used to steer the sub-commutated data items, and thus to make up the telemetry format. The motor position read-out (XMOTOR) is particularly complex, as 14 bits of motor position

are interleaved with 4 bits of TCOUNT, and two bits from the sun sensors. TCOUNT is the binary value for the current number of spectral scans. This whole sub-group is transmitted in such a format that time resolution of the LSB of the motor position is 16 msec. A secondary feature of this circuit is the generation of a position-dependent suppression signal for the SOLEX detectors (see Section 4.7).

The main telemetry output of CRLS-229 is the readout of the SOLEX A (or 1) and B (or 2) and the MONEX A (or 1) and B (or 2) detectors. These four values are accumulated in 16 bit counters and serially shifted out once per main frame. This corresponds to an overflow counting rate of 2.56×10^5 counts sec^{-1} input to any of the four. They are interleaved by steering signals from the frame sync pulse circuits. See Figure 7.3 for a description of the 29-1 telemetry format which includes the four main payload outputs above as well as others mentioned in this section.

The telemetry clock and strobe signals are received in this system (although the strobe is unused by the command box) at a burst rate of 125 kHz gated clock pulses. The output telemetry signal is driven into the spacecraft harness by an active-low LM139 driver in series with 400 ohms for surge protection. The level is clamped at an upper limit of 12 volts by a zener diode. Pull-up is provided by the receiver circuit in the spacecraft. Data is positive TRUE as noted above.

The discrete commands "Go to Lambda 1 On/Off" and "Go to MAGMAP Position On/Off" drive latching relays. These relays will store the command state sent, independent of the presence of power in the command box. Discrete command "Go to Reference Zero" causes a momentary switch closure.

The optical boresight axis of the CRLS-229 collimator is coaligned with the optical axis of the collimators. These sensors give rise to one-bit signals in the digital telemetry. Analog amplifiers, type LM124, are used for the purpose. The digital

4-9

threshold is set at 1 arc minute on the sun sensors, and is interpreted by monitoring the time of switching during a spacecraft raster operation. The two telemetry bits (B1,B2) are both 1 whenever the Spacecraft Pointed Instrument Assembly is pointing to within about 1 arc min of the center of the sun (as well as at night).

4.3   Command Box Power

The power supply section of the command box is required to provide operating DC power for the command box only. The power consumption is 0.9 watt, independent of mode. The requirements of the Interface Control Drawing regarding input-output isolation are met by making use of a self-excited inverter circuit operating on a 25 kHz symmetrical square wave. The secondary of the isolation transformer is operated at 15 volts DC, both positive and negative, with active series regulators used to provide ± 10 volts for the logic system power. Current limits on these lines are set to allow for up to a four-fold increase in the amount of DC power demanded by the logic system, as the inevitable effects of radiation damage to the CMOS slowly raise the requirements. Thus, some increase in the life expectancy of the circuit is provided. The end-point failure mode is expected to be a collapse of the power bus with load demand of about 2 watts.

4.4   Control Word Option Bits and Commands

When standby (or launch) power is initially turned on, all memory registers are reset to the hard-wired pre-programmed values (mentioned later in this section), and the SOLEX crystal and detector motors are driven to Reference Zero. If the spacecraft is rastering (Offset Mode Status from the spacecraft greater than 2V), the satisfaction of the Reference Zero condition is followed by motion to the first lambda position (λ_1).

After M rasters are counted while at position λ_1, the motors drive to position λ_2. After M rasters are counted at position λ_2, the motors drive to position λ_3. This continues until position λ_{2N} is completed, at which time another call for Reference Zero position occurs. 2N can be any even number from 2 to 8. Values of M and N are stored in Control Register 1.

If RTE (Raster End, a signal constructed within the command box) occurs during the above sequence, then the sequence terminates at that point, and Reference Zero position is called. The lambda sequence of positions (LCALL) is reset at this time to the first position if control bit P is "1", or is left at the current location if P is "0". This option bit P is stored in Control Register 1; it can be altered by reloading this register. If WLC (a signal from the S/C called Pattern Generator Disconnect) is received during the above rastering sequence, signifying that a coronagraph exposure request from the NRL-401 experiment is being allowed, then option bit P allows or disallows the lambda sequence reset as above.

When the signal 'Raster' is False (Offset Mode Status less than 2V), the above operation is modified: the motors drive to the first stored lambda position beyond the location defined by value N. This is called a λ_e ("end") value. These λ_e's are stored in pairs, and the allowed values of N given above permit storage for 1, 2, 3, or 4 pairs of λ_e's. The sequence of λ_e pairs is then called, with the motors driving back and forth between the two members of a λ_e pair until a total of T passages ("rocks") has taken place. T is a number stored as three bits in Control Register 1, and can require any odd number of one-way passages (2T-1) from a λ_e to its mate, from 1 up to a maximum of 13. The end of such a set of rocks calls for the motor to go to the position for the next rock between the next stored pair of λ_e's. When all stored pairs of λ_e's have been scanned, position Reference Zero is called. The above sequence then restarts as before, until the signal 'Raster' is received from the spacecraft. During rocking, the telemetry

4-11

read-out contains the current passage number TCOUNT. Time resolution of this number is 64 msec. The passage number TCOUNT will be zero while the motors are traversing the region between rocking regions. An example of SOLEX rocking programs is given in Figure 4.1 for the case of N=1.

Option bit R is available to determine if the spacecraft signal, WLC, is to be allowed to call Reference Zero during rastering sequences. If this bit is "0", then WLC itself has no effect on the raster sequencing, unless bit P is one, in which case WLC resets the raster wavelength to $\lambda 1$.

Option bits P' and P" are available to choose the effects of the end of rastering (not a WLC interrupt, but a spacecraft change from rastering to a pointing mode). If P' is "1", it allows the M counter to be reset by the end of rastering. If P" is "1", it allows the λ_e counter TCOUNT to be reset by the end of rastering. As stated above, if the option bit P is "1", it allows the spectrum line counter to be reset to $\lambda 1$ by the start of rastering. Thus, the three option bits P, P', and P" are available to determine the condition of storage of the sequence, and the point in the subsequent routine where interrupted events are to be recommenced.

A further option bit Q is available to determine if the sequence of T rocks between each of the stored λ_e pairs is to be followed by a transition to full rocks (scans from one microswitch limit to the other) or by a repeat of the previously described sequence of stored rocks (Q=0).

Option bit S is assigned to allow or to prevent the continuance of the routines during the presence of a MAGMAP state. It is possible that while the instrument is held in the MAGMAP state, SOR, WLC, and Raster signals are still received and appropriately counted. If this is what is desired, bit S is set at "1". Otherwise bit S = "0" will prevent
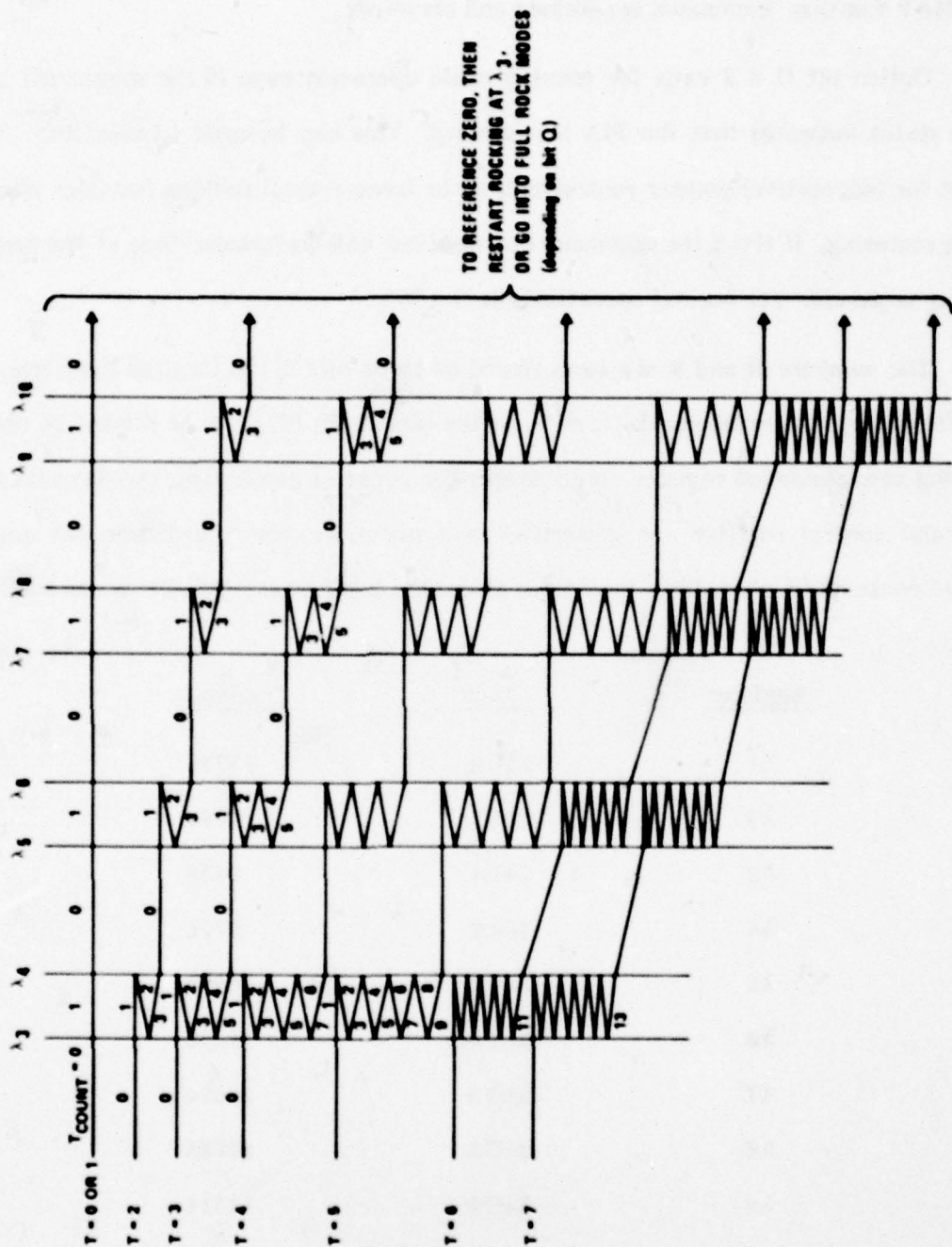
Figure 4.1. SOLEX Spectrometer Rocking Motion as a Function of T for N = 1. Several values of TCOUNT are given.

the system from recognizing any external events until the "Go to MAGMAP Position Off" command is given. In this state, the original configuration, interrupted by the "Go to MAGMAP Position "command, is retained and resumed.

Option bit $G = 1$ calls for rocking mode operation even if the spacecraft offset mode status indicates that the PIA is rastering. This can be used to substitute for an absent (or inoperative) pointer rock signal, or to force crystal rocking behavior when the PIA is rastering. If $G = 1$ the command box does not call Reference Zero at the end of a rocking sequence. For normal operation, bit $G = $ "0".

The numbers M and N are each stored as three bits in the Control Registers. Any modification of the numbers M, N, or T, or the bits P, P', P", Q, R or S must be done by entering new command register contents. In the event of power loss, the numbers in the command control register are generated in a pre-determined hardwired set and any altered contents (if alterations have been made) are lost. These default values are:

Register	Hex	Decimal
$\lambda 1$	35DA	13786
$\lambda 2$	318E	12686
$\lambda 3$	24EA	9450
$\lambda 4$	260A	9738
$\lambda 5$	29CA	10698
$\lambda 6$	2CDA	11482
$\lambda 7$	2D9A	11674
$\lambda 8$	31CA	12746
$\lambda 9$	34CA	13514
$\lambda 10$	3DEA	15850
CONT 1	22C7	8903
CONT 2	282A	10282

4-14

The default values are M=2, N=1, P=0, P'=1, P''=1, Q=0, R=0, S=0, T=7, V12=01, V34=01, G=0, V5=0, V6=0, and F=0. CONT1 and CONT2 are described later in this section.

In the event of a WLC interrupt during a non-raster interval (as, say, when the spacecraft is offset pointing for spectrometer rocking), no action is taken; the instrument simply continues its rocking mode sequence. The RAS rastering and the WLC (or PGD) signals are included in the telemetry data with time resolution of 1.024 sec, so that confusion as to the actual sequence of the pointer during these signals can be resolved.

To allow MAGMAP observations and calibrate SOLEX, the latching command "Go to MAGMAP Position" is given. This initiates a Go to Reference Zero action, after which only the crystal motor is driven to the Bragg Zero position, leaving the detector in the Reference Zero position. This arrangement is held until the "Go to MAGMAP Position Off" command is given. Receipt of this command causes the original routines to apply after the crystal panel is driven to Reference Zero and "picks up" the detectors.

The command "Go to Reference Zero Position", is a momentary command which can be used to cause the system to drive into the -60 degree limit position and zero the motor position counter. This will be sent during orbit nights and if a noisy environment is suspected of causing counter skip so that the SOLEX motor position is properly indexed at the start of day operation.

The command "Go to λ_1 Position" is a latching command which can be used to interrupt the routine in either rastering or non-rastering operation. The stored value in the memory location 1 is used to hold the motor position of both crystal and detector, while any spacecraft pointer operation takes place. This permits time dependence of a particular spectral line to be developed while in a raster or pointing mode. The $\lambda 1$ position is held until the command "Go to λ_1 Position Off" is given.

4-15

Several nonsense values can conceivably be sent for values of the numbers M, N, or T. These three bit groups are decoded in such a way that if N=000 (signifying that no λ_i values of memory are to exist), then a value of N=001 is substituted (four regions of rocking). This is because of hardware conflict that would arise otherwise. The actual condition N=000 is however a recognized condition, and it is used to do the same as bit G="1" described above, i.e., it forces rocking, as is implied by no λ_i values. Since the memory is limited to a total of ten locations, the N group is not allowed to recognize values in excess of the binary number 100. Thus, if the values 101, 110, or 111 are sent, the hardware substitutes 100 for these: otherwise the memory pointer which marks the boundary between λ_i values and λ_e values would go off scale. No action is taken on receipt of these suppressed codes. M can be sent as a value 000, for which the number 001 is substituted since zero rasters per λ_i is not recognized. Likewise, the T group is prevented from seeing a 000, and 001 is the substituted value.

Included in the control registers are six HV bits, which can be used to command the output value of any of the four SOLEX and MONEX high voltage power supplies. The normal On state of these power supplies is with V12="00", V34="11", V5="1" and V6="1".

4.5   Serial Magnitude Command Structure

1. λ (lambda or wavelength) Registers and Control Registers contain 16 bits each:

        1 2 3 4 5 6 7 8 9 10 11 12 13 14 15 16

The MSB (1) is leftmost. SOLEX operation is determined by these registers.

4-16

2. Serial magnitude commands should always be sent to the CRLS-229 experiment in groups of 3. (The circuitry was originally designed for a 21 bit SMC.)

3. First SMC (9 bits):

    1 0 0 0 0 X X X X   The X bits give the storage register address within CRLS-229 as follows:

$$0\ 0\ 0\ 1 = \lambda_1$$
$$0\ 0\ 1\ 0 = \lambda_2$$
$$0\ 0\ 1\ 1 = \lambda_3$$
$$0\ 1\ 0\ 0 = \lambda_4$$
$$0\ 1\ 0\ 1 = \lambda_5$$
$$0\ 1\ 1\ 0 = \lambda_6$$
$$0\ 1\ 1\ 1 = \lambda_7$$
$$1\ 0\ 0\ 0 = \lambda_8$$
$$1\ 0\ 0\ 1 = \lambda_9$$
$$1\ 0\ 1\ 0 = \lambda_{10}$$
$$1\ 0\ 1\ 1 = \text{Control} \quad 1$$
$$1\ 1\ 0\ 0 = \text{Control} \quad 2$$

"1" indicates an address;

MSB and first bit in leftmost.

4. Second SMC (9 CRLS-229 bits):

    0 1 2 3 4 5 6 7 8

"0" indicates not an address, but data.

MSB and first bit in leftmost.

4-17

5. __Third SMC__ (9 CRLS-229 bits):

0 9 10 11 12 13 14 15 16

6. In each lambda register, bits 1 and 2 are always zero, bit 3 corresponds to 8192, bit 4 to 4096, ... and bit 16 to 1. Therefore, the following sequence of SMCs:

$$1\ 0\ 0\ 0\ 0\ 0\ 0\ 1\ 0$$

$$0\ 0\ 0\ 1\ 1\ 1\ 1\ 1\ 1$$

$$0\ 1\ 1\ 1\ 1\ 1\ 1\ 1\ 1$$

would load λ Register 2 with the largest possible wavelength value, namely 16383_{10} or $3FFF_{16}$. (To protect the SOLEX drive, do not command to a wavelength value greater than 16055_{10} or $3EB7_{16}$).

7. Construction of Control Register Words

MSB and first bit in leftmost.

	MSB															LSB
Bit Number	1	2	3	4	5	6	7	8	9	10	11	12	13	14	15	16
Control 1	-	M1	M2	M3	N1	N2	N3	P	P'	P"	Q	R	S	T1	T2	T3
Control 2	-	V1	V2	V3	V4	G	V5	V6	-	F	-	-	-	-	-	-

- indicates bit is unassigned.

For multi-bit numbers in Control Register 1, the bit called "1" is the MSB.

For example, M1 is the MSB of M.

4-18

8. A summary of the definitions (and allowed values) of the Control Register contents previously described is given below:

F - If 0, fast motor speed (62.5 Hz)

If 1, slow motor speed (31.25 Hz)

(0 or 1).

G - If 1, forces crystal rocking (independent of PIA mode)

(0 or 1).

M - Number of sequential rasters at each wavelength

(1 to 7, inclusive).

2N - Number of stored wavelengths (λ_i's) for raster maps; the number of scan pairs is therefore 5-N.

(N x 2 = 2, 4, 6, or 8).

P - If 1, there is a reset to the first λ position at the start of rastering (RAS goes from 0 to 1); or if RAS is one and PGD changes from 0 to 1; if P = 0, the pointer position does not change at this time.

(0 or 1).

4-19

P' - If 1, the M counter is reset by the end of rastering (S/C, not ITS derived); if P' = 0, this counter is not reset at this time. (The ITS circuit is described in Section 4.8.5.)

(0 or 1).

P" - If 1, the λ_e pair is reset to λ_{2N+1}, λ_{2N+2} at the end of a raster sequence. (The T counter is always reset at the end of a raster sequence.)

(0 or 1).

Q - If 1, starts full rocks after stored rocking sequence, if 0, calls Reference Zero and repeats stored rocking sequence.

(0 or 1).

R - If 0, Pattern Generator Disconnect from ITS does not reset counters; if 1, calls to Reference Zero and then continues where it left off.

(0 or 1).

S - If 0, MAGMAP operation freezes SOLEX MCOUNT register and SOR's are not counted; if 0, M counter changed by SOR's.

(0 or 1).

2T-1 - Number of rocks between two end wavelengths (T = 1 through 7) (1, 3, 5, 7, 9, 11, 13).

4-20

V1, V2 - 3 increasing values of SOLEX A (PC) high voltage

(00, 11, 01).

V3, V4 - 3 increasing values of SOLEX B (CEMA) high voltage

(00, 11, 01).

V5 - 2 increasing values of MONEX A (LEM) high voltage

(1 or 0).

V6 - 2 increasing values of MONEX B (HEM) high voltage

(1 or 0).

4.6   Spacecraft Signals Affecting SOLEX

There are 3 signals from the spacecraft to the command box which influence the SOLEX operational sequences.

1.   Offset Mode Status. This analog signal is used to indicate the configuration of the PIA. The amplitude of this signal is 5, 3, 1, and 0 V in the large raster, small raster, offset point, and sun centered point modes, respectively. In DFORM1, RAS equals 1 in either raster mode.

2.   Start-of-Raster (SOR) Pulse. The SOR pulse is generated at the start of each large or small raster of the PIA. SOLEX operation is affected by the

leading edge of this pulse. Receipt of an SOR pulse is reflected in the housekeeping word DFORM1.

3. Pattern Generator Disconnect (PGD) Status. This signal goes high (to 5 V) when the ITS (see Section 4.8.5) system releases the PIA from pattern generator control and goes to sun center pointing as a result of the WLC exposure request and remains high until pattern generator control is resumed. This status is also given in DFORM1.

4.7 SOLEX Angle High Voltage Cutoff

In order to protect the SOLEX detectors from directly viewing the sun (see also Section 6.3), the command box automatically disconnects the low voltage input to both SOLEX HVPS's between XMOTOR step number 5120 and 9216. S_{HV}, the least significant bit of DFORM 2, equals 0 when this condition occurs. The SOLEX high voltage is also disabled when the spectrometer is heading for Reference Zero position, for the same reason.

4.8 SOLEX Operational Modes

The operational modes of the SOLEX experiment are discussed below for a situation in which the CRLS-229 experiment has full control of the PIA (see Section 3.10). When the ITS system is in operation (described later in this section), SOLEX may continue its program of observations while NRL-401 (the other experiment sharing the PIA) returns the pointing to sun center or it may restart the raster sequence, call Reference Zero, or both. Which alternative is operative depends on the status of certain bits in the control registers.

4-22

4.8.1 Spectrometer Spectral Scan Mode

(1) PIA is in the offset point mode (not in raster mode except if control register allows spectrum mode while rastering).

(2) $2N$ λ registers (N set in control register 1) contain λ_is. There are thus 5-N pairs of spectral scan end points (λ_e pairs).

(3) Spectrometer performs $2T - 1$ (T = 1 - 7, set in Control Register 1) scans (or rocks) between the first pair of λ_e's.

(4) Spectrometer repeats step 3 with each λ_e pair until all pairs are done.

(5) Spectrometer drives to wavelength reference point.

(6) Sequence repeats unless PIA mode or Control Register has changed.

(7) If $Q = 1$ (bit in control register 1) each complete set of scans between all λ_e pairs is followed by full end-to-end spectral scans until the PIA mode is changed or the spectrometer is commanded out of the full scan mode.

This mode is illustrated in Figures 3.29 and 4.1 and will be used frequently.

4.8.2 Raster (Spectroheliograph) Mode

(1) PIA is in the large or small raster mode.

(2) M (1-7, set in Control Register 1) rasters are performed with the spectrometer parked at wavelength position set in the first λ register.

(3) Repeat step two at each position up to the Nth λ register.

(4) Spectrometer returns to wavelength reference point.

(5) Sequence repeats if the PIA mode and control registers are unchanged.

Raster maps are illustrated in Figures 3.27 and 3.28. This mode of operation will be frequently implemented.

4.8.3 Time Variation Mode

(1) PIA is pointed at a specific location (no raster).

(2) Spectrometer observes, while stationary, at a specified wavelength position (λ_1).

This mode will be used infrequently.

4.8.4 Crystal Rocking in Raster Mode

(1) P78-1 PIA in the small or large raster mode.

(2) SOLEX control bit G = 1 forces crystal rocking.

This mode will be used infrequently.

4.8.5 Instrument Time Share

There exists a spacecraft module called the Instrument Time Share (ITS) circuit which is used to shift control of the spacecraft PIA between CRLS-229 and NRL-401. From the flowchart in Figure 4.2, it is evident that the PIA will alternate between offset point or raster and sun center operation when it is controlled by the ITS module. This mode will be used frequently in conjunction with the modes described in Sections 4.8.1 and 4.8.2. Control bits P and R mentioned in Section 4.4 can affect the raster observation program.

4-24
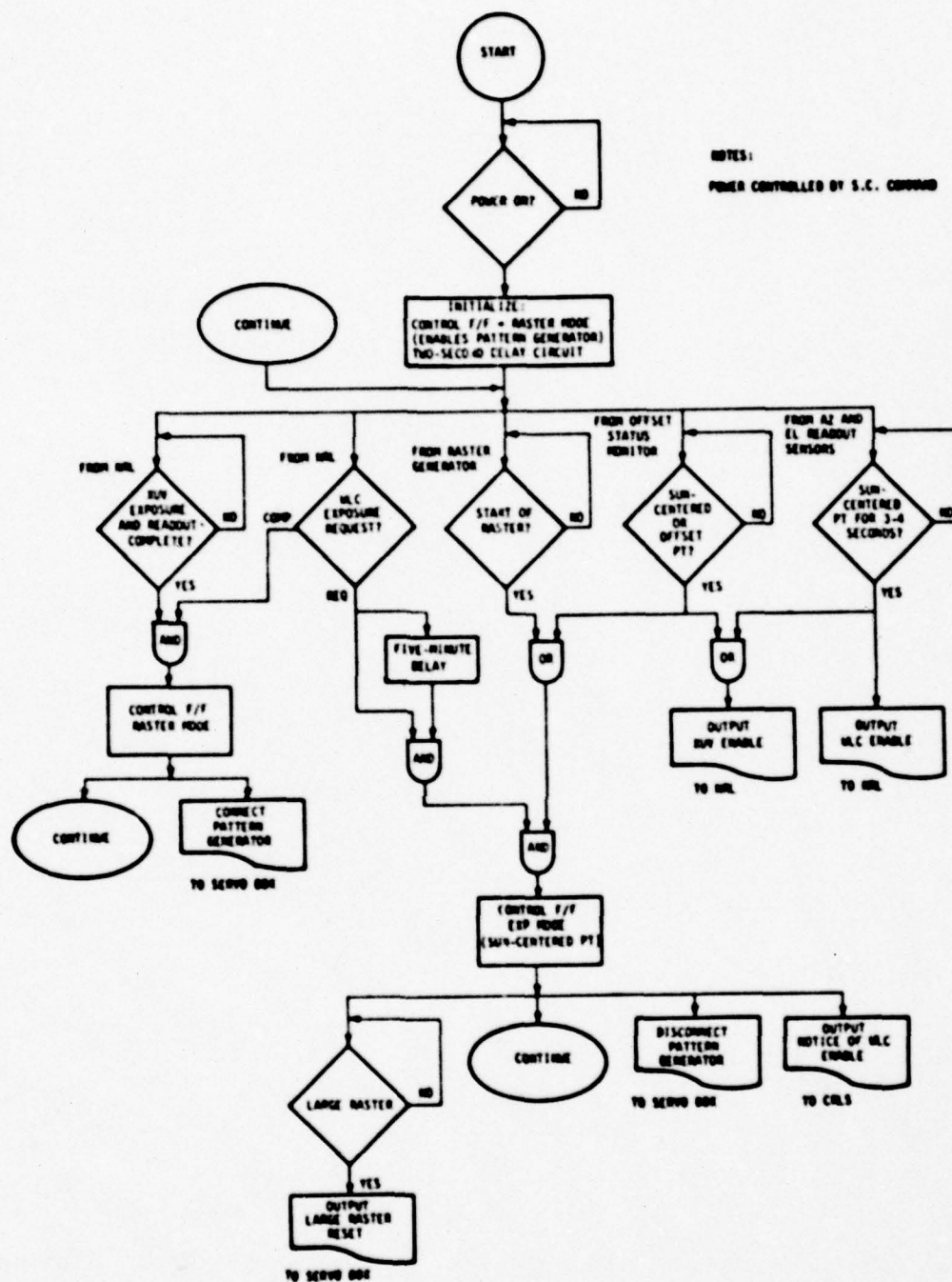
Figure 4.2. P78-1 Instrument Time Share Flow Chart.

5.   MONEX LOW ENERGY MONITOR

5.1   Module Description

The MONEX Low Energy Monitor (LEM) module (also called MONEX A) consists of a small stationary sealed proportional counter and associated electronics, and is designed to monitor the solar soft X-ray flux in the energy range 1-22 keV during flares. Its main utility lies in separating temporal from spectral and spatial effects in the SOLEX and SOLFLEX flare measurements, in the determination of flare line-to-continuum ratios and in providing a quick-look measure of the daily level of solar activity. A photograph of the flight LEM Module is presented in Figure 5.1.

A summary sheet for this experiment is given in Table 5.1. A drawing of the proportional counter is presented in Figure 5.2. Measurements of the LEM detector effective beryllium window and gas thicknesses were made by comparison with a calibrated standard counter of known efficiency. The window thickness of the LEM detector was first determined using Al K and Mg K X-rays for which the gas efficiency of the standard counter was expected to be unity; it was found to be $1.06 \pm .03 \times 10^{-2}$ gm cm^{-2}. The gas pressure was then found to be about 1.0 atmospheres by making comparisons to the standard counter efficiency with an Fe^{55} radioactive source (Mn Kα, 5.9 keV). The counter manufacturer claims that the window thickness is $9.4 \pm 0.9 \times 10^{-3}$ gm cm^{-2} and the gas pressure at 24°C is 1.10 atmospheres. The LEM counter efficiency as a function of energy was determined by assuming a window thickness of $1.00 \pm 0.06 \times 10^{-3}$ gm cm^{-2} and a gas pressure of 1.10 atm and then calculating the efficiency using the window and gas absorption coefficients, tabulated by Storm and Israel (1970). The results of this calculation are given in Figure 5.3. Note that the lower and upper e^{-1} cutoff energies are 1.9 and 8.5 keV, respectively. Six pulse height channels divide the energy range between 1 and 22 keV as shown in Table 5.2.
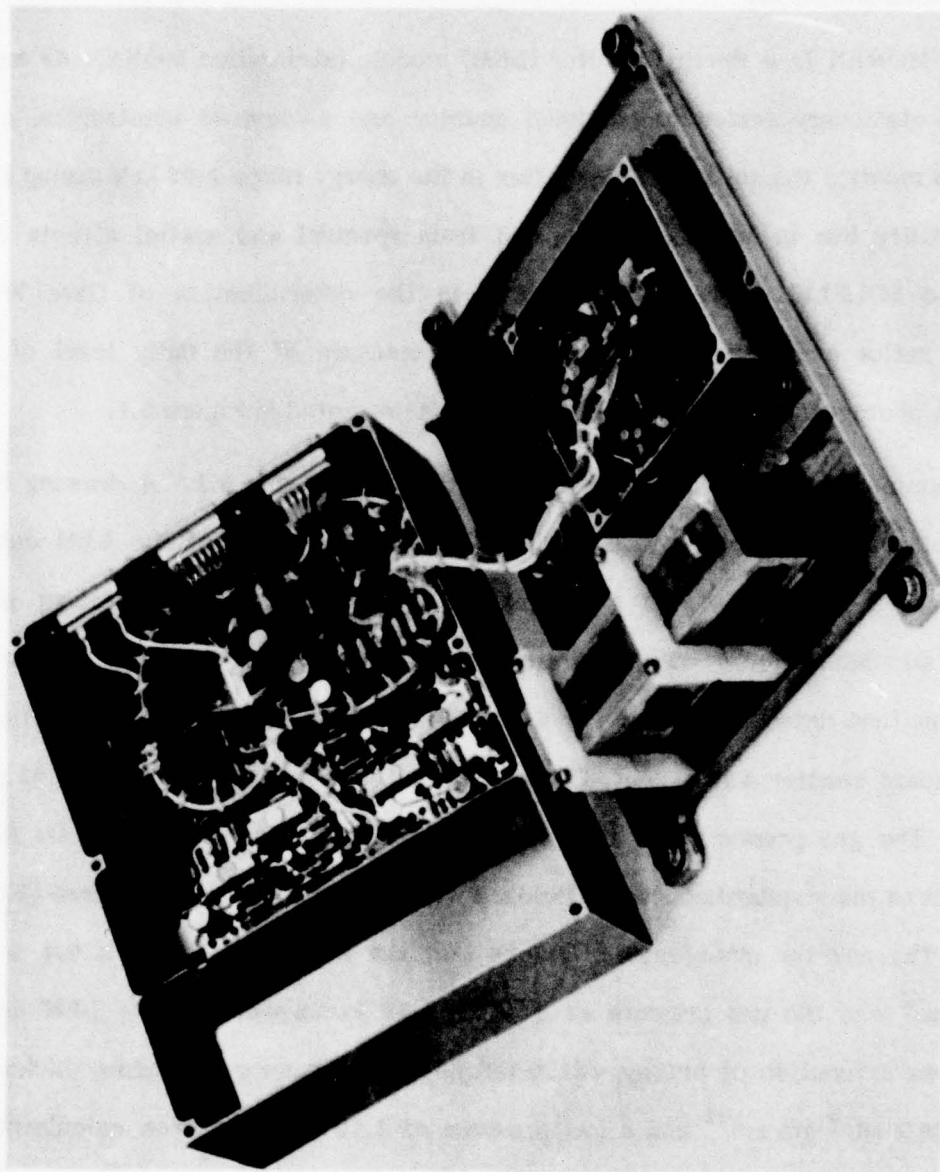
Figure 5.1. Partially Disassembled Low Energy Monitor Module, MONEX Experiment.

Table 5.1. MONEX Low Energy Monitor

Proportional Counter Size: 1.00 in x 1.00 in x 3.00 in

Counter Window Area: π (0.020)^2 = 0.00126 in^2 = 0.00811 cm^2
   (collimated)

Collimation: Two circular holes of diameter 0.250 in
                                  and 0.040 in separated by 9.0 in

                                  100% transmission for offset angle $\leq$ 0.668°

                                  0% transmission for offset angle $\geq$ 0.923°

Counter Window Thickness: 0.0021 in = 0.010 gm cm^{-2} beryllium ($\pm$ 10%)

Counter Fill Gas: 80.0% Argon, 10.0% Xenon, 10.0% Carbon Dioxide

Counter Gas Thickness: 0.750 in = 0.00429 gm cm^{-2}

Counter Gas Pressure: 1.10 atm = 836 Torr

LND Counter Model Number: 424 (S/N 60840)

Time Resolution: Integrated count rate data = 32.0 msec
                                  Pulse Height Data = 1.024 sec

Efficiency Calculation: Same cross section as used in HEM

                                  Direct calculation

                                  Computer program LAND

Background Counting Rate: 0.4 sec^{-1}
   (at sea level)

5-3

BERYLLIUM WINDOW

$\frac{3}{4}$ DIA.

3"

$1\frac{1}{2}$

MATERIAL
ALUMINUM

BLANK SIZE

SCALE 1:1

LND, INC.

TITLE SQUARE, SIDE WINDOW, PROPORTIONAL COUNTER

TUBE TYPE 424

PLOT NO. 424-2

Figure 5.2.   MONEX Low Energy Monitor Detector.
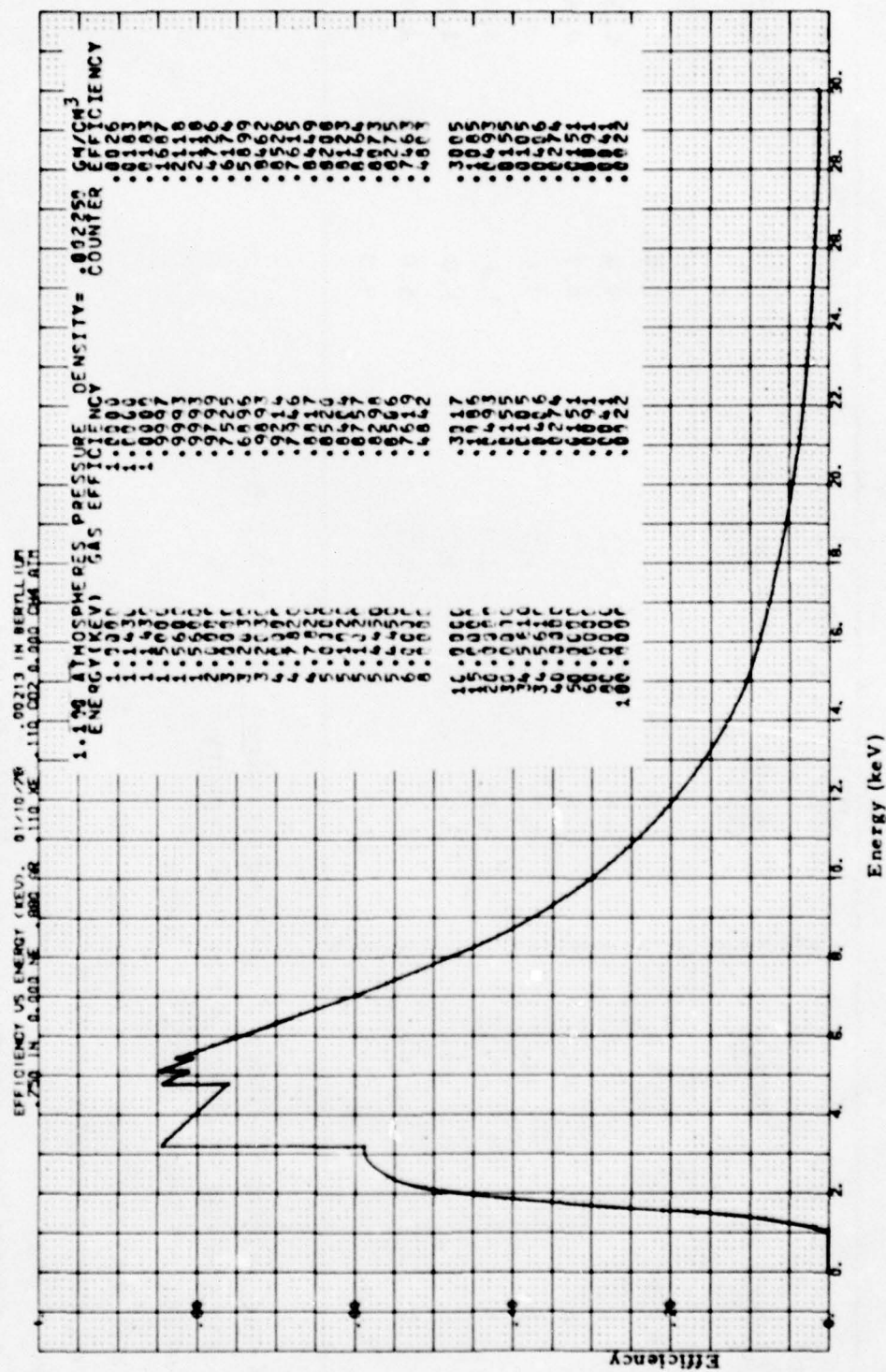
Figure 5.3. Calculation of CRLS-229 MONEX Low Energy Monitor
Efficiency as a Function of Energy.

Table 5.2. MONEX Low Energy Monitor Spectral Information.

Channel	Threshold (mV)	LEMHVPS Monitor = 1.7 V (V5 = "1")		LEMHVPS Monitor = 1.8 V (V5 = "0")	
		Threshold (keV)	Channel Width (keV)	Threshold (keV)	Channel Width (keV)
RTD	15.0*	1.0		0.4	
1	15.0*	1.0	0.6	0.4	0.3
2	24.4	1.6	1.1	0.7	0.4
3	41.2	2.7	1.7	1.1	0.7
4	67.1	4.4	2.9	1.8	1.2
5	111	7.3	4.7	3.0	2.0
6	183	12.0	9.9	5.0	4.0
ULD	334	21.9		9.0	

X-ray counting efficiency of rise time circuitry = 99.2 $\pm$ 0.2 %

Y-ray counting efficiency of rise time circuitry = 51 $\pm$ 1 %

Counter resolution = $\dfrac{FWHM}{MAX} = \dfrac{0.43}{\sqrt{E(keV)}}$

Ratio of gains at higher vs lower high voltage = 2.4

Data above taken at about 22°C

Gain changes an average of -0.7%/°C between 0° and 39°C

High voltage across counter (Volts) ≈ LEMHVPS x 1050

V5 = "1" is the normal operating mode

*Thresholds independently set

The requirement that the MONEX counters be simple precluded the use of an aperture wheel to broaden the LEM dynamic range. Thus a single aperture size had to be chosen. Since it was likely that the SOLFLEX experiment would observe many more flares than SOLEX, the LEM was designed to have a sensitivity similar to that of SOLFLEX. This required a window diameter of about one millimeter. As a check on the reasonableness of a window this size, LEM counting rates were computed for four of the larger flares observed by the proportional counters included in the S-056 experiment on Skylab. Calculated counting rates for flares of X-ray classes M1 to X1 ranged between 650 and 5000 $\sec^{-1}$ (SOLRAD X-ray flux F of $1.0 - 1.1 \times 10^{-2}$ and $1.0 - 1.1 \times 10^{-1}$ erg $cm^{-2}\sec^{-1}$ respectively in a 1-8Å band). Thus the LEM should be able to detect flares near the SOLFLEX detectability threshold but should not saturate for any but the largest flares. The on-orbit signal will be dominated by X-rays from the non-flaring sun.

5.2   LEM Electrical Design

The signals from the LEM proportional counter are processed in the same manner as described in Section 3.7 and illustrated in Figure 3.18. The basic signal detection criterion is the establishment of lower and upper amplitude thresholds. Signals within these limits were further analyzed in pulse risetime (see Section 3.7.3).

The output V of the charge amplifier at the lower high voltage setting is

$$V \text{ (volts)} = 1.5 \times 10^{-2} \ E_x \text{ (keV)}.$$

The lower level discriminator (LLD) threshold is set at 15 mV and the upper level discriminator (ULD) threshold is set at 334 mV as is shown in Table 5.2.

Nine different accumulator outputs are available in the telemetry stream (see Figure 7.3).

5-7

1. MONEX A, the number of events between LLD and ULD with acceptable risetime per 32 msec.

2. MAULD, the number of events with an amplitude greater than the ULD threshold per 1.024 sec.

3. MARTD, the number of events between LLD and ULD with excessive risetime per 1.024 sec.

4. PHA1A-PHA6A, the number of events with acceptable risetime in each of 6 pulse height channels listed in Table 5.2. The pulse height analyzer is of the differential type and is shown in Drawing L-5769 (not included in this report).

The low voltage and high voltage power supply outputs are monitored as analog signals in the telemetry stream (see Table 7.3). The LVPS and HVPS outputs are first attenuated by a factor of 2 and 1050, respectively. Telemetry buffers identical to those used in SOLEX are employed.

There are 4 discrete commands which affect the operation of the LEM as follows.

Command	Low Voltage Circuit Active	Detector Active
(1) MONEX +28V 1 On	Yes	No (unless (2) also on)
(2) MONEX HVPS 1 On	Yes (only if (1) also on)	Yes (only if (1) also on)
(3) SOLEX/MONEX +28V Off	No	No
(4) SOLEX/MONEX HVPS Off	Yes (only if (1) also on)	No

The seventh most significant bit in Control Register 2 affects the value of the LEM high voltage. The lower (and normal) high voltage value occurs when this bit is equal to 1.

The LEM module requires 25 mA at 28V to operate, corresponding to a power level of 0.7 W.

5.3   LEM Efficiency Calculation

Details of the system efficiency calculation are given in Table 5.3. A computer program CAL 229 was used in this calculation. The conversion from counts sec^{-1} to photons cm^{-2}sec^{-1} can be made by dividing the number of counts sec^{-1} by CTS/FLUX given in Figure 5.4.

Table 5.3. Calculation of MONEX System Efficiency

$$N(E) = C \, F(E) \, E_d(E)$$

where

$N(E)$ = Counts sec^{-1} at energy E

$F(E)$ = Incident flux (photons $\text{cm}^{-2} \, \text{sec}^{-1}$)

$E_d(E)$ = Detector quantum efficiency

and

$$C = A_o \, e_{rt} \, f_d$$

where

A_o = Nominal detector area (cm^2)

e_{rt} = Efficiency of risetime circuit

f_d = Fraction of detector aperture that is open.

For example, for MONEX A at 2 keV,

A_o = 0.00811 cm^2

e_{rt} = 0.991

f_d = 1.000

C = 8.037 x 10^{-3} cm^2

$E_d(E)$ = 0.4726

and

$$\frac{N(E)}{F(E)} = 3.80 \times 10^{-3} \quad \frac{\text{counts sec}^{-1}}{\text{photons cm}^{-2} \text{sec}^{-1}}$$

For the case of MONEX B,

C = 26.44 cm^2

To convert from counts per main frame to flux in photons $\text{cm}^{-2} \, \text{sec}^{-1}$, divide the recorded number of counts per MF by "CTS/MF/FLUX" listed in Figure 5.4.
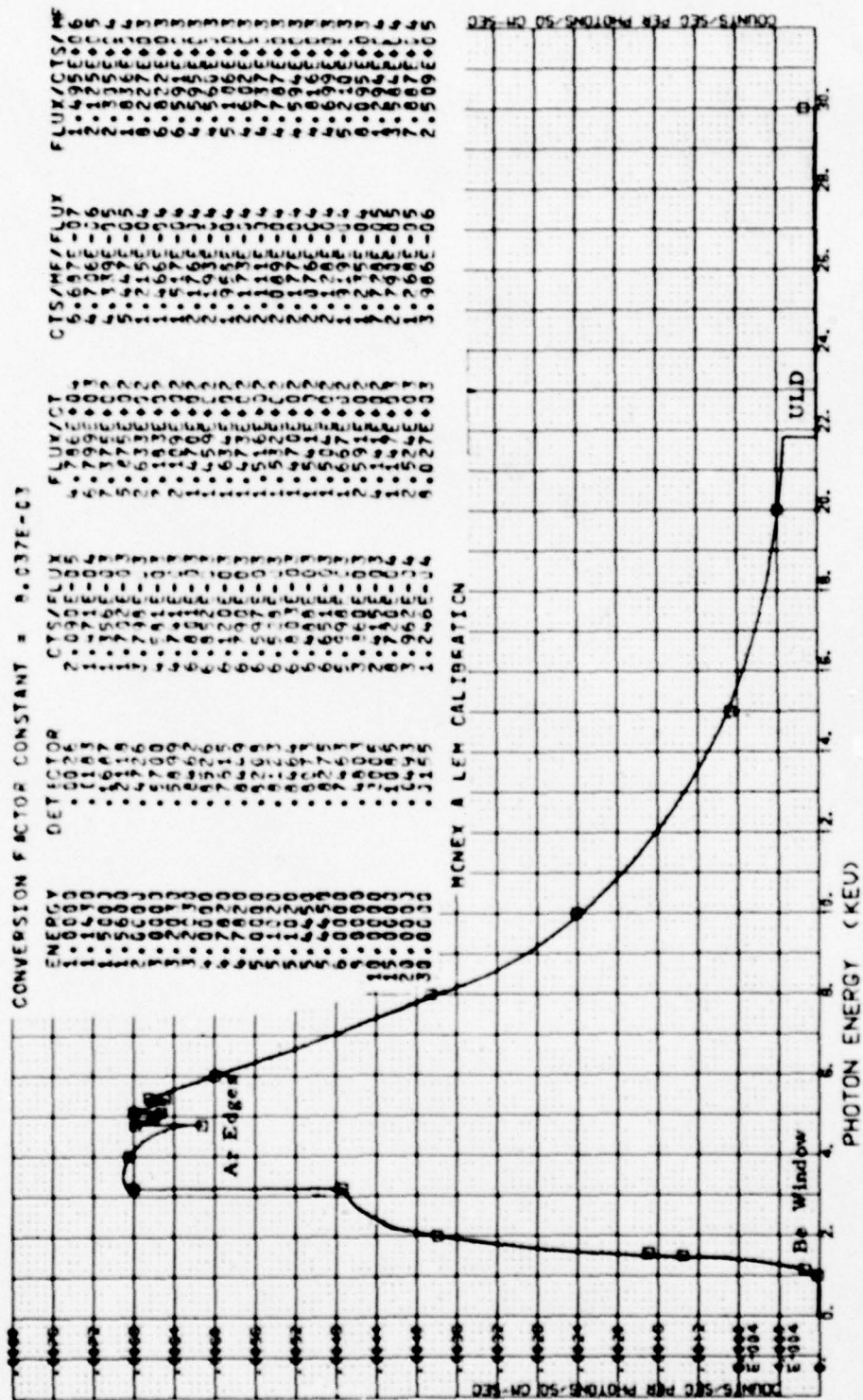
Figure 5.4.   CRLS-229 MONEX A LEM Calibration.

6. MONEX HIGH ENERGY MONITOR

6.1 Module Description

The MONEX High Energy Monitor (HEM) module (also called MONEX B) consists of a stationary sealed proportional counter and associated electronics, and monitors the occurrence of hard X-ray bursts in the energy range 11-140 keV. It will aid in the analysis of SOLEX and SOLFLEX data as well as be used in the study of solar X-ray bursts with excellent time resolution (32 msec). The HEM also has the capability to shut off the SOLEX detectors automatically in the presence of large charged particle fluxes. Considerations of space, weight, and especially time dictated that the HEM be simple. Hence the use of an actively shielded scintillation counter, which has superior background suppression, was precluded, and a large area proportional counter was chosen. A photograph of the flight HEM module is given in Figure 6.1.

A summary sheet for this experiment is given in Table 6.1. The window was chosen to provide a low-energy e^{-1} cut-off at 20 keV so that the counter would have negligible response to X-rays at energies below about 10 keV. The gas fill was chosen to obtain the highest practical efficiency for hard X-rays.

6.2 Shielding Considerations

Since active shielding was precluded for the HEM, passive absorbers had to be used to limit the background. The criterion was to shield so that at 34.6 keV, just above the xenon K absorption edge, the background due to diffuse cosmic X-rays was small compared to the unavoidable (with passive shielding only) background due to cosmic rays. At the time of this analysis it was thought that the counter X-ray efficiency would have
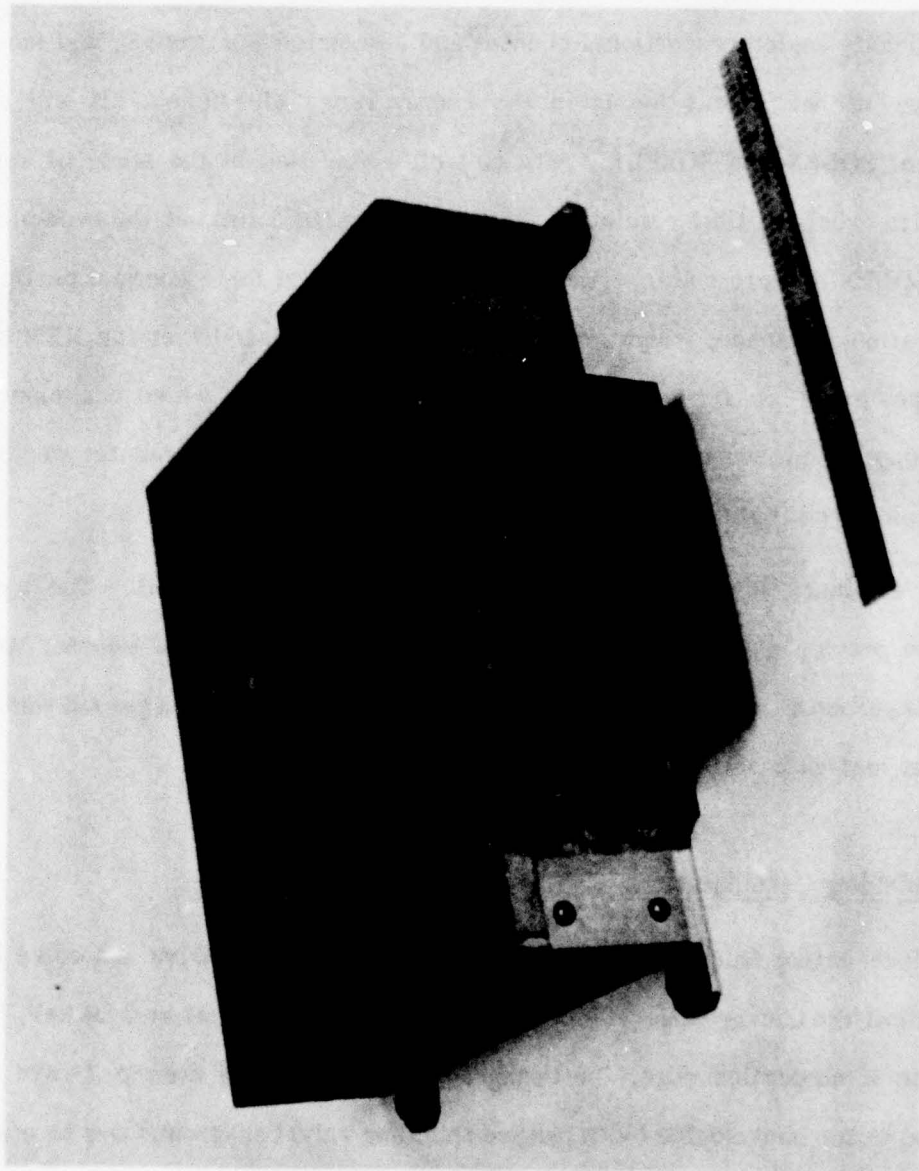
Figure 6.1. Assembled High Energy Monitor Module, MONEX Experiment

Table 6.1.   MONEX High Energy Monitor.

Proportional Counter Size:	2.00 in x 2.00 in x 6.09 in
Counter Window Area:	1.50 in x 3.50 in = 5.25 in^2 = 33.9 cm^2
Collimation:	Perpendicular slats of 0.032 in thick brass FWHM = 16.95° in Y and 17.17° in Z direction Transmission = 84.77% (on axis) Net collimated window area = 28.7 cm^2
Counter Window Thickness:	0.044 in = 0.30 gm cm^{-2} aluminum ($\pm$ 2%)
Counter Fill Gas:	97.0% Xenon, 3.0% CO_2
Counter Gas Thickness:	1.75 in = 1.59 x 10^{-2} gm cm^{-2}
Counter Gas Pressure:	3.00 atm = 2280 Torr
LND Counter Model Number:	428 (S/N 60850)
Time Resolution:	Integrated count rate data = 32.0 msec Pulse height data = 1.024 sec
Background Counting Rate: (at sea level)	10 sec^{-1}

a substantial local maximum at 34.6 keV, but when a proper Monte Carlo analysis was made it was found that K photon escape very substantially lowers the efficiency above the K edge and that the efficiency just below the edge is only negligibly smaller than that above the edge (see Section 6.4). In determining the amount of absorber needed by the criterion above we assumed the HEM would have no rise time discrimination circuit to reject cosmic rays; such a circuit was later added and it provides about 50 percent rejection.

The HEM aperture and shielding are shown in Figure 6.2. The box and collimator are made of brass of thickness 0.67 gm cm^{-2}. The collimator limits the field of view to 17 x 17 degrees FWHM and there is, of course, no brass over the window behind the collimator. The calculated in-orbit background rates at 35 keV with the shielding used are 0.4 keV^{-1} sec^{-1} from the diffuse X-rays and 1 keV^{-1}sec^{-1} from cosmic rays. In fact, we expect the instrument components around the HEM to provide additional X-ray shielding and the risetime discrimination circuitry to cut the cosmic ray background in half. Thus, outside regions of energetic trapped charged particles the HEM background should be much less than 1 keV^{-1}sec^{-1}. The HEM makes use of only the central part of the counter anode because resolution degradation is expected near the ends of the wire. The total window area for solar X-rays is 29 cm^2. The tin sheets shown in Figure 6.2 are provided to prevent energetic solar X-rays from entering the counter outside the nominal window. The 0.74 gm cm^{-2} of tin provides 90 percent absorption at 80 keV. The brass inside the tin will absorb all tin characteristic X-rays produced, and the aluminum counter body will absorb any copper or zinc X-rays escaping the brass box. Thus most 80 keV X-rays not passing through the detector window are degraded to 1.5 keV, far below the HEM threshold energy.

0.04 in. TIN OUTSIDE SHIELD,
THIS SURFACE ONLY

COLLIMATOR

1.50

1.50

3.50

PROPORTIONAL COUNTER
(aluminum anode)
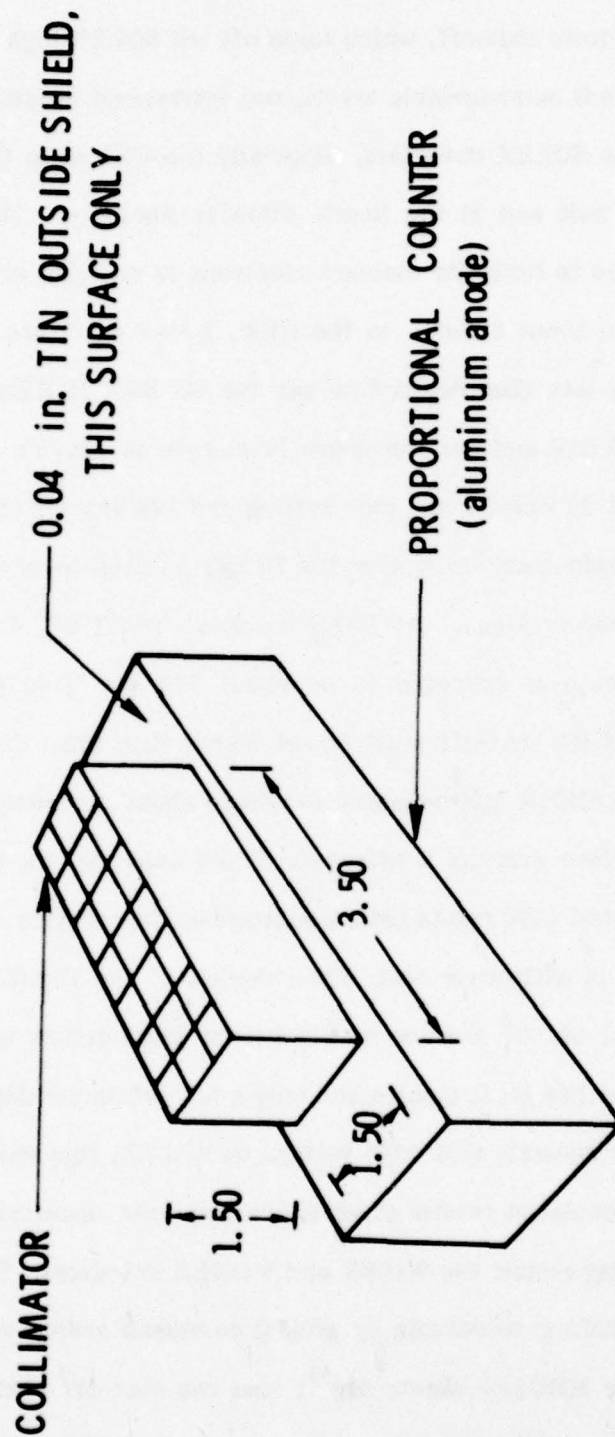
COLLIMATOR CELL SIZE 0.457 x 0.463 in.
COLLIMATOR CENTERED ON PROPORTIONAL COUNTER WINDOW

Figure 6.2. MONEX HEM Detector and Collimator.

6.3   SOLEX HV Shutoff

The HEM charged particle shut-off, which turns off the SOLEX high voltage when the HEM counting rate exceeds commandable levels, was introduced because of concern regarding degradation of the SOLEX detectors, especially the CEMA, in the "horns" of the Earth's outer radiation belt and in the South Atlantic Anomaly.   The absorption around the CEMA is expected to limit the incident electrons to energies above 1.5 MeV, while the HEM is shielded to about 3 MeV. In the HEM, 3 MeV electrons will deposit, typically, about 70 keV. It was thus decided to set the MONEX B HEM upper level discriminator (ULD) near 70 keV and use the upper level rate to provide the shut-off. The ULD is at present set at 86 keV for one gain setting and 140 keV for the other. The 86 keV threshold should perform nearly as well as the 70 keV nominal level that was used in making the following considerations. At latitudes above about 65° the HEM ULD background due to cosmic rays is expected to be about 300 sec^{-1}, so the threshold counting rate for the SOLEX HV shut-off must be set higher than this. For a threshold of 500 sec^{-1}, we expect each CEMA microchannel to record about one count per orbit in passing through the horns before shut-off is effected. This means that the CEMA can be active for at least an estimated 1000 orbits before substantial degradation occurs due to trapped charged particles. In a lifetime test, 100 channels of the flight spare CEMA were irradiated with a total of 10^9 X-rays; no significant degradation was observed. Since the nominal experiment life is six months and only a few orbits per day will involve passage through the horns or anomaly with high voltage on SOLEX, this shut-off scheme should be adequate. The calculated results given above are quite uncertain because of the complexity of the shielding around the SOLEX and MONEX detectors. Therefore the HEM SOLEX shut-off threshold is selectable by ground command among values of 250, 500, and 4000 HEM ULD (or MBULD) events sec^{-1}; also the shut-off circuitry can be totally disabled by command. Additional information about the HEM control capability is given in the table below.

Table 6.2. Commands Affecting the SOLEX High Voltage Shutoff

Commands Sent	MF 112, SF 50 HEM Rate In	MBULD Rate Threshold (sec^{-1})
Cmd S3931	1V	250
+Cmd S3934 Only	2V	500
+Cmd S3935 Only	3V	4000
+Cmd S3934 and S3935	4V	Infinite

A ratemeter with a 1 sec integration time is used to compare the MONEX B ULD (MBULD) rate to the selected threshold. This HEM Rate Out ratemeter output measurement (MF or mainframe word 112, SF or subcom frame 51) equals about 1V when each selected threshold is attained and about 0 V when the MBULD rate is close to zero. When the MBULD threshold counting rate is exceeded, i.e. when HEM Rate Out exceeds 1 V, input power to both SOLEX HVPS's is automatically disconnected and they remain off until the MBULD counting rate decreases below the chosen threshold. The fourth threshold effectively disables this circuit (HEM Rate Out is forced to 0 V) and the SOLEX high voltage power supplies remain on. When the MBULD threshold rate is exceeded, the HEM control changes to 0 V, and the SOLEX high voltage is turned off. However, when the MBULD threshold rate has not been exceeded, the HEM Control (MF 112, SF 52) is 5 V, and the SOLEX high voltage will not be turned off by this circuit. The HEM Rate In, the HEM Rate Out and the HEM Control are analog telemetry values included in Table 7.3.

The MBULD threshold can be reset to 250 sec^{-1} by turning the HEM low voltage off and then on. When the HEM low voltage is off, SOLEX will operate normally. The additional control of the SOLEX high voltage power supplies will occur only when the MONEX HEM low voltage is on.

6.4 HEM Detector Efficiency

The efficiency of the HEM was determined by measuring the effective window thickness in gm cm^{-2} of aluminum and the effective gas thickness in gm cm^{-2} of xenon and then using the absorption coefficients tabulated by Storm and Israel (1970). The window thickness was determined by irradiating the counter with collimated X-ray beams at normal and 45 degree incidence. The ratio of counting rates obtained in the two configurations should be

$$\frac{R_{90}}{R_{45}} = e^{+(0.414 \mu \rho x)_{window}} \quad \frac{1 - e^{-(\mu \rho x)_{xenon}}}{1 - e^{-\sqrt{2}(\mu \rho x)_{xenon}}} \quad ,$$

where μ is the mass absorption coefficient for the X-rays used, ρ the density and x the path length through the material. Note that some knowledge of the xenon path is needed to complete this calculation. The X-rays chosen, Ag Kα and Mo Kα have high absorption coefficients in xenon so that with the nominal three atmosphere fill the bracketed term in the equation is 0.86 and 0.94, respectively. Using this technique we measured the entrance window and the side opposite it obtaining 0.28 gm cm^{-2} for the window and 0.68 gm cm^{-2} for the back side. The window result shows reasonable agreement with the nominal value of 0.30 gm cm^{-2}. The gas density was then determined by measuring the normal incidence X-ray counting rate for a detector then interposing the HEM in the beam and repeating the measurement. The counting rate ratio is then

$$r = e^{-(\mu \rho x)_{window}} e^{-(\mu \rho x)_{back}} e^{-(\mu \rho x)_{xenon}} .$$

Since the window and back aluminum thicknesses are known, x for xenon may be derived from the above formula. It is then necessary to put the derived xenon density back into

the previous equation and to continue iterating until a consistent set of aluminum and xenon thicknesses is obtained. Using characteristic X-rays of barium, we found a xenon pressure of 3.5 atmospheres as compared to a nominal value of 2.9. In view of the uncertainties of this technique we regarded these two values consistent and used 2.9 atmospheres in computing the counter efficiency.

In the determination of the MONEX HEM efficiency, cross sections by Storm and Israel (1970) were used. Below the xenon K-absorption edge at 34.58 keV, efficiencies were calculated directly. Above the edge, a Monte Carlo Program HEMEFF was utilized. A random number generator was used in conjunction with the relevant cross sections to determine the sequence of scattering and absorption events for each photon. The pulse height of K-escape events will be distributed about the incident photon energy less 29.8 keV. When the counter resolution of $0.334 \, E^{1/2}$ (E in keV) was assumed based on laboratory measurements, the distribution in recorded energy was calculated for incident photon energies from 10 to 150 keV. It was thus possible to determine the K-escape and photo peak efficiencies as well as the expected pulse height distributions as a function of incident photon energy. Results of this calculation are listed in Table 6.3 and drawn in Figure 6.3.

Six pulse height channels divide the energy range between 11 and 140 keV as shown in Table 6.4.

6.5   HEM Electrical Design

The signals from the HEM proportional counter are processed in a manner similiar to that described in Sections 3.7 and 5.2 and illustrated in Figure 3.18. The main data out, MONEX B, gives the number of events between the lower and upper level discriminators with fast risetime in 32 msec. In addition, the number of risetime reject

Table 6.3. MONEX High Energy Monitor Efficiency Results.

Photon Energy (keV)	Gas Detection Efficiency		Aluminum Window Transmission	Total Efficiency	
	Photopeak	K-escape		Photopeak	K-escape
10.0	1.000	0.000	0.0004	0.0004	0.000
15.0	0.978	0.000	0.109	0.107	0.000
20.0	0.823	0.000	0.397	0.327	0.000
25.0	0.606	0.000	0.632	0.383	0.000
30.0	0.427	0.000	0.771	0.329	0.000
34.58-	0.318	0.000	0.847	0.270	0.000
35.0	0.318+.006	0.565+.008	0.854	0.272+.005	0.483+.007
40.0	0.291+.005	0.495+.007	0.898	0.261+.005	0.445+.006
45.0	0.244+.005	0.434+.007	0.929	0.227+.005	0.403+.007
50.0	0.207+.005	0.363+.006	0.946	0.196+.005	0.343+.006
55.0	0.178+.004	0.299+.005	0.960	0.171+.004	0.287+.005
60.0	0.145+.004	0.257+.005	0.968	0.140+.004	0.249+.005
65.0	0.123+.004	0.205+.005	0.974	0.120+.004	0.200+.005
70.0	0.099+.003	0.187+.004	0.978	0.097+.003	0.183+.004
75.0	0.088+.003	0.160+.004	0.981	0.086+.003	0.157+.004
80.0	0.072+.003	0.133+.004	0.984	0.071+.003	0.131+.004
85.0	0.066+.003	0.116+.003	0.985	0.065+.003	0.114+.003
90.0	0.057+.002	0.101+.003	0.987	0.056+.002	0.100+.003
100.0	0.041+.001	0.072+.002	0.989	0.041+.001	0.071+.002
150.0	0.012+.001	0.020+.001	0.992	0.012+.001	0.020+.001
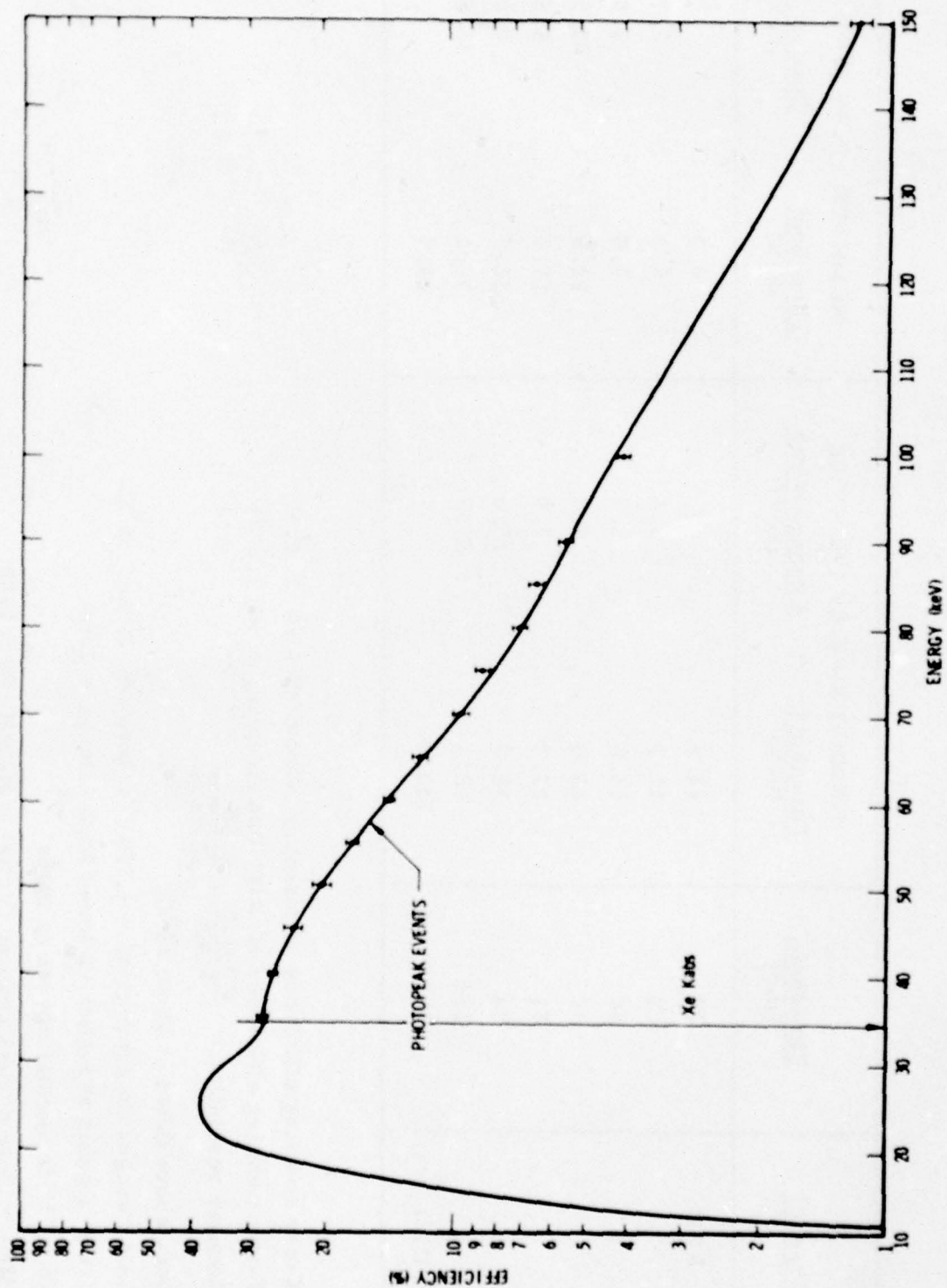
Figure 6.3. CRLS-229 MONEX High Energy Monitor Window Plus Counter Gas Efficiency.

Table 6.4 MONEX High Energy Monitor Spectral Information.

Channel	Threshold (mV)	HEMHVPS = 2.8V (V6 = "1") Threshold (keV)	Channel Width (keV)	HEMHVPS = 2.9V (V6 = "0") Threshold (keV)	Channel Width (keV)
RTD	29	11.3		6.9	
1	29	11.3	3.3	6.9	2.1
2	40	14.6	5.7	9.0	3.5
3	52	20.3	7.4	12.5	4.5
4	71	27.7	9.0	17.0	5.5
5	94	36.7	15.6	22.5	9.6
6	134	52.3	87.7	32.1	53.8
ULD	359	140.0		85.9	

X-ray counting efficiency of risetime circuitry = 89 ± 3 %

γ-ray counting efficiency of risetime circuitry = 48 ± 2 %

Counter resolution = $\dfrac{FWHM}{MAX} = \dfrac{0.88}{\sqrt{E(keV)}}$

Data above taken at about 22°C

Gain changes an average of -0.35%/°C between -2° and 45°C

Ratio of gains at higher vs lower high voltage = 1.63

V6 = "1" in normal operating mode

High voltage across counter (Volts) ≈ HEMHVPS x 1000

events (MBRTD), upper level discriminator events (MBULD) and events in each of 6 pulse height channels (with acceptable risetime) are telemetered every 1.024 sec. The telemetry format is given in Section 7.2.

The HEM risetime discriminator circuit is significantly different from that of the LEM and SOLEX PC due to the slower HEM gas mixture. HEM pulse risetimes from X-ray events are mostly less than 700 nsec vs 100 nsec for the other two detectors. The HEM risetime circuitry stores the peak amplitude value of a pulse and determines the 10% and 70% pulse height values of this peak. The pulse meanwhile has been delayed 1.5 μ sec while these 10% and 70% threshold levels stabilize. The delayed pulse is then processed by the 10%/70% threshold circuit which yields a pulse whose width is equal to the time for the delayed pulse to go from 10% to 70% of its peak value, i.e. its risetime. Since most X-ray events have risetimes less than 700 nsec, events which exceed this risetime are rejected.

As discussed in Sections 3.7 and 5.2, the amplitude of the detector's charge amplifier output at the lower operating value of high voltage is

$$V \text{ (volts)} = 3 \times 10^{-3} \ E_x(\text{keV}).$$

The lower, differential PHA and upper level thresholds are given in Table 6.4.

Discrete commands affecting the HEM are given in Table 7.1 as well as in Table 6.5 below.

6-13

Table 6.5. HEM Discrete Commands

Command No.	Command Title
S3916	SOLEX/MONEX +28V Off
S3917	SOLEX/MONEX HVPS Off
S3931	MONEX +28 2 On
S3933	MONEX HVPS 2 On
S3934	MONEX HEM Rate 1
S3935	MONEX HEM Rate 2

The HEM has 5 analog outputs; these are included in Figure 7.3 and described in part in Section 6.3. The low and high voltage monitors are identical to those used in SOLEX (Section 3.7.6) and the MONEX LEM (Section 5.2).

The power required to operate the HEM is 1.4 watts.

6.6   HEM Efficiency Calculation

Details of the system efficiency calculation are given in Table 5.3. A computer program CAL 229 was used in this calculation. The conversion from counts sec^{-1} to photons $cm^{-2}sec^{-1}$ can be performed by dividing the recorded number of counts sec^{-1} by CTS/FLUX given in Figure 6.4.
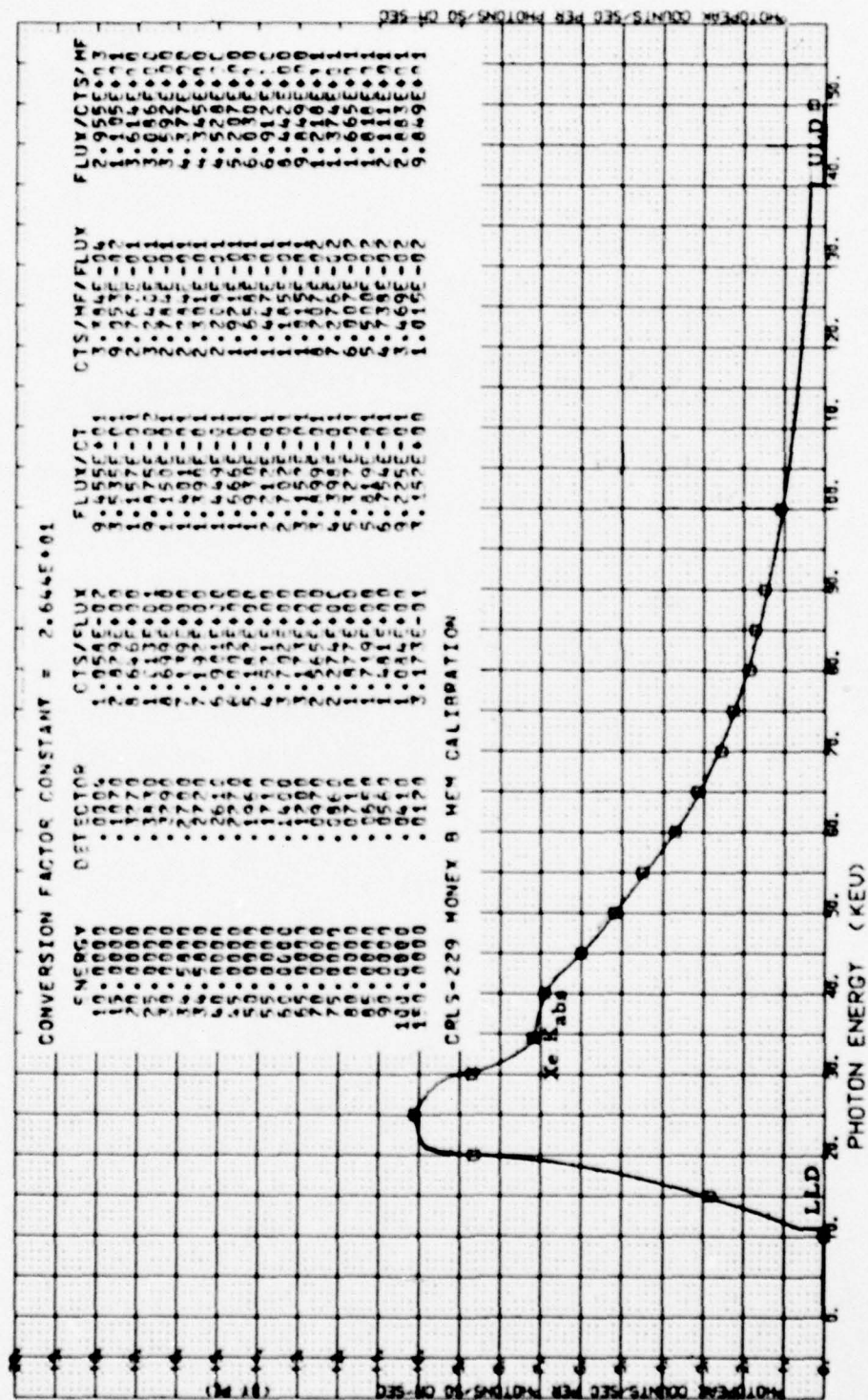
Figure 6.4. CRLS-229 MONEX B HEM Calibration.

7. COMMAND AND TELEMETRY

7.1 Command List

The CRLS-229 experiment uses two types of commands: 1 serial magnitude command and 29 discrete commands. The serial magnitude command is almost always used in real time, while the discrete commands are frequently used as commands stored in the spacecraft's command storage memory. In addition, both stored and real time discrete commands are required to be sent to control the PIA operation.

A list of CRLS-229 Commands and their corresponding USAF Satellite Control Facility (SCF) command number is given in Table 7.1. Launch power is used in the command box and day power is used in other modules of CRLS-229. Descriptions of the effects of the various SOLEX and MONEX discrete commands are given in the corresponding electronics sections earlier in this report. A discussion of the structure of the serial magnitude commands is given in Section 4.5. A block diagram showing the modules affected by the various discrete commands is shown in Drawing L-5972 (not included in this report) and Figure 7.1.

The SOLEX part of the CRLS-229 experiment requires most of the commands. Its operation is controlled by twelve 16-bit lambda and control registers and by the mode information from the PIA. The λ (lambda) registers allow the experiment to select wavelengths for rasters or for spectral scan limits. The control registers allow the experimenter to exercise options in the SOLEX operations. The 9-bit command format makes it necessary to uplink 3 serial magnitude commands to fill a single register. Since the use of stored commands would then require 9 serial magnitude commands per register, realtime serial magnitude commands are used, except under unusual circumstances.

Table 7.1. CRLS-229 Commands and P78-1 Command Number.

Discrete Commands		Serial Magnitude Commands		
Cmd Num	Cmd Title	Cmd Num	Cmd Title	Remark
3902	CRLS-229 Lch Pwr On	3971	λ Register 1	100000001
R3903	CRLS-229 Lch Pwr Off	3972	λ Register 2	100000010
3900	CRLS-229 Day Pwr On	3973	λ Register 3	100000011
3901	CRLS-229 Day Pwr Off	3974	λ Register 4	100000100
3910	SOLEX +28V On	3975	λ Register 5	100000101
3911	SOLEX HVPS 1 On	3976	λ Register 6	100000110
3912	SOLEX HVPS 2 On	3977	λ Register 7	100000111
3913	Go to Ref Zero Position	3978	λ Register 8	100001000
3914	Go to λ 1 Position	3979	λ Register 9	100001001
3915	Go to λ 1 Position Off	3980	λ Register 10	100001010
3916	SOLEX/MONEX +28V Off	3981	Control Register 1	100001011
3917	SOLEX/MONEX HVPS Off	3982	Control Register 2	100001100
3930	MONEX +28V 1 On	4000	Command 0	000000000
3931	MONEX +28V 2 On	4001	Command 1	000000001
3932	MONEX HVPS 1 On	4002	Command 2	000000010
3933	MONEX HVPS 2 On	4003	Command 3	000000011
3934	MONEX HEM Rate 1	:	:	:
3935	MONEX HEM Rate 2	4255	Command 255	011111111
3950	SOLFLEX +12 On			
3951	SOLFLEX HVPS 1 On			
3952	SOLFLEX HVPS 2 On			
3953	SOLFLEX Motor Direction			
3954	SOLFLEX Motor Dr On			
3955	SOLFLEX Motor Dr Rate 1			
3956	SOLFLEX Motor Dr Rate 2			
3957	SOLFLEX Motor Dr Rate 3			
3958	SOLFLEX Motor Dr Rate 4			
3959	SOLFLEX/MAGMAP +28V Off			
3960	SOLFLEX MAGMAP HVPS Off			
3961	MAGMAP +12V On			
3962	MAGMAP HVPS On			
3963	Go to MAGMAP Position On			
3964	Go to MAGMAP Position Off			
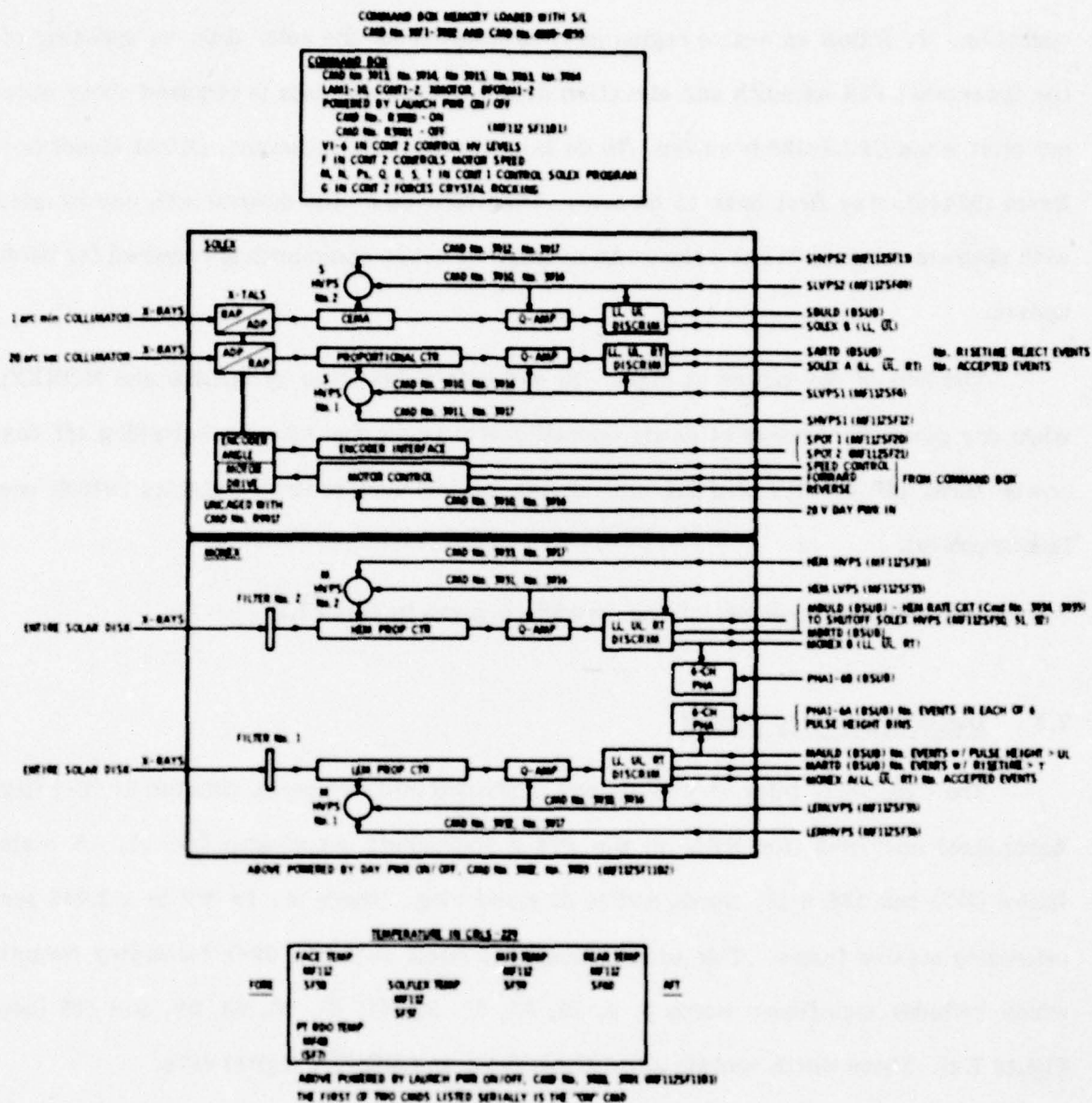
Figure 7.1. CRLS-229 SOLEX/MONEX Command and Telemetry
Block Diagram.

The SOLEX experiment requires an offset pointing capability for its optimum operation. To follow an active region as it rotates across the solar disk, an updating of the spacecraft PIA azimuth and elevation offset and vernier bits is required about once per orbit when CRLS-229 is active. To do this, the discrete command, Offset Generator Reset (S2440), may first have to be sent. Then turn-on of the desired bits, one by one, with discrete commands can occur. An average of seven commands is required for each update.

The loss of day power at night will end data acquisition by SOLEX and MONEX; when day power is restored at dawn, operation will again commence. Switching off day power turns off the HV without erasing the lambda and control registers (which use launch power).

The power requirement of each module is given in Table 7.2.

7.2 Digital Telemetry Format

The CRLS-229 telemetry allotment is divided into two parts, denoted as 29-1 (for Aerospace) and 29-2 (for NRL) in the P78-1 spacecraft mainframe format. A main frame (MF) has 128 8-bit words and is 32 msec long. There are 64 MF in a 2.048 sec telemetry master frame. This section concerns itself with the 29-1 telemetry format which includes mainframe words 3, 4, 35, 36, 51, 52, 67, 68, 83, 84, 99, and 100 (see Figure 7.2). These words contain all of the SOLEX and MONEX digital data.

The twelve 29-1 mainframe words are divided into two groups, one in the first half of the frame and the other in the second half. These 48-bit groups are the fundamental 29-1 telemetry units. Figure 7.3 displays the division of each 48-bit unit. The first 13 bits read out alternately the SOLEX B and SOLEX A detector counts as

Table 7.2. CRLS-229 Power Budget.

		NUMBER OF WATTS AT 28 VOLTS	
		DAY POWER	NIGHT POWER*
CMD BOX	AVERAGE	0.9	0.9
	MAX	0.9	0.9
SOLEX	AVERAGE	5.7	0.0
	MAX	5.7	0.0
MONEX HEM	AVERAGE	1.0	0.0
	MAX	1.0	0.0
MONEX LEM	AVERAGE	0.7	0.0
	MAX	0.7	0.0
SOLFLEX	AVERAGE	4.8	0.0
	MAX	5.5	0.0
MAGMAP	AVERAGE	0.2	0.0
	MAX	2.2	0.0
TOTAL	AVERAGE	13.3	0.9
	MAX	16.0	0.9

*From "Launch" Power Bus
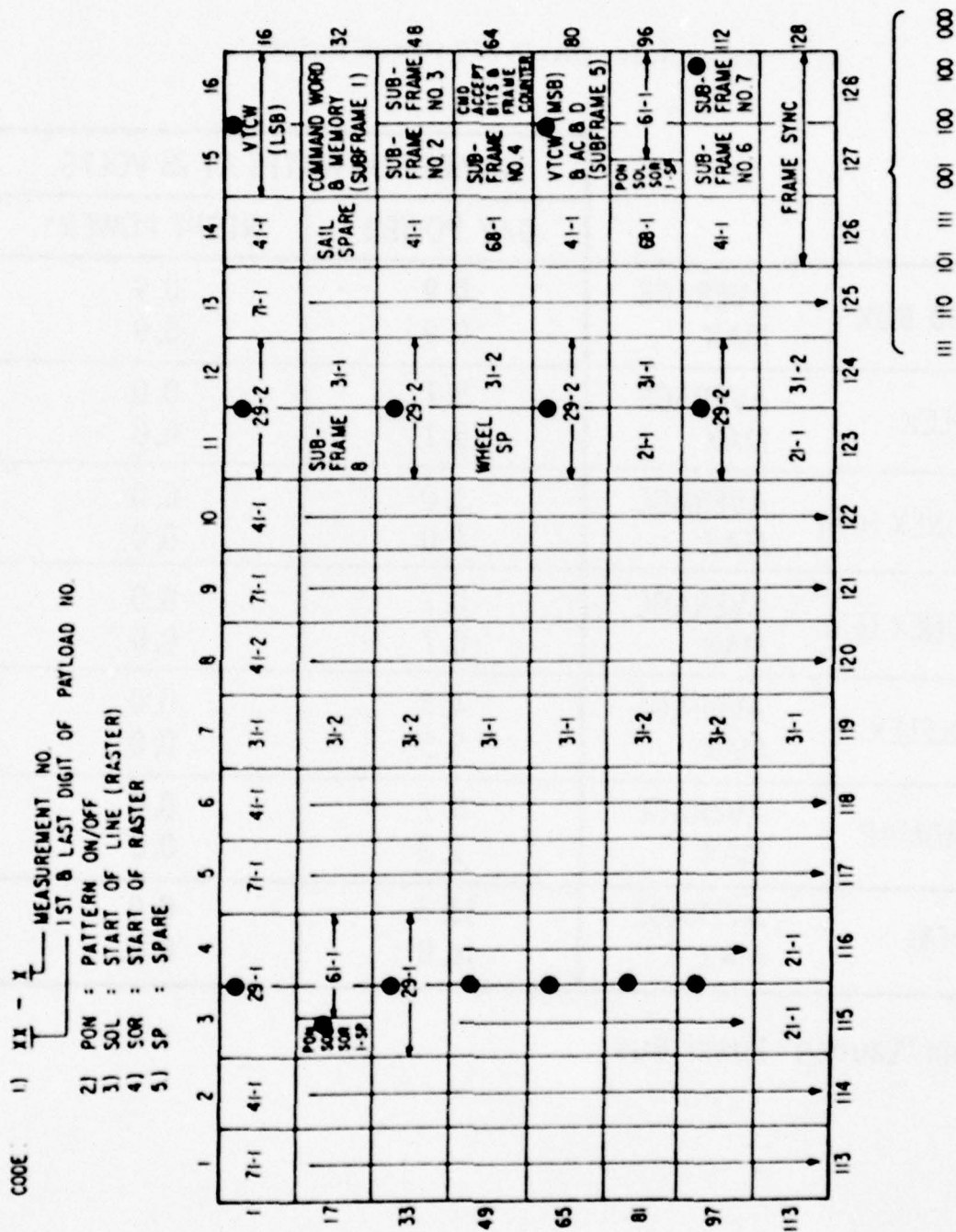
Figure 7.2. P78-1 Mainframe Format. The dots refer to telemetry relevant to CRLS-229.

7-6

Figure 7.3. 29-1 Telemetry Format.

MAIN FRAME WORD NO.

| FIRST HALF FRAME | 3 | 4 | 35 | 36 | 51 | 52 |
| SECOND HALF FRAME | 67 | 68 | 83 | 84 | 99 | 100 |

FUNCTION

| FIRST HALF FRAME | SOLEX B | MONEX B | XMOTOR | MFCT1 | BSUB |
| SECOND HALF FRAME | SOLEX A | MONEX A | XMOTOR | MFCT2 | BSUB |

12 8-bit words/32 msec = 3 kbps

MF # 1, 33 — MFCT2

SUBCOM 32 TIMES PER MASTER FRAME

8	7	6	5	4	3	2	1
12	11	10	9		3	2	1
B_2	B_1		13	4		2	1
B_6	B_5		B_4	B_3		2	1

B_1 = XZ BIT OF BORESIGHT CELL

B_2 = XY BIT OF BORESIGHT CELL

B_3 = LSB OF TCOUNT (1)

B_6 = MSB OF TCOUNT (8)

14 = MSB OF MOTOR POSITION (8192)

1 = LSB OF MOTOR POSITION (MTR POS)

SARTD 1
SBULD 3
MAULD 5
MBULD 7
MARTD 9
MBRTD 11
PHA1A 13   12, 44
PHA2A 15   13, 45
PHA3A 17   14, 46
PHA4A 19   15, 47
PHA5A 21   16, 48
PHA6A 23   17, 49
PHA1B 25   18, 50
PHA2B 27   19, 51
PHA3B 29   20, 52
PHA4B 31   21, 53
PHA5B 33   22, 54
PHA6B 35
DFORM1 37
DFORM2 39
LAM1 41
LAM2 43

30, 62 LAM10 59
31, 63 CONT1 61
32, 64 CONT2 63

32 16-bit words twice per MASTER FRAME

LCALL — LASSMC

| RAS | SOR | PGD | JKH | R5R5 | F5R5 |
| | | | | 3 4 | 9 10 |

SMOTOR

DFORM1

DFORM2

η_D S	λ_e λ_i	A_x B_x	A_d B_d
C_6 S	MCOUNT C8	C9 S	
7		10	HV

One Master Frame = 2.048 sec = 64 Main Frames

binary numbers, with MSB first. Thus each SOLEX detector rate is read out once per mainframe, with SOLEX B in the first half frame and SOLEX A in the second half frame. Bits 14-26 read out the MONEX counter integral counts in the same way as bits 1-13 read out the SOLEX counters. All four counters are reset to 1, not 0. Bits 27-34 read out the SOLEX motor position (mnemonic XMOTOR) which indicates the X-ray wavelength under observation. The four LSBs are read out twice per mainframe while the remaining bits are read out as displayed in the figure. The "T count" referred to gives the number of times the crystal has been scanned between a specified pair of wavelengths. This number is internally compared with a preset value in Control Register 1. When the two numbers are equal, a new set of wavelengths is scanned or the entire sequence is started again. Bits 35-40 give the minor frame count and serve to identify the measurements in bits 41-48 which are subcommutated. The subcom consists of 32 16-bit words and is consequently cycled twice per master frame.

The subcom in the last eight bits of each 48-bit unit requires further explanation. The functions being subcommutated are shown in Figure 7.3. Each function requires 16 bits, hence an entire mainframe (with two 48-bit units), to read out. The first six functions are event counts above the upper level discriminators or longer than the rise time discriminations of the SOLEX and MONEX detectors. These are followed by pulse height analysis counting rate spectra for the two MONEX proportional counters. The following two words are called "Discrete Format 1" and Discrete Format 2" (DFORM 1 and DFORM 2). These formats are also displayed in Figure 7.3. The four LCALL bits designate the "target" spectrometer motor step number. The next four command bits give the address in the 12-location memory that was last addressed by a serial magnitude command. The next four bits give PIA mode information as indicated, and the last four

7-8

bits give information on the SOLEX motor status. As indicated in the figure, the bits of DFORM 2 are assigned to the motor direction, the microswitch status, the discrete command status, the SOLEX HV control status, and the raster counter.

The contents of the SOLEX lambda and the control registers are also subcommutated in the final eight bits of the 48-bit unit. There are 12 registers: 10 lambda registers and 2 control registers. These are given the mnemonics LAM 1 through LAM 10 and CONT 1 and CONT 2. The total number of measurements in each subcom is 32; the entire list is read out twice per telemetry master frame.

Additional discussion about items in the 78-1 telemetry format is given in Section 4 and elsewhere in this report.

7.3   Analog Monitors

There are 16 analog housekeeping values assigned to the Aerospace part of CRLS-229. These are given in Table 7.3. Nominal operating and redline values are also given in this Figure. The P78-1 Spacecraft digitizes these values using the conversion 20 mV per count.

It is possible to determine uniquely the angular position of the SOLEX crystal shaft using the SOLEX Pot 1 output; this is shown in Figure 7.4. An electrical potentiometer is mechanically attached to the shaft and the voltage across the pot changes as the shaft rotates. Figure 7.4 also gives the non-unique angular position of the SOLEX detector shaft as a function of the voltage output from SOLEX Pot 2. At the MAGMAP position, SPOT1 = 2.2 V and SPOT 2 = 4.5 V.

The MONEX analog outputs are discussed in the MONEX section of this report.

Table 7.3. CRLS-229 Aerospace Analog Monitors. All are in P78-1
telemetry main frame No. 112.

NAME	Sub Frame No.	Nominal Value (Volts)	Redline (Volts) (Problem if outside limits below)
SOLEX LVPS 1	4	2.3	
SOLEX LVPS 2	49	2.5	
SOLEX HVPS 1 *	12	"00" = 1.95	0 - 2.3
SOLEX HVPS 2	13	"11" = 2.70	0 - 3.0
SOLEX Pot 1 *	20	0.9 - 3.8	
SOLEX Pot 2 *	21	0.0 - 4.6	
MONEX LEM LVPS	35	2.5	
MONEX LEM HVPS	36	"1" = 1.7	1.5 - 2.0
MONEX HEM LVPS	33	2.6	
MONEX HEM HVPS	34	"1" = 2.8	2.6 - 3.1
MONEX HEM Rate In	50	1, 2, 3, or 4	
MONEX HEM Rate Out	51	0 - 5	
MONEX HEM Control	52	0 or 5	
CRLS-229 Face Temp #	58	2.0 - 3.7	
CRLS-229 Middle Temp #	59	2.0 - 3.7	1.8 - 5.5
CRLS-229 Rear Temp #	60	2.0 - 3.7	

* power source is SOLEX LVPS 1

power source is command box power supply (launch power)
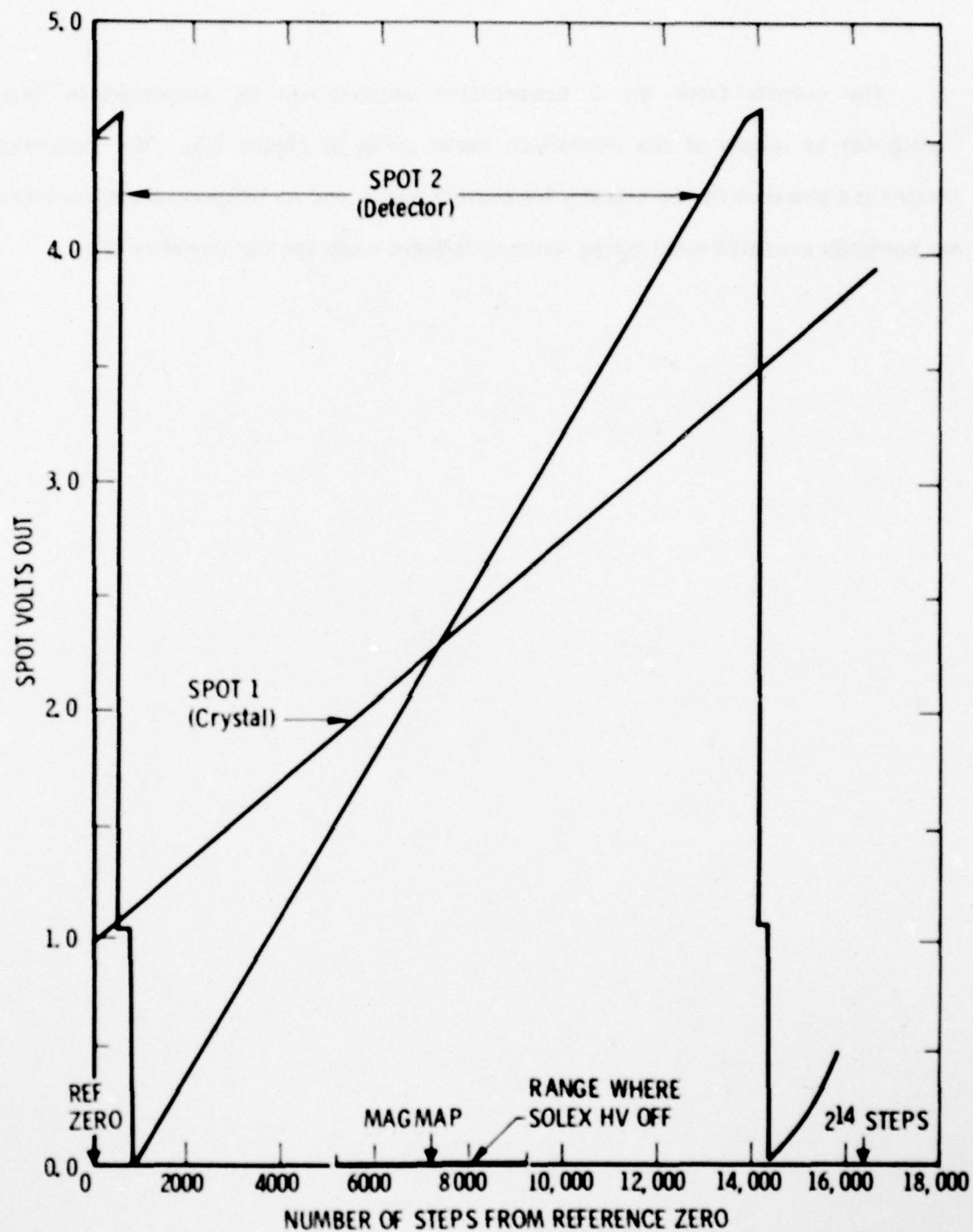
Figure 7.4. CRLS-229 SOLEX Pot Readout Calibrations.

7-11

The outputs from the 3 temperature sensors can be converted to degrees Centigrade by means of the conversion curve given in Figure 7.5. The temperature sensors are powered by the standby (or launch) power and so temperature measurements are normally available even during spacecraft night when the day power is off.

Figure 7.5. CRLS-229 Temperature Conversion Curve.

8. CRLS-229 MILESTONES

6/12/75	Beginning of Program - design started.
7/28/75	Decision that NRL build and test MAGMAP and SOLFLEX. Aerospace to build the MAGMAP collimator.
8/1/75	RFQ for Spacecraft released.
9/9/75	Aerospace to build NRL HVPS and proposes design features of SOLFLEX experiment.
9/23/75	Completion of review of spacecraft proposals.
1/20/76	Decision that SOLEX will contain 2 (and not 3) pairs of crystals.
2/15/76	Payload Requirements Questionnaire completed.
2/2/76	P78-1 spacecraft contract awarded to Ball.
2/24/76	Aerospace and NRL telemetry format determined.
3/15/76	Drop polarimeter from CRLS-229 complement of instruments.
4/6/76	Command structure defined in terms of 21-bit serial magnitude commands.
5/13/76	Interface Control Document agreement between Ball and Aerospace.

6/4/76	Completion of Definition Phase Design Review at Ball.
9/15/76	Command structure altered by direction of the SPO to be 9-bit serial magnitude commands.
10/8/76	Preliminary Design Review of P78-1 at Ball completed.
12/13/76	CRLS-229 Preliminary Design Review at Aerospace completed (see Landecker et al., 1976).
1/22/77	P78-1 Critical Design Review completed at Ball.
3/29/77	SCF displays determined.
4/15/77	Mechanical simulator delivered to Ball and electrical simulator completed.
5/5/77	Quick-look data requirements at SCF negotiated.
9/15/77	Initial mechanical assembly of CRLS-229 at Aerospace.
9/27/77	Delivery of CRLS-229 electrical simulator to Ball.
10/15/77	Delivery of NRL hardware to Aerospace for fit check.
11/13/77	Vibration testing of CRLS-229 at AETL.

11/15/77	Start of CRLS-229 thermal vacuum test at Aerospace.
12/10/77	Completion of EMI/EMC tests at Genisco.
12/18/77	Completion of thermal-vacuum testing and calibration at Aerospace.
12/23/77	CRLS-229 Consent-to-Ship Review at Aerospace (see Landecker et al., 1978).
1/4/78	CRLS-229 Payload received at Ball.
1/5/78	Bench Check of CRLS-229 at Ball.
1/19/78	SAMTEC tape format determined.
2/10/78	Upgrade CRLS-229 collimator from 1 arc min to 20 arc sec at Ball.
2/17/78	CRLS-229 Minicomputer functional at Ball.
2/27/78	IST-1 Completed at Ball (electrical simulator test).
3/8/78	CRLS-229 Payload Integration Test completed at Ball.
4/15/78	CRLS-229 Calibration Book completed at Aerospace.
6/15/78	Integrated System Test-2 completed at Ball (EMI/EMC).
6/21/78	SCF Training Session presentation made at Sunnyvale (see Landecker and McKenzie, 1978).

7/18/78	Scaled Integrated System Test 1 and Aliveness Test completed at Ball.
8/2/78	SIST-2 completed at Ball.
9/7/78	SIST-3 completed at Ball.
11/10/78	Integrated System Test-3 completed at Ball (Thermal-Vacuum).
12/16/78	SOLEX modified at Aerospace and redelivered to Ball.
1/10/79	P78-1 arrives at Vandenberg.
1/23/79	Launch Base IST completed at VAFB.
2/24/79	Launch of P78-1.
2/27/79	CRLS-229 power on in orbit.

9. REFERENCES

W. E. Behring, L. Cohen, U. Feldman and G. A. Doschek, 1976, "The Solar Spectrum: Wavelengths and Identifications from 160 to 770 Angstroms," Astrophys. J. 203, 521-527.

R. L. Blake, P. F. Santos, D. M. Barrus, W. Brubaker, E. Fenimore, and R. Puetter, 1976, "Collimators for Soft X-Ray Measurements," Space Sci. Inst. 2, 171-196.

A. J. Burek, 1977, 1978, private communications.

W. Eng, 1978, "ADP and RAP Single Crystal Rocking Curve Tests," Aerospace Technical Memorandum No. ATM-78(3960-01)-5, 10 pp.

B. L. Henke and M. A. Tester, 1975, "Techniques of Low Energy X-Ray Spectroscopy (0.1 to 2 keV Region)," Adv. in X-Ray Anal. 18, 76-106.

S. W. Kahler, A. S. Krieger, and G. S. Vaiana, 1975, "Morphological Evolution of X-Ray Flare Structures from the Rise through the Decay Phase," Astrophys. J. (Letters), 199, L57-L61.

C. K. Howey, and D. L. McKenzie, 1978, "The Arc-Second Alignment of Sun-Seeking Optical Detectors," Aerospace Technical Report No. TR-0079(4960-01)-1, 14 pp.

P. B. Landecker, W. T. Chater, C. K. Howey, D. L. McKenzie, and R. L. Williams, 1976, "CRLS-229 Solar X-Ray Spectrometer/Spectroheliograph Preliminary Design Review," Aerospace Technical Memorandum No. ATM-77-(2960-01)-1, 54 pp.

P. B. Landecker, W. T. Chater, C. K. Howey, D. L. McKenzie, and R. L. Williams, 1978, "CRLS-229 Solar X-Ray Spectrometer/Spectroheliograph Consent-to-Ship Review," Aerospace Technical Memorandum No. ATM-78 (3960-01) - 1, 64 pp.

P. B. Landecker and W. Eng, 1978, "CRLS-229 SOLEX CEMA Shield Transmission", Aerospace Technical Memorandum No. ATM-78 (3960-01) - 2, 6 pp.

P. B. Landecker and W. Eng, 1979, "Properties of Channel Electron Multiplier Arrays," Aerospace Report in preparation.

P. B. Landecker and D. L. McKenzie, 1978, "CRLS-229 SCF Training Session," Aerospace Technical Memorandum No. ATM-78 (3960-01)-3, 42 pp.

M. Malinovsky and L. Heroux, 1973, "An Analysis of the Solar Extreme Ultraviolet Spectrum between 50 and 300 Å," Astrophys. J. 181, 1009-1030.

J. F. McGrath, Jr., 1968, "New Technique for the Design of an Extreme Ultraviolet Collimator," Rev. Sci. Inst. 39, 1036-1038.

D. L. McKenzie, C. K. Howey, and R. M. Young, 1978, "Compact and Lightweight Multigrid Collimators for a Satellite-Borne Solar X-Ray Spectrometer Experiment," SAMSO-TR-78-105, 39 pp.

D. L. McKenzie, P. B. Landecker, and J. H. Underwood, 1976, "Crystals and Collimators for X-Ray Spectroscopy," Space Sci. Inst. 2, 125-139.

R. Meyer, McDonnell Douglas Astronautics Co., 1973, "Iso-Grid Design Handbook," NASA-CR-124075, 222 pp.

W. M. Neupert, W. A. White, W. J. Gates, M. Swartz, and R. M. Young, 1969, "X-Ray and Extreme Ultraviolet (1-400 Å) Spectroscopy of the Sun from OSO-III," Solar Phys. 6, 183-192.

H. R. Rugge and A. B. C. Walker, Jr., 1978, "Observation and Analysis of Fe XVIII Solar X-Ray Emission," Astrophys. J. 219, 1068-1078.

H. R. Rugge and A. B. C. Walker, Jr., 1968, Space Res. 8, 439-449.

E. Storm and H. I. Israel, 1970, "Photon Cross Sections from 1 keV to 100 MeV for Elements Z=1 to Z=100," Nuclear Data Tables A7, 565-681.

J. A. Vorpahl, E. G. Gibson, P. B. Landecker, D. L. McKenzie, and J. H. Underwood, 1975, "Observations of the Structure and Evolution of Solar Flares with a Soft X-Ray Telescope," Solar Phys. $\underline{45}$, 199-216.

A.B.C. Walker, Jr. and H. R. Rugge, 1970, "Solar X-Ray Observations of Forbidden Lines in the Helium Isoelectronic Sequence," Astron. and Astrophys. $\underline{5}$, 4-11.

A. B. C. Walker, Jr., H. R. Rugge, and K. Weiss, 1974, "Relative Coronal Abundances Derived from X-Ray Observations III: The Effect of Cascades in the Relative Intensity of Fe XVIII Line Fluxes, and a Revised Iron Abundance," Astrophys. J. $\underline{194}$, 471-482.

10. CRLS-229 GLOSSARY

$\overset{\circ}{A}$ Angstrom - 1 $\overset{\circ}{A}$ = 10^{-8}cm.

A_D Bit 7 in DFORM 2 which equals 0 whenever SOLEX detector microswitch A is depressed.

ADP Ammonium Dihydrogen Phosphate crystals used in SOLEX and SOLFLEX. The crystal lattice spacing 2 d = 10.64 $\overset{\circ}{A}$.

AF Air Force.

AFB Air Force Base.

AFS Air Force Station.

A_x Bit 5 in DFORM 2 which equals 0 whenever SOLEX crystal microswitch A is depressed.

AZ Azimuth.

B_1 XZ bit of SOLEX boresight cell. The data is located in XMOTOR.

B_2 XY bit of SOLEX boresight cell. The data is located in XMOTOR.

BASD Ball Aerospace Systems Division located in Boulder, CO.

BBRC Ball Brothers Research Corporation (now BASD).

BBRT	Bird Buffer Recording Tape records all incoming data line transmissions on magnetic tape at the SCF.
B_D	Bit 8 in DFORM 2 which equals 0 whenever SOLEX detector microswitch B is depressed.
BSUB	B priority subcom contains 32 16-bit words, each read out every 1.024 sec.
B_x	Bit 6 in DFORM 2 which equals 0 whenever SOLEX crystal microswitch B is depressed.
C6/7	If this housekeeping bit No. 9 in DFORM 2 equals 1, the Go To MAGMAP POS latching relay is on. This bit returns to 0 after the Go To MAGMAP POS OFF command is received.
C8	Bit 14 in DFORM 2 momentarily goes to 1 when the Go To Reference Zero command is sent.
C9/10	If this housekeeping bit No. 15 in DFORM 2 equals 1, the Go To LAMBDA 1 POS latching relay is on. This bit returns to 0 after the Go To LAMBDA 1 POS OFF command is received.
C and DP	P78-1 Command and Data Processing units.
CEMA	Channel Electron Multiplier Array. X-ray detector used in SOLEX B.
CG	Center of Gravity.

1·0
1·1
1·25

2·8
3·15

2·5
2·2
2·0
1·8
1·6

1·4
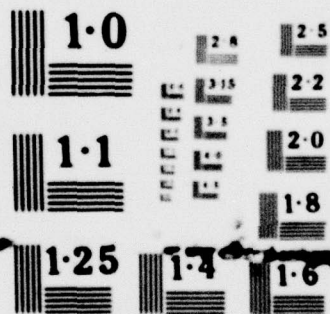
NATIONAL BUREAU OF STANDARDS
MICROCOPY RESOLUTION TEST CHART

CMD	Command.
CMOS	Complementary Metal Oxide Semiconductor.
C of R	Center of Rotation.
CONT 1-2	These 16 bit words 31-32 and 63-64 in BSUB contain the control register values stored in the command box memory.
CRLS	Cambridge Research Laboratory Subcontract
CRLS-229	Solar X-Ray Spectrometer/Spectroheliograph on P78-1.
DA	Data Analysis line printer at the SCF.
DFORM 1-2	Discrete Format No. 1 and No. 2 each contain 16 bits of housekeeping data that are sampled twice per master telemetry frame in BSUB words 19-20 and 51-52, respectively.
DOZE	Office code for SCF Field Test Force Director.
DP	Data Presentation line printer at the SCF.
EED	Electro-Explosive Device. There is one squib in CRLS-229 which is used to release the SOLEX detector shaft after launch.
EICD	Electrical Interface Control Document.

EL	Elevation.
EM	Estimation Module software used to determine P78-1 attitude and ephemeris.
F	If this bit No. 10 in CONT 2 is 0, SOLEX runs at the fast (62.5 Hz) motor speed; if this bit is 1, it runs at the slow (31.25 Hz) rate.
FOV	Field of View.
FTFD	SCF Field Test Force Director.
FWHM	Full Width at Half Maximum is a measure of the resolution of a detector or collimator.
G	If this bit No. 6 in CONT 2 is 1, it forces SOLEX crystal rocking, even in spacecraft raster modes.
GICD	General Interface Control Document.
GMT	Greenwich Mean Time.
HEM	High Energy Monitor experiment also called MONEX B. The energy range is 11-140 keV.
HEM CONTROL	Analog voltage equal to 5V when HEM has no control over SOLEX and 0 V when the SOLEX HVPS are turned off by the HEM or SOLEX is in the critical angle region. It is located in MF 112, SF 52.
HEMHVPS	HEM High Voltage Power Supply analog output located in MF 112, SF 8.

HEMLVPS	HEM Low Voltage Power Supply analog output located in MF 112, SF 7.
HEM RATE IN	Four level analog output indicating the threshold HEM MBULD required to turn off the SOLEX high voltage. It is located in MF 112, SF 50.
HEM RATE OUT	Analog voltage which is a function of MBULD and located in MF 112, SF 51.
HV	High Voltage.
ICD	Interface Control Document.
IRON	Interrange Operations Number. The P78-1 mission corresponds to IRON 2265.
ITS	Instrument Time Share circuit in the P78-1 spacecraft. It is used to shift control of the spacecraft PIA between CRLS-229 and NRL-401.
JK 11	This housekeeping bit No. 12 in DFORM 1 equals 1 after the PIA has just changed to the raster mode and while the first SOR is locked out.
λ	Lambda or photon wavelength.
λ_e	1) This 3rd MSB in DFORM 2 equals 1 when SOLEX is in the crystal rocking mode. 2) Wavelength end point of a crystal block.
λ_i	1) This 4th MSB in DFORM 2 equals 1 when SOLEX is in a raster mode. 2) Fixed wavelength in raster mode.

LAM 1-10	These 16 bit words 21-30 and 53-62 in BSUB contain the wavelength step number (from Ref Zero) stored in the wavelength register part of the command box memory for wavelengths 1-10, respectively.
LASSMC	Binary number in DFORM 1 (bits 5-8) indicating the address of the last serial magnitude command received by the SOLEX command box.
LCALL	Four most significant bits of DFORM 1 indicating the current position of the SOLEX wavelength pointer (as a binary number).
LEM	Low Energy Monitor experiment also called MONEX A. The energy range is 1-22 keV.
LEMHVPS	LEM High Voltage Power Supply analog output located in MF 112, SF 10.
LEMLVPS	LEM Low Voltage Power Supply analog output located in MF 112, SF9.
LLD	Lower Level Discriminator pulse height setting.
LR	Large Raster mode of PIA.
LSB	Least significant bit.
LV	Low Voltage.

M	Number of sequential SOLEX rasters at each wavelength (Binary bits 2-4 or M1, M2, M3 in CONT 1 total 1 to 7, inclusive).
MAF	P78-1 telemetry Master Frame (2.048 sec).
MAGMAP	Magnesium Mapping experiment on CRLS-229. NRL detectors look through the Aerospace SOLEX B 1 arc min collimator.
MARTD	This 16 bit word 5 and 37 in BSUB gives the number of MONEX A risetime reject events in 1.024 sec (number events with risetimes slower than the risetime discriminator setting).
MAULD	This 16 bit word 3 and 35 in BSUB gives the number of MONEX A (LEM) upper level discriminator reject events in 1.024 sec (number of events with amplitude greater than that of the upper level discriminator).
MBRTD	This 16 bit word 6 and 38 in BSUB gives the number of MONEX B risetime discriminator reject events in 1.024 sec.
MBULD	This 16 bit word 4 and 36 in BSUB gives the number of MONEX B (HEM) upper level discriminator reject events in 1.024 sec.
MCC	Mission Control Complex at SCF includes test control room, analysts room and technical advisor's room.
MCOUNT	Housekeeping bits 11-13 in DFORM 2 which indicate the current number of rasters at the current wavelength position (MCOUNT less than or equal to M).

MF	P78-1 telemetry Main Frame (32 msec).
MFCT (MFCT1, MFCT2)	Minor frame count (0–63 in 1.024 sec). '. can be found in 6 LSB's of MF Word 1 and 99.
MICD	Mechanical Interface Control Document.
MID	Middle.
MONEX A	Monitor Experiment data from the Low Energy Monitor experiment built by The Aerospace Corporation.
MONEX B	Monitor Experiment data from the High Energy Monitor experiment built by The Aerospace Corporation.
MSB	Most Significant Bit.
MTRPOS	Number of steps SOLEX is from Reference Zero Position. This 14 bit number can be constructed from XMOTOR and is reset to zero whenever the spectrometer is enroute to Reference Zero.
N	Number of stored wavelengths (λ_i's) for SOLEX rasters equals 2 N. (Binary bits 5-7 in CONT 1: N1, N2, N3 x 2 totals 2, 4, 6, or 8). There are 5-N pairs of endpoints in the spectrometer mode.
N/A	Not Applicable.
NASA	National Aeronautics and Space Administration.
NRL	Naval Research Laboratory.

10-8

OM	Output Module software used to determine P78-1 attitude.
ORD	Orbital Requirements Document.
OSO	Orbiting Solar Observatory.
OTWG	Orbital Test Working Group.
P	8th MSB in CONT 1. When P = 1 and RAS changes from 1 to 0 or PGD goes from 0 to 1 in a raster mode, there is a reset to the first position. When P = 0, the pointer location does not change when either of the above conditions is met.
P'	9th MSB in CONT 1. Only if it equals 1 is MCOUNT reset when RAS goes from 1 to 0. If P' = 0, MCOUNT is increased by 1 at the end of rastering.
P"	10th MSB in CONT 1. Bit P" clears the λ_e pair to λ_{2N+1}, λ_{2N+2} at RTE.
P78-1	Designation of spacecraft carrying CRLS-229.
PC	Proportional Counter X-ray detector.
PGD	Housekeeping bit 11 in DFORM 1 which equals 1 whenever the Pattern Generator Disconnect signal is high, and WLC controls the PIA in the spacecraft sun center point mode.
PHA 1-6A	These 16 bit words 7-12 and 39-44 in BSUB give the number of MONEX A (LEM) events in each of 6 pulse height channels every 1.024 sec.

PHA 1-6B   These 16 bit words 13-18 and 45-50 in BSUB give the number of MONEX B (HEM) events in each of 6 pulse height channels every 1.024 sec.

PIA   Pointed Instrument Assembly of the P78-1 spacecraft. It is the solar pointing system of the spacecraft sail.

PRD   Program Requirements Document.

PST   Pacific Standard Time.

Q   11th MSB in CONT 1 which when equal to 1 generates full rocks at the end of a raster sequence. When $Q = 0$ at the end of a raster sequence, Reference Zero is called before the rock sequence is repeated.

QA   Quality Assurance.

R   If this 12th MSB in CONT 1 is 0, the Pattern Generator Disconnect signal from the ITS does not reset any counters. If this bit is 1 the PGD signal commands the spectrometer to go to Reference Zero before continuing.

RAP   Rubidium Acid Phthalate crystals were used in SOLEX. The crystal lattice spacing $2 d = 26.12 Å$.

RAS   9th MSB in DFORM 1. It equals 1 only when the PIA is in the raster mode (independent of whether the pattern generator is connected).

REV   Revolution.

10-10

RLW2   See HEM RATE IN.

RLW3   See HEM RATE OUT.

RLW4   See HEM CONTROL.

RS3   Housekeeping bit No. 13 in DFORM 1 which
                                  equals 1 while SOLEX is en route to
                                  Reference Zero.

RS4   Housekeeping bit No. 14 in DFORM 1 which is
                                  set to 1 by the closure of detector
                                  microswitch A.

RS9   Housekeeping bit No. 15 in DFORM 1 which is
                                  set to 1 by the closure of crystal
                                  microswitch A and cleared to 0 by the
                                  closure of crystal microswitch B.

RS10   Housekeeping least significant bit in DFORM 1
                                  which equals 1 while SOLEX is rastering
                                  end-to-end.

RTC   Real Time Command.

RTD   Risetime discriminator pulse shape setting.

RTS   Remote Tracking Station.

S   If this bit No. 13 in CONT 1 is 0, MAGMAP
                                  operation will freeze the SOLEX MCOUNT
                                  register so that SOR pulses are not
                                  counted.

SAMSO   Air Force Space and Missile Systems Organi-
                                  ation located at Los Angeles AFS, CA.

10-11

SAMTEC	Air Force Space and Missile Test Center located at Vandenberg AFB, CA.
SARTD	This 16 bit word 1 and 33 in BSUB gives the number of SOLEX A risetime reject events in 1.024 sec.
SAFS	Sunnyvale Air Force Station.
SBULD	This 16 bit word 2 and 34 in BSUB gives the number of SOLEX B upper level reject events in 1.024 sec.
S/C	Spacecraft.
SCF	Air Force Satellite Control Facility in Sunnyvale, CA.
SF	Telemetry Sub-Frame.
S_{HV}	This housekeeping least significant bit in DFORM 2 goes to 0 when XMOTOR is scanning the 5120-9216 region or scanning to Reference Zero. SOLEX high voltages are disabled at this time.
SHV1 or SHVPS1	SOLEX A High Voltage analog readout located in MF 112, SF 12.
SHV2 or SHVPS2	SOLEX B High Voltage analog readout located in MF 112, SF 13.
SLC	Spacecraft Launch Complex.

SLVPS1   SOLEX Low Voltage Power Supply analog out-
                                put located in MF 112, SF 4.

SLVPS2   SOLEX Low Voltage Power Supply analog
                                output located in MF 112, SF 49.

SMC   Serial Magnitude Command.

SMOTOR   The 4 LSB's of DFORM 1 which include RS3,
                                RS4, RS9 and RS10.

SOL   Start of Line in a PIA raster.

SOLEX A   Solar Experiment proportional counter 20 arc
                                sec collimator data. SOLEX was built by
                                The Aerospace Corporation.

SOLEX B   Solar Experiment Channel Electron Multiplier
                                Array 1 arc minute collimator data.
                                SOLEX was built by The Aerospace
                                Corporation.

SOLFLEX   Solar Flare Experiment on CRLS-229. This is
                                an uncollimated crystal spectrometer built
                                by NRL.

SOR   Housekeeping bit No. 10 in DFORM 1 which
                                equals 1 when the Start of Raster line is
                                high.

Sp   Spare bits 2 and 10 in DFORM 2.

SPO   Air Force Systems Program Office.

SPOT 1, 2   SOLEX Pot reads out angular position of
                                crystals and detectors, and located in MF
                                112, SF 20, 21, respectively.

10-13

SR	Small Raster mode of PIA.
SSL	Space Sciences Laboratory at Aerospace.
STC	Satellite Test Center.
STG	Space Test Group.
STP	Space Test Program.
SV	Space Vehicle.
T (T1, T2, T3)	Number of rocks between two end wavelengths equals 2T-1.
TCOUNT	Bits B3-B6 in XMOTOR give the spectral scan number, i.e. the current number of wavelength rocks. TCOUNT is less than or equal to 2T-1.
TCT	Telemetry Conversion Tables.
TFACE	CRLS-229 face temperature located in MF 112, SF 58.
TMID	CRLS-229 middle temperature located in MF 112, SF 59.
TOO	Test Operations Order of SCF.
TRD	Telemetry Requirements Document.
TREAR	CRLS-229 rear temperature located in MF 112, SF 60.

U/D   Housekeeping most significant bit in DFORM 2
                        which equals 1 when XMOTOR is increas-
                        ing and when the spectrometer is enroute
                        to Reference Zero, and 0 when it is
                        decreasing.

ULD   Upper Level Discriminator pulse height set-
                        ting.

UT   Universal Time.

VAFB   Vandenberg Air Force Base.

VDC   Voltage (direct current).

V1, V2   2nd and 3rd MSB in CONT 2 which set the
                        value of the SOLEX HVPS 1 as follows:

                                Lowest 00 or 10
                                Middle 11
                                Highest 01.

V3, V4   Bits 4 and 5 in CONT 2 which set the value of
                        the SOLEX HVPS 2 as follows:

                                Lowest 00 or 10
                                Middle 11
                                Highest 01.

V5   Bit 7 in CONT 2 which selects the value of the
                        MONEX A (LEM) high voltage as follows:

                                Lower 1
                                Higher 0.

V6   Bit 8 in CONT 2 which selects the value of the
                        MONEX B (HEM) high voltage as follows:

                                Lower 1
                                Higher 0.

WLC

1) White Light Coronagraph part of the NRL-401 experiment.

2) See PGD.

XMOTOR

CRLS-229 telemetry containing SOLEX MOTOR position, TCOUNT and bore sight cell data.

XTAL

Crystal.

YCTA

Office code for SAMSO P78-1 Program Office.

Z

Zulu or Universal Time.

LABORATORY OPERATIONS

The Laboratory Operations of The Aerospace Corporation is conducting experimental and theoretical investigations necessary for the evaluation and application of scientific advances to new military concepts and systems. Versatility and flexibility have been developed to a high degree by the laboratory personnel in dealing with the many problems encountered in the nation's rapidly developing space and missile systems. Expertise in the latest scientific developments is vital to the accomplishment of tasks related to these problems. The laboratories that contribute to this research are:

Aerophysics Laboratory: Launch and reentry aerodynamics, heat transfer, reentry physics, chemical kinetics, structural mechanics, flight dynamics, atmospheric pollution, and high-power gas lasers.

Chemistry and Physics Laboratory: Atmospheric reactions and atmospheric optics, chemical reactions in polluted atmospheres, chemical reactions of excited species in rocket plumes, chemical thermodynamics, plasma and laser-induced reactions, laser chemistry, propulsion chemistry, space vacuum and radiation effects on materials, lubrication and surface phenomena, photosensitive materials and sensors, high precision laser ranging, and the application of physics and chemistry to problems of law enforcement and biomedicine.

Electronics Research Laboratory: Electromagnetic theory, devices, and propagation phenomena, including plasma electromagnetics; quantum electronics, lasers, and electro-optics; communication sciences, applied electronics, semiconducting, superconducting, and crystal device physics, optical and acoustical imaging; atmospheric pollution; millimeter wave and far-infrared technology.

Materials Sciences Laboratory: Development of new materials; metal matrix composites and new forms of carbon; test and evaluation of graphite and ceramics in reentry; spacecraft materials and electronic components in nuclear weapons environment; application of fracture mechanics to stress corrosion and fatigue-induced fractures in structural metals.

Space Sciences Laboratory: Atmospheric and ionospheric physics, radiation from the atmosphere, density and composition of the atmosphere, aurorae and airglow; magnetospheric physics, cosmic rays, generation and propagation of plasma waves in the magnetosphere; solar physics, studies of solar magnetic fields; space astronomy, x-ray astronomy; the effects of nuclear explosions, magnetic storms, and solar activity on the earth's atmosphere, ionosphere, and magnetosphere; the effects of optical, electromagnetic, and particulate radiations in space on space systems.

THE AEROSPACE CORPORATION
El Segundo, California

. . .